A Study Of Nramp1 Function And Targeting

UNIVERSITY OF SOUTHAMPTON

FACULTY OF SCIENCE

MOLECULAR CELL BIOLOGY

Doctor of Philosophy

By Stephen Timothy Baker

July 2002

UNIVERSITY OF SOUTHAMPTON

ABSTRACT

FACULTY OF SCIENCE

MOLECULAR CELL BIOLOGY

Doctor of Philosophy

A STUDY OF NRAMP1 FUNCTION AND TARGETING

By Stephen Timothy Baker

The *Nramp1* gene is a member of a family of divalent cation transporters found in a variety of species. Mammalian *Nramp1* is found exclusively in cells of haematopoietic lineage, namely monocytes/macrophages and polymorphonuclear leukocytes. Studies in mice have shown *Nramp1* to confer resistance to a number of taxonomically and antigenically distinct organisms including *Leishmania*, *Salmonella* and *Mycobacteria*. It is recruited to phagolysosomes upon ingestion of bacteria where it is believed to affect the microenvironment within the phagolysosome. Two hypotheses have been formulated: one in which *Nramp1* depletes the microenvironment of iron, starving the bacteria; and the other in which *Nramp1* supplies iron for radical production and active attack of the bacteria.

Through the use of *in vitro* expression systems, induction studies in murine macrophages and sequence analysis, the following has been achieved: *Nramp1* expression is regulated by its substrate, iron, and also by oxygen derived radicals. In addition, putative sites for this type of regulation have been identified in the promoter sequence.

Stable transfectant cell lines containing constitutively expressed *Nramp1* grow at a slower rate compared to controls, as measured by cell staining and [^{3}H]-thymidine uptake. These cell lines also show greater resistance to superoxide-induced stress, and attenuation of PKCβI protein levels, the gene transcription of which has been shown to be sensitive to labile iron pool concentrations. Together the results imply that Nramp1 protein may act to sequester iron in an intracellular vesicular system.

Lastly analysis of EGFP wildtype and mutant Nramp1 tagged proteins indicates that N-terminal phosphorylation of Nramp1 is not important in its targeting, as has been suggested. It is also shown that under an appropriate stimulus Nramp1 can translocate to the plasma membrane; the functional significance of this is discussed.

In conclusion these results support a model for *Nramp1* whereby it may effect microbial replication through production of radicals brought about by Fenton chemistry. These results also suggest the possibility of two other Nramp1 roles, namely as an antioxidant and/or iron recycling protein.

Contents:

Tables:

Figures:

Major abbreviations:

PBM	primary bone marrow macrophages.
R	resistant functional Gly169 *Nramp1*
S	susceptible functional null Asp169 *Nramp1*
FAS	ferric ammonium sulphate
SNP	sodium nitroprusside
(HMW)	high molecular weight – i.e. 90-100kDa.
(LMW)	low molecular weight – i.e. 45kDa.
37	*Nramp1*^{Gly169} sense stably transfected RAW264.7 cells.
32	*Nramp1*^{Gly169} sense stably transfected RAW264.7 cells.
21	*Nramp1*^{Gly169} anti-sense stably transfected RAW264.7 cells.
S4	*Nramp1*^{Gly169} sense stably transfected L1 3T3 fibroblasts.
S7	*Nramp1*^{Gly169} sense stably transfected L1 3T3 fibroblasts.
AS3	*Nramp1*^{Gly169} anti-sense stably transfected L1 3T3 fibroblasts.
AS7	*Nramp1*^{Gly169} anti-sense stably transfected L1 3T3 fibroblasts.
P6	p-nut stably transfected RAW264.7 cells.
p-nut	*Nramp1* N-terminal phosphorylation mutant construct under constitutive β-actin promoter control.
p-wil	Wildtype *Nramp1* construct under constitutive β-actin promoter control.
TB	Tuberculosis
Mtb	*Mycobacterium tuberculosis*
TMD	Transmembrane domain
ROS	Reactive oxygen species
RNI	Reactive nitrogen intermediates

Acknowledgements

I would like to dedicate this thesis to my dad who always supported me and gave me the confidence to achieve my goals.

I would especially like to thank my supervisor, Dr Howard Barton, for his help and insight and also Dr Thelma Biggs for her support and help. I would also like to say a big thank you to my mum who has given me great financial and emotional help throughout my PhD.

Last but not least are the people I spent my time in the lab with, thanks to: Dr Andrew Bingham, Holly, Emma, Joe, Helen, Roisin, and Karen.

Chapter 1

Introduction

1.1 Antimicrobial Resistance

Antimicrobial agents are among the wonder drugs of the twentieth century, and have transformed our ability to treat many infectious diseases that were previously killers. One of the most revolutionary finds was that of penicillin by Alexander Fleming in 1928, which changed the treatment of bacterial infections forever. Pharmaceutical industries now widely use the mass production of synthetically made compounds in an attempt to find novel drug activities. This is not a new technique however, and was used by a German scientist at the turn of the previous century. Paul Ehrlich produced synthetically made substances, not necessarily of natural origin, to treat Syphilis and later coined the term 'chemotherapy'. This term now encompasses 'antibiotics' which described the substances produced by some microorganisms that kill or inhibit the growth of other microorganisms. Chemotherapy has also been more recently applied to those drugs used in the treatment of malignant or cancerous cells. Subsequently substances used in the treatment of microbial infections are now classed as antimicrobials.

The wonder drugs of the twentieth century are more recently becoming the Pentium processors of the past as for every one produced a new market of resistant microbes appears requiring more powerful or novel treatment making previous treatments obsolete. This is the result of misdiagnosis, misuse and overuse putting

selective pressure on bacteria, causing development of mutated strains carrying resistance.

Antimicrobial agents are used in agriculture such as livestock and crop production, as well as in fish farming and to treat and control animal diseases, enhancing growth and yield. The widespread use of antimicrobials for disease control and growth promotion in animals has been paralleled by an increase in resistance in those bacteria that can spread from animals, often through food, to cause infections in humans. Bacteria that are harmless to livestock can be fatal to humans. One example occurred in Denmark in 1998, when strains of multi drug-resistant *Salmonella typhimurium* struck 25 people, killing two (1). Cultures confirmed that the organisms were resistant to seven different antibiotics. Epidemiologists eventually traced the microorganism to pork and to a swineherd where it originated.

1.2 Multidrug-resistant Tuberculosis, a Global Crisis

Multidrug-resistant tuberculosis is defined as resistance to at least isoniazid and rifampicin (WHO).

After decades of decline, tuberculosis case rates are increasing worldwide. Tuberculosis (TB) is the most frequent cause of death from a single infectious disease in persons aged 15–49 years. It is estimated that if current trends continue, nearly five million people will be newly infected each year, 10 million people will get sick, and about 1.5 million will die from TB if control is not further strengthened (WHO). Two major problems regarding the control of TB are emerging: co-infection with human immunodeficiency virus (HIV) and resistance of *M. tuberculosis* (Mtb) to the currently used regimen of tuberculostatics. Co-infection with HIV means the disease can achieve pulmonary TB quickly; that is without the body's natural immune

defence TB can run riot in the lungs leading to infectious sputum with high bacilli counts. This allows faster transit of the disease to uninfected individuals. In addition HIV is highly prevalent in developing countries and people being treated for co-infection of Mtb in these countries will often have interrupted or inappropriate medical care, which can lead to selection of resistant bacteria with subsequent growth and spread of resistant strains. Indeed, resistance of Mtb to anti-tuberculosis drugs is a man-made amplification of a natural phenomenon. Unlike the situation in many bacteria, with Mtb there is believed to be no horizontal gene transfer (2); as a result natural resistance to antimicrobial drugs is believed to be a very rare event. Spontaneous mutations in a given gene in a population derived from a single bacterium only occur with a frequency of 10^{-12}-10^{-7} making this type of resistance in any given patient unlikely [184]. Natural resistance to specific drugs has been documented however, for example *M. bovis* has an efficient transporter for the active form of pyrazinamide where as Mtb does not (3;4). Therefore drug resistance occurs by the selective sorting of drug resistant bacteria from susceptible bacteria during treatment.

Genetic mutations resulting in resistance of Mtb to rifampicin, an RNA polymerase inhibitor, occur at a rate of 10^{-10} per cell division and lead to an estimated prevalence of 1 in 10^8 bacilli in drug-free environments; the rate for isoniazid is approximately 10^{-7} to 10^{-9}, resulting in resistance in 1 out of 10^6 bacilli (WHO). Acquired resistance is defined as the suppression of susceptible bacilli during a single drug treatment that leads to multiplication of resistant microbes. Subsequent delivery of these bacilli to another host, causing infection, results in drug resistance from the outset and is known as primary resistance. To avoid this, the rules of probability are employed. The mutational rate leading to resistance of the above genes to their

cognate drugs is high enough to make spontaneous resistance possible. However if multiple drugs are used then it is the product of their individual probabilities. For example using the above drug probabilities: 10^6 X 10^8 is 10^{14} a much lower probability of any single bacteria becoming resistant. This is the reason multi-drug schemes are used in the treatment of Mtb and other infectious diseases. However if base-line resistance occurs then multi-drug resistance can occur, a phenomenon seen in parts of the world.

Multi-drug resistant strains have been found in Iran and also in Eastern Europe, South Africa and especially the countries of the former Soviet Union. Strains are also arising in Asia, especially parts of India and provinces in China (WHO). Most countries of the world have drug-resistant TB although these are on the decline due to better therapy and follow up of patients. This does not mean they are free from risk however, as travel between countries has become routine for a large population of the world increasing the probability that such a strain could be imported.

1.3 Development Of New Antimicrobial Strategies

1.3.1 Prevention By Vaccination

200 years ago Edward Jenner, after seeing the pox-free skin of milkmaids, rationalised that exposure of the cowpox virus to humans (where it is non-virulent) may confer resistance to human smallpox. This theory turned out to be correct and led to modern vaccination.

The theory is to allow the body to respond to precursors or an avirulent/dead form of the pathogen. This initiates presentation of antigens associated with the disease to T-cells and subsequent production of cell mediated and humoral immunity.

In turn it is hoped that this will facilitate production of memory cells that will recognise infection with the virulent pathogen, producing a specific and rapid inflammatory response.

In TB prevention an attenuated form of *M.bovis* is used, bacille Calmette-Guerin (BCG). Albery Calmette and Camille Guerin who isolated *M.bovis* from a cow produced this in the early years of the previous century. Today BCG is widely used throughout the world as a vaccine against TB and leprosy (caused by *Mycobacterium leprae*). The problem with this vaccine is that it might not work (5), a trend that is variable between countries but is thought to be caused by a number of factors:

- Incorrect preparation of vaccines,
- Interference by exposure to local environmental mycobacteria; this may be the reason the vaccine has a higher efficacy in children.

New methods for vaccine production are now being established. These include DNA vaccines, which are plasmids with mammalian promoters that control the expression of Mtb genes. Injection of such constructs into the muscle of the animal allows production of the coded protein and immune-reactivity against it.

Subunit vaccines, in adjuvant, are also being produced in combination with cytokine therapy to specifically produce a Th1 response [5], a response that ultimately causes activation of macrophages and their infiltration to the site of infection through the activities of a subset of T lymphocytes called Th1 cells. This is known as the cell mediated immune response and subsequently boosts the macrophages' ability to remove intracellular Mtb/*M.bovis*.

1.3.2 Analysis Of Host Resistance

Host infection by intracellular parasites such as Salmonella, Mycobacterium and Leishmania requires the immune response to develop a set of Th1 helper cells. These cells target the immune system against pathogens that 'veil' themselves in host cells and are otherwise protected against the humoral response. The above pathogens favour phagocytes, in particular resident macrophages, perhaps partly as they are highly phagocytic allowing straightforward entry. Here the parasites can hide and replicate but first they need to avoid the macrophage's antimicrobial activity. They do

Figure 1.3.21

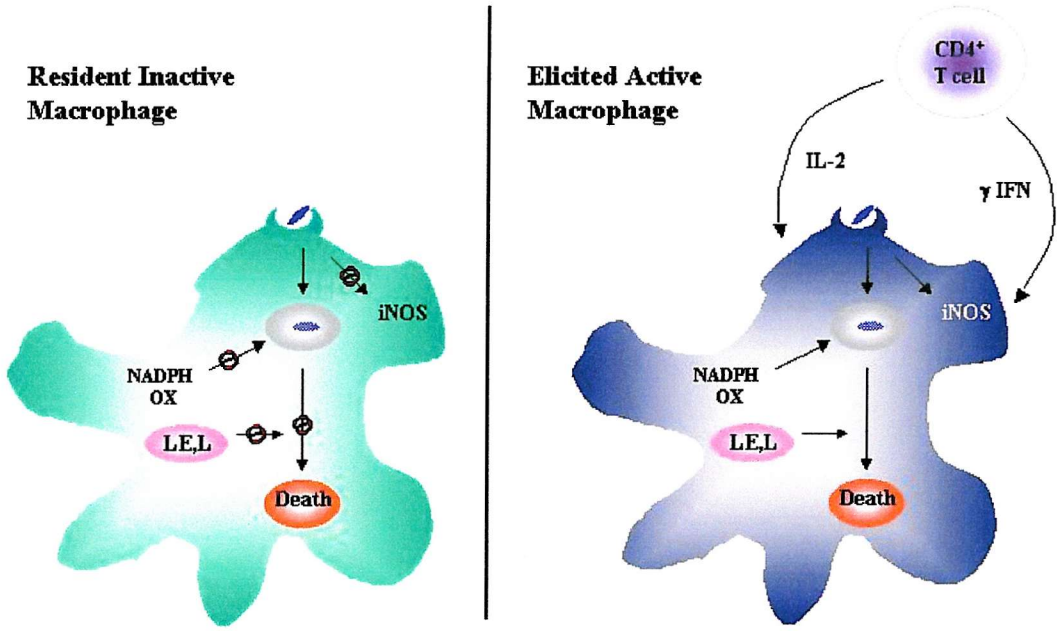

Figure 1.3.21. Macrophage inflammatory activation: the diagram depicts an un-stimulated resident macrophage that has little antimicrobial activity. Elicited active macrophages are however primed by cytokine signalling from T-cells; allowing pathogens that could once block phagosome maturation to be removed. NADPH ox = NADPH oxidase that is recruited to the phagosome. LE = late endosome, L = lysosome.

this by inhibition of phagosome maturation allowing survival in less mature phagolysosomes. For macrophages that are not activated this can pose a problem as priming allows them to react through production of reactive oxygen/nitrogen intermediates, occurring via NADPH oxidase and iNOS (inducible Nitric Oxide Synthase) activation, respectively. NADPH oxidase consists of five subunits two of which are membrane bound, $gp91^{phox}$ and $p22^{phox}$, and three that form a cytosolic complex, $p47^{phox}$, $p67^{phox}$ and $p40^{phox}$, that is recruited to the plasma or phagosomal membrane subunits upon an appropriate stimulus. Recruitment of the small cytosolic GTPase Rac is also required for correct functioning of NADPH oxidase and culminates in the transfer of a single electron to molecular oxygen to produce superoxide anion. In order for this to arise Th1 helper cells need to be activated allowing secretion of cytokines (IFN-γ, IL-2) that activate elicited macrophages that have entered the inflammatory site (Fig. **1.3.21**). These macrophages upon bacterial uptake can also abrogate bacterial mediated attenuation of phagosome maturation leading to pathogen destruction [185].

The above response is ideal but it is not activated to the same degree in all people; demonstrated by the small percentage of people that develop clinical Mtb, 5-10%, while tens of millions of people are actually infected with the causative pathogens (6). This apparent degree of susceptibility has created an area of research devoted to identifying host genetic traits, either in innate or acquired immunity, causing vulnerability. Identification of these genes may in the future allow design of novel therapies.

1.3.3 Identification Of Susceptibility Genes

Abundant evidence exists to suggest that infectious disease susceptibility is under the control of host genetic loci (7;8). These susceptibility traits have been the

focus of concentrated study, which currently suggests that most are multi-genic. For example leprosy can manifest itself as a spectrum of disease phenotypes, ranging from lepromatous leprosy to tuberculoid leprosy. Lepromatous leprosy is associated with a potent humoral response but little delayed type hypersensitivity characteristic of anergy to leprosy antigens. Disfiguring and sensory nerve loss is thought to be due to uncontrolled growth of bacilli. At the opposite end is tuberculoid leprosy that is associated with a good delayed type hypersensitivity and cell-mediated immunity. Nerve damage in these cases is believed to be due to the inflammatory response as bacilli growth is under much better control. This variety of phenotypes implies a range of gene interactions leading to disease susceptibility *per se* and to the spectral differences.

Study of the genes that affect these outcomes has been achieved in a number of different ways, often using multiple techniques to achieve the final goal. The candidate gene approach has been used in family and population association studies, but is based on prior knowledge of influencing factors. For instance, mutations were identified in the IFN-γ receptor of six children with atypical mycobacterial dissemination, immunological screening showing that they had impaired IFN-γ production in response to mycobacterial antigens. Detection of the deficiency was followed by a genome wide search and identification of a region of linkage that was known to contain the IFN-γ receptor gene. Continued research identified that this receptor was mutated and missing on the children's leukocytes (9;10). Such alleles are unlikely to be associated with the 10% of the population, which have susceptibility to TB, as estimations of the frequency of disseminated infection following vaccination with BCG are ~ 0.59 per million (11).

The vitamin D receptor has also been used as a candidate gene implicated in susceptibility to TB; these studies were initiated by several findings: the active metabolite of vitamin D (1,25 di-hydroxyvitamin D_3) was known to influence the immune system; vitamin D receptors were present on monocytes and activated B and T lymphocytes; epidemiological studies suggested links between dietary intake of vitamin D and onset of TB (12); and monocytes exposed to 1,25 di-hydroxyvitamin D_3 *in vitro* showed enhanced bacteriostatic activity against Mtb. Subsequent association analysis identified that one particular vitamin D receptor genotype was significantly under-represented in individuals with TB [5].

The difficulty is that no single gene has been shown to be the major cause of susceptibility to TB; associations to gene mutations in one population that are not with held in others make the problem complex. An example of this is the variable association of MHC haplotypes with malaria susceptibility possibly due to geographical location and exposure to malaria that are antigenically polymorphic (13). This adds yet another dimension to infection genomics, with the possibility of tailor made susceptibility based on geographical location, and displays an important point in that environmental factors also effect disease progression.

The sequencing of the human genome and production of informative markers has significantly decreased the time period in which linkage analysis can be performed. Aided by the introduction of high throughput fluorescence-based genotyping it will allow future family based linkage studies to have a greater impact. Isolation of parts of the genome in this way will also complement knowledge of the genome, and the proteins encoded therein, highlighting candidate genes.

Animal models are yet another technique used in the identification of susceptibility genes or those involved in resistance. In particular mice are used as

they rapidly breed and high-resolution genetic maps are available for them, there is also extensive homology between human and mouse chromosomes (>85%) (8). Transgenic technology in mice is and has been hugely beneficial; it allows the insertion of genes or use of homologous recombination to specifically remove/replace functional or mutant genes respectively. This is achieved by removal of the inner cell mass from blastocysts and culture of embryonic stem cells. These cells can then be transfected, as with other tissue culture cells, selected and then replaced into a blastocyst. Using this method both expression of transgenes and specific replacement of genes creating knockout (KO) animals can be made with genes of interest, allowing their effects to be analysed. This technology has been enhanced using the established Cre/lox system(14) involving the insertion of gene sequences, as above, that are partly flanked by loxP sites themselves targets for the bacteriophage recombinase, Cre. This enables genes to be switched on or off in spatially and temporally specific manners upon crossing with mice that display the desired pattern of Cre expression.

Congenic animals can be made by back crossing, which are identical in their genetic backgrounds except for the gene of interest. Informative crosses can be used to analyse inheritance patterns, and in more detail linkage analysis in association with recombinational frequency, to dissect particular phenotypes aiding acquisition of genes by positional cloning methods.

The identification in the 1970s-80s of inbred strains of mice susceptible to infection with antigenically and taxonomically distinct intracellular parasites led to the exciting possibility of an animal model for human infectious disease susceptibility (15-19). Since then the gene involved in natural resistance of these mice has been positionally cloned and designated *Nramp1*, later leading to the isolation of the human homologue, *NRAMP1*. Polymorphisms in the promoter of *NRAMP1* have since been

associated with susceptibility, in some populations, to TB and leprosy (20) (1.6.1). Although both mouse and human *NRAMP1* have been associated with disease susceptibility to intracellular parasites there are fundamental differences between the actions of the two, discussed later (1.6.2). This research however should provide a paradigm for analysis of future candidate genes showing that parallels can be drawn from animal infectious disease susceptibility and related to the human multigenic control. The identification of a mouse strain resistant to endotoxin shock may also provide a suitable model for cloning of a gene involved in the inflammatory response to lipopolysaccharide (LPS) (21). It was found that the genetic locus determining resistance contained the toll-like receptor 4 (*Tlr4*) (with a point mutation), a receptor found on macrophages and involved in intracellular signalling upon interaction with CD14 that has bound LPS. Separately Yuan *et al.* have suggested that *Tlr4* is not solely responsible for resistance and another protein, Ran GTPase that is part of the Ras family (22), may have a role in CD14 independent responses to LPS; implying that more than one genetic change has occurred in these mice to account for LPS resistance (23).

Natural Resistance Associated

Macrophage Protein 1

1.4 Discovery of *Nramp1*

Three independent groups in the 1970s-80s headed by Bradley & Kirkley, Plant & Glynn, and Gros and his group found a phenotype in mice that suggested a single gene could control innate resistance to intracellular pathogens. The three groups were working independently on infections of mice with *Salmonella typhimurium* (*Ity*) (15), *Leishmania donovani* (*Lsh*) (17) and *Mycobacterium bovis,* (*Bcg*) (16), giving the gene its original name, *Lsh/Ity/Bcg*. Pathogen infected mice showed a biallelic phenotype, and alleles were designated susceptible and resistant, this was based on either rapid growth of the pathogen in the reticuloendothelial organs (susceptible) or reduced growth (resistant) in the first few weeks of infection. The early halt to the progression of the disease suggested that an enhancement of innate immunity was occurring. The kinetics of the disease were similar in both *Bcg* and *Lsh* infection showing a pre-immune phase controlled in resistant mouse strains, followed by a recovery phase where both resistant and susceptible lines showed the same outcome (24). This did not occur in *Ity* infection however as the rapid growth of this pathogen inevitably led to the death of susceptible mice before the recovery phase. The recovery phase is believed to occur due to the onset of acquired immunity. Resistant mice fed with the macrophage poison, silica, (25) became susceptible suggesting that the macrophage was the housing for the gene's expression. Furthermore, explanted macrophages from the two phenotypes showed differential

abilities to restrict the growth of ingested *Bcg* (26), *M.smegmatis* (27), *S.typhimurium* (28), *L.donovani* (29) and *M.intracellulare* (30).

Crossing of resistant and susceptible mice (fig.**1.4.1**) (17) showed that the trait followed a typical Mendelian ratio, and that the now termed *Lsh/Ity/Bcg* resistant phenotype was dominant. This was useful as it meant the phenotype was under the control of a single gene and that it should be possible to identify a candidate gene.

Figure 1.4.1

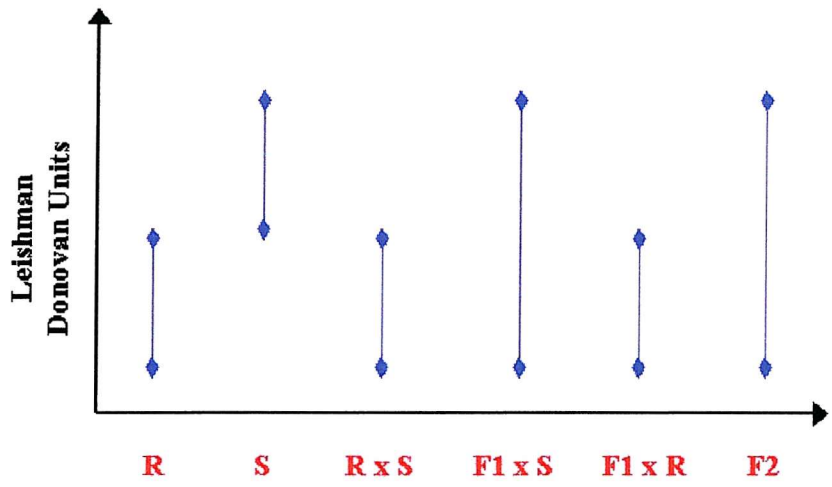

Figure 1.4.1. Diagrammatic graph showing differential parasitic growth in mice of resistant and susceptible backgrounds: Graph was adapted from Bradley *et al.* [17]. Leishman donovan units - ratio of parasites to reticuloendothelial cell nuclei. R = homozygous *Nramp1* Gly169 resistant mice, S = homozygous Asp169 susceptible mice, R x S = crossing of resistant and susceptible strains. F1 test-crosses and F2 generations are also shown.

In 1993 Vidal *et al.* (31) positionally cloned the *Lsh/Ity/Bcg* gene. The phenotype responsible was genetically mapped through linkage analysis in back crossed and recombinant inbred strains of mice. It was mapped to the proximal region of chromosome 1 and the maximum genetic interval containing it determined. Probes from this interval were then used to generate a high-resolution linkage map to determine further the limits of the genomic fragment containing the *Lsh/Ity/Bcg* gene.

Two probes from this interval on both proximal and distal sides of *Lsh/Ity/Bcg* showing no recombination defined a maximum genetic interval of 0.3cM. Pulse field gel electrophoresis (PFGE) of restriction endonuclease digested mouse genomic DNA and fluorescence in-situ hybridisation was then used to produce a physical map spanning a maximum interval of 1.1Mb. The two probes that showed no recombination, and therefore the most tightly linked to the *Lsh/Ity/Bcg* gene, were consequently used to screen a mouse yeast artificial chromosome (YAC) library producing one positive clone and a second was isolated using chromosomal walking. The two YAC clones were then subjected to restriction endonucleases followed by Southern blotting using the markers from the genomic interval containing the *Lsh/Ity/Bcg* gene. This allowed the two clones to be mapped according to the genomic DNA.

A contig. of cosmid and bacteriophage clones for each YAC clone was then produced and ordered. This allowed closer analysis of the DNA with identification of six CpG islands observed through the clustering of enzymes able to recognise and subsequently cut sequences containing CpG dinucleotides. These islands are often associated with, bi-directionally, the 5' end of transcribed genes. Cosmid fragments from clones spanning the six CpG islands were then used for exon trapping, achieved by subcloning the genomic inserts of the cosmids into a vector known as pSPL1 (32) (fig.**1.4.2**).

This mRNA derived from vector has the ability to splice together competent exons, *ex vivo*, producing RNA that can be reverse transcribed to cDNA to allow detection of competent exons by PCR. The exons produced from the genomic DNA using this method, were then subjected to a number of tests. This was done to ensure

Figure 1.4.2

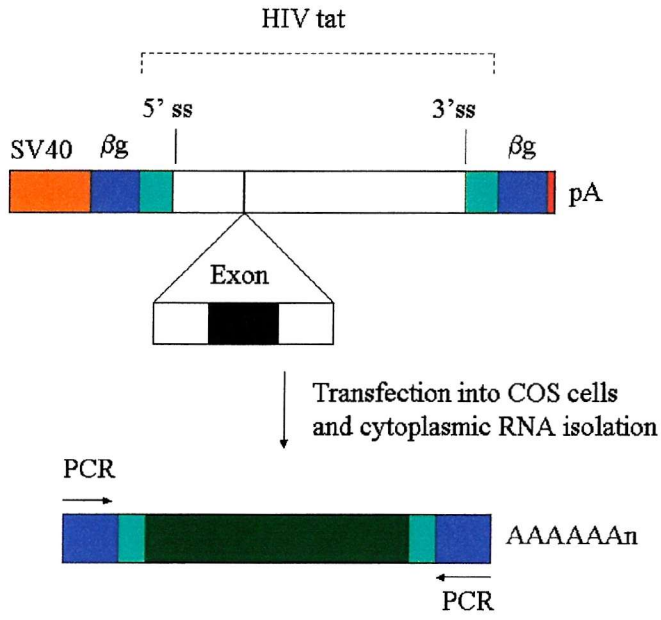

Figure 1.4.2. Diagram showing the characteristics of pSPL1 exon trapping: adapted from Buckler *et al.* [32]. The vector contains an intron from the HIV-1 tat gene with flanking 5' and 3' splice sites (ss). Either side of these splice sites contain sequences from the intron of rabbit β-globin (βg) that are used for RT PCR and PCR amplification after transfection into COS-7 cells and isolation of cytoplasmic RNA. In addition the SV40 early promoter drives expression and there is also a polyadenylation signal (pA) derived from SV40 downstream of the βg sequence. The genomic DNA of interest is inserted into the cloning site and any functional exon will be spliced together with the tat splice sites.

that any exons isolated were from actual genes and not false positives. These included:

1. 'Zoo blots', where genomic DNA from other species is screened for identity to the isolated exons through hybridisation; exons are likely to be conserved between species whereas introns are not.
2. Sequence identity to searches in GenBank and EMBL databases.

3. Northern blots were used to detect groups of exons recognising the same mRNA transcripts and tissue specificity of expression; expression believed to be in macrophages of the reticuloendothelial system.
4. Orphan exons: Any exons not recognising transcripts from Northern blotting were assumed to either be in low abundance or expressed in a tissue specific manner. These exons were used to screen mouse precursor B cell line and rat brain cDNA libraries.

The above searches identified 7 possible candidate transcription units, but only one was consistent with previous studies of the *Lsh/Ity/Bcg* gene. This gene mapped 50kb proximal to Vil, a known gene closely linked to *Lsh/Ity/Bcg*, and was transcribed in the centromere to telomere direction. Northern blotting analysis showed its expression in the reticuloendothelial organs, liver and spleen. Moreover fractionation of spleen cells showed great enrichment of this mRNA in macrophages consistent with previous findings. This gene was correspondingly named natural resistance associated macrophage protein, *Nramp*, but later modified to *Nramp1* upon the identification of a second sequence related gene. More recently the *Nramp* family has been renamed the 'solute carrier family 11' of which *Nramp1* is member 1, abbreviated in its entirety to Slc11a1.

Computer assisted analysis of a 484 amino acid open reading frame for *Nramp1* suggested a structure that resembled and had regions common to the nitrate transporter Crna from *Aspergillus nidulans*. Not unlike Nramp1 it contained ~ 484 amino acids, ~ 10 transmembrane domains and a transport motif between putative membrane domains 6 and 7 (1.5), leading people to believe that *Nramp1* may be a transporter, possibly of nitrate. In 1994 Barton *et al.* (33) demonstrated that Nramp1

actually contained an additional N-terminal 64 amino acids, with a total length of 548 amino acids and manifested through an additional two exons with a more proximal ATG codon. Analysis of this region displayed a sequence rich in proline, serine and basic amino acids having homology to *Drosophila* dynamin, a microtubule motor protein (1.5).

Haplotyping of chromosome 1 polymorphic markers in close vicinity of *Nramp1* was used to screen 27 inbreed strains of mice of both susceptible and resistant background. In addition cDNA sequencing of *Nramp1* from these strains identified 5 polymorphisms 4 of which were silent but one of which was shown to be a substitution likely responsible for susceptibility; a glycine for aspartic acid substitution at amino acid 169 believed to be contained in putative transmembrane domain 4. This was a result of a single guanine to adenine transition at nucleotide 596 (34) and was contained in every susceptible, but not resistant, mouse strain examined. In addition the polymorphisms used in the haplotype mapping showed that infection resistant mice were divergent but susceptible mice contained a conserved core over 2.2Mb overlapping and including *Nramp1*. This suggested that not only was susceptibility caused by a single mutation of 1 ancestral chromosome but also that it occurred recently. Finally divergence of the resistant allele implies it was the allele carried by wildtype mice, as it was present in resistant mice with differing haplotypes over the *Nramp1* region suggesting it is of distant origin.

More recently *Nramp1* was confirmed as the *Lsh/Ity/Bcg* gene when *Nramp1* knockout mice (35), created by homologous recombination, displayed the susceptible phenotype. These mice housed in a barrier facility were viable, healthy and fertile. However when subjected to challenge with *S.typhimurium*, *M.bovis* or *L.donovani* displayed characteristics identical to susceptible homozygous Asp169 mice. This

produced the first direct evidence to suggest the G169A substitution was affecting functional protein formation, but Vidal and colleagues also concluded that removal of *Nramp1* might affect other genes in close vicinity. One worry was that the cellular receptor for interleukin 8, that is in very close proximity to *Nramp1* and is expressed in similar tissues, could be modulated. To this end the group latter produced transgenic *Nramp1* animals on a C57/BL6 (susceptible) background (36), through injection of whole *Nramp1* DNA including 5kb of 5' promoter sequence into male pronuclei. Progress of the transgenic mice was tested through Bcg infection and displayed the resistant phenotype. In addition immunoprecipitation of Nramp1 isolated from peritoneal macrophages cultured in the presence of [^{35}S]-methionine showed the absence of Nramp1 from susceptible mice but the appearance of a 90-100kDa Nramp1 band in resistant mice and transgenic mice of a susceptible background. Transgenic mice appeared to be normal, developed normally and showed fitness and longevity similar to those of non-transgenic littermates.

In 1995 a second *Nramp* gene was reported (37) and subsequently named *Nramp2* (new nomenclature, Slc11a2). Isolation was achieved by low stringency cross-hybridisation to cDNA and the gene was mapped to chromosome 15 between markers D15Mit41 and D15Mit15. Unlike *Nramp1* this gene is expressed at low levels in all tissues tested. Homologous *Nramp1* sequences have been found in diverse phyla from both prokaryotes and eukaryotes. Computer assisted analysis of these sequences has highlighted regions of high conservation (38), permitting putative predictions of Nramp1 secondary structure.

1.5 The *Nramp* Family and Structure

Since the cloning of murine *Nramp1* many homologous *Nramp* genes have been isolated (table **1.5.1**). These have been identified in worms, insects, plants, fish,

bacteria and mammals highlighting the importance of this transporter and an ancient origin.

Table 1.5.1

	Murine Nramp1	Murine Nramp2	*Drosophila* Mvl	*O.sativa* OsNramp1	Yeast SMF1	Yeast SMF2	*M.leprae* Nramp	*C.elegans* Nramp
Murine Nramp1	100	**66.4**	**54.9**	**40.1**	**25.4**	**28.9**	**31**	**55.5**
Murine Nramp2		100	**57.4**	**39.9**	**26.2**	**26**		**55.5**
Drosophila Mvl			100	**36.2**	**29.0**	**29.0**		**58.5**
O.sativa OsNramp1				100	**33.2**	**37.7**		**41**
Yeast SMF1					100	**51.7**	**37**	
Yeast SMF2						100		
M.leprae Nramp							100	
C.elegans Nramp								100

Table 1.5.1. Table showing the homology of Nramp1 like proteins: adapted from M.Cellier *et al.* [38]. Data show the percentage identity between a set of Nramp orthologues. Yeast = *S.cerevisiae*, *Drosophila* = *Drosophila melanogaster*.

Murine *Nramp*1 encodes a polypeptide of 548 amino acids with a predicted molecular weight of 59.7 kDa. Through the use of sequence identity to paralogues and

orthologues and production of hydropathy plots it is believed to contain 10-12 membrane spanning domains and a number of consensus protein motifs (fig.**1.5.3**). Analysis of *Nramp* sequences suggests that the transmembrane domains (TMD) contain the most striking conservation particularly TMD 1-10 (38). The last two domains are either non-essential or confer different characteristics, as they are variable in some bacterial *Nramp* orthologues (39) and missing in Malvolio *Nramp* from *Drosophila melanogaster*.

Figure 1.5.2

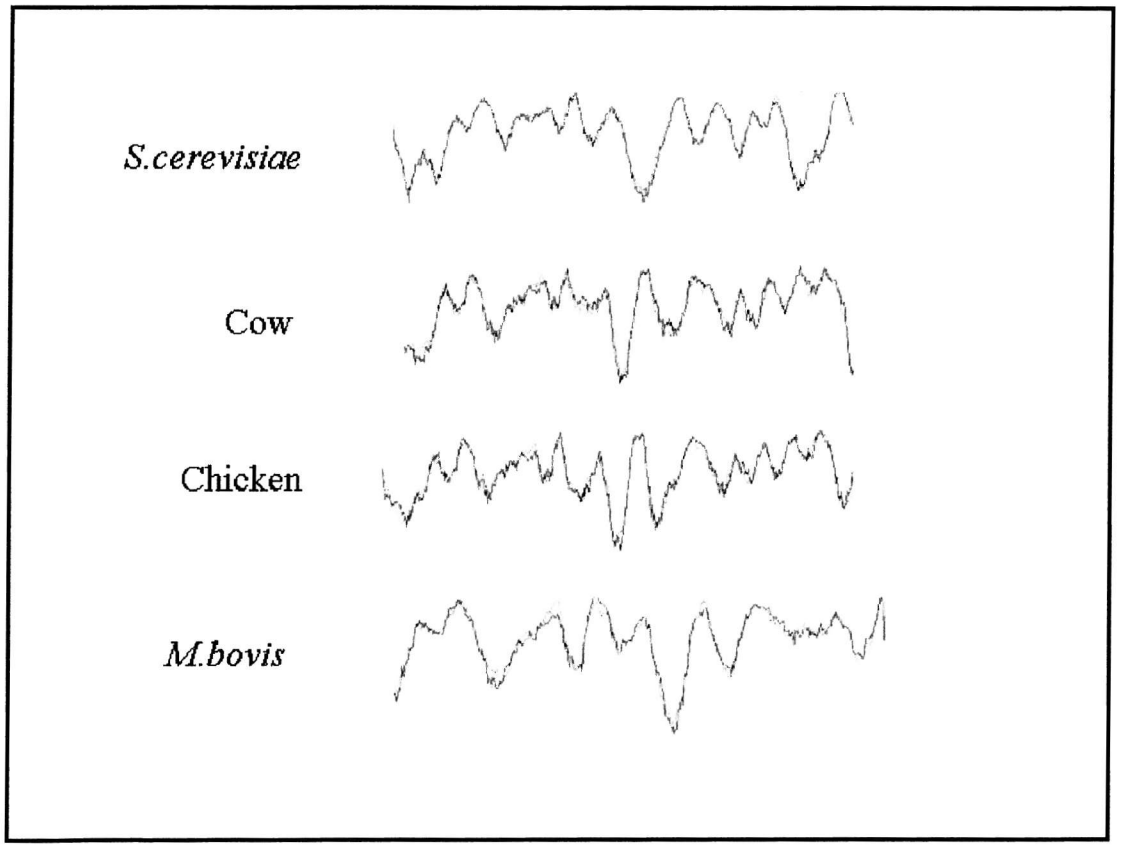

Figure 1.5.2. Aligned hydropathy plots for distantly related Nramp1 sequences. These were produced using the K.Hofmann & W.Stoffel Tm-base.

Figure **1.5.2** displays hydropathy plots using *Nramp* sequences from the organisms shown, it demonstrates the conservation of amino acid residues giving rise to very similar hydropathy profiles across distant species. Topological predictions by Cellier and colleagues (38) using five *Nramp* related sequences positions the N-terminal domain intracytoplasmic and TMD 10-12 with the hydrophilic tail after TMD 10 intracytoplasmic. The N and C terminal domains show little conservation between species suggesting these regions have undergone change to suit the characteristics of the organism.

Motifs found in murine Nramp1 include five protein kinase C (PKC) phosphorylation motifs (S/T-X-R/K) three contained in the N-terminal cytoplasmic tail, positions 3,37 and 51, 1 between TMD 6-7 (position 269) and the last in the C-terminal cytoplasmic tail, position 530. Two N-linked glycosylation motifs (N-X-S/T) at positions 321 and 335 within the highly hydrophilic outer loop between TMD 7 and 8, and a consensus transport motif known as the 'binding-protein dependent transport system inner membrane component signature.' This motif has been described in a range of bacterial transport proteins (31) and more recently, eukaryotic transporters. It is thought to be involved in physical interaction with other proteins or an important protein fold for transporter activity. Indeed an alignment of Nramp1 protein sequences shows that this motif is largely conserved in both prokaryotes and eukaryotes (fig.**1.5.3**). Nramp1 also contains a putative src kinase (sarcome) homology 3 (SH3) binding domain, which consists of a proline, serine and basic rich 64 amino region at the N-terminal portion of the protein. This area itself has 55% identity over 20 residues to Drosophila dynamin, which has also been implicated in binding anionic phospholipids and microtubules in addition to SH3 domains.

Figure 1.5.3

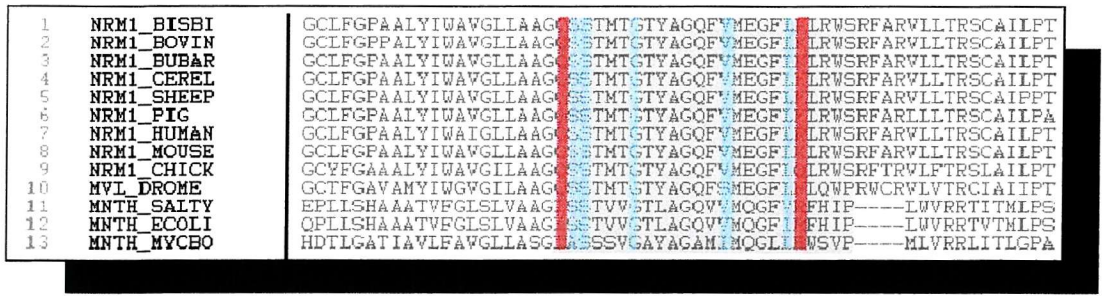

Figure 1.5.3. Nramp family sequence alignments showing the conservation of the bacterial inner membrane transport signature. Sequence alignment using Clustal X; sequences from the swissprot database. The red highlights depict the start and finish of the motif and blue the other essential residues. The motif consists of: (E,Q), (S,T,A)2, 3X, (G), 6X, (L,I,V,M,F,Y,A), 4X, (F,L,I,V), (P,K). Numbers are as follows: **1** American Bison, **2** cow, **3** domestic water buffalo, **4** red deer, **5** sheep, **6** pig, **7** human, **8** mouse, **9** chicken, **10** fruit fly, **11** *S.typhimurium*, **12** *E.coli*, **13** *M.bovis*

Interestingly human NRAMP1 has been shown to bind α and β tubulin (40;41) and it is possible that phosphorylation of this domain could regulate Nramp1 association with the microtubules and control the protein's translocation around the cell. However the identity of the N-terminal domain of Nramp1 and NRAMP1 is less that that of the respective whole sequences compared to one another (83% compared to 88%) suggesting this domain is less critical for activity than others.

Figure **1.5.4** shows the putative positioning of charged residues in the Nramp1 sequence. Many of the membrane charges are highly conserved between species and other bacterial transport proteins with this motif (38) and as a result are likely to be important to its function. Interestingly if topology predictions are correct there will be a potential difference across the protein, the lumenal extension having a net negative charge, as does the membrane partitioned section of the protein, and the cytosolic a

net positive charge. This has been speculated to be important for transport activity and/or necessary for correct membrane insertion (38).

Figure 1.5.4

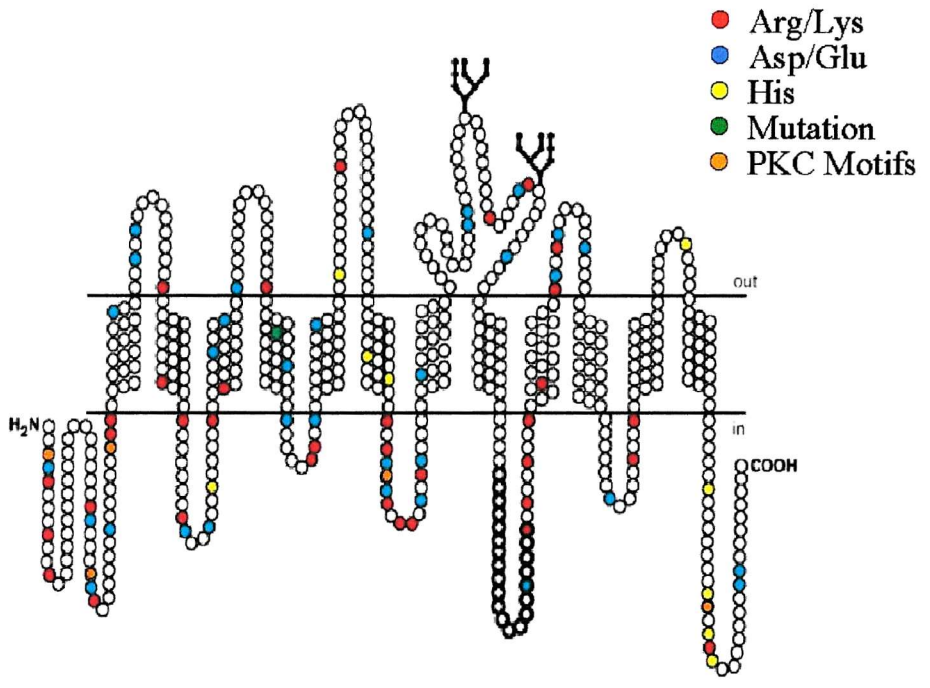

Figure 1.5.4. Diagram of putative Nramp1 structure: Cartoon is a modified version from (42). Branches on the loop between TMD 7 and 8 are possible glycosylation sites. Coloured residues refer to key. Bold circles depict the cytoplasmic transport motif. The protein is believed to contain 12 TMD and is orientated so that the glycosylated side protrudes into the lysosome.

Nramp1 is extensively glycosylated (43) with the protein running on an SDS gel as several distinct/diffuse polypeptide bands (fig.**1.5.5**). The protein has a predicted MW of 59.7kDa but immune precipitation using specific Nramp1 antibodies led to the identification of a diffuse 90-100kDa protein (44); reported to occur with glycosylated proteins and supported by Nramp1's own sensitivity to glycosidase treatment. It is also sensitive to metabolic labelling with orthophosphate suggestive that in all

Nramp1 is a phosphoglycoprotein with approximately 50% of its MW attributable to glycosylation.

In addition to 90-100kDa proteins, studies by Atkinson and Barton (43) also recognised the presence of a smaller and sharper 45kDa protein band. Furthermore treatment of Nramp1 from N11 cell extracts, a microglial cell line derived from a resistant mouse background, with a glycosidase lead to the reconstitution of a 45kDa polypeptide and the disappearance of 90-100kDa Nramp1. The 45kDa polypeptide is believed to be the precursor form of the protein before it becomes glycosylated and the 90-100 kDa, the mature glycosylated protein. As indicated in figure **1.5.4** there is also a 65kDa inducible band. There is convincing evidence that this is Nramp1 (45) but its function is unknown. It may be that the differential glycosylation events lead to changes in Nramp1 trafficking around the cell or affect its function, a phenomenon that has occurred in other proteins (46).

Figure 1.5.5

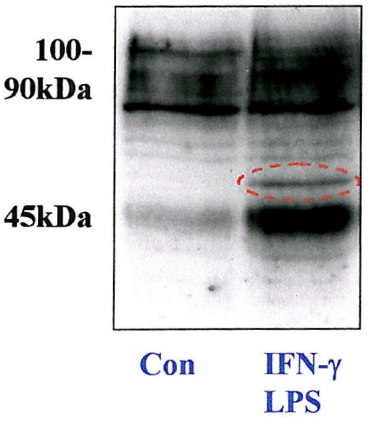

Figure 1.5.5. Characteristic western blot of Nramp1: Cells were treated for 24 hours then harvested for western blotting. 20μg of protein was loaded. Treatments were carried out on primary bone marrow macrophages from CBA mice that carry the resistant *Nramp1* allele. Con = cells grown in normal media, IFN-γ (50 units/ml) plus LPS (100 ng/ml) treated murine macrophages show increased Nramp1 immune reactivity (result from a routine experiment).

The susceptible phenotype in mice is caused by a non-conservative glycine 169 to aspartic acid mutation in putative TMD 4. This change to a highly hydrophilic and bulky residue in a hydrophobic part of the protein is thought to cause incorrect protein folding, which leads to the loss in functional activity (1.4). Mice carrying this mutation still express mRNA but not the 90-100 kDa diffuse polypeptide band. In addition to this the *mk* mouse and belgrade rat *Nramp2* mutation causing anaemia in these animals and the *Lsh/Ity/Bcg* mutation in *Nramp1* occur at adjacent, conserved residues within predicted TMD 4. This lends further evidence to the hypothesis that the *Nramp1* susceptible allele produces non-functional protein. Mislocalisation of susceptible Nramp1 does not occur as studies by Searle and colleagues have localised this protein to the same compartment as resistant Nramp1 (47).

1.6 The *Nramp1* Promoter

The mouse *Nramp1* gene consists of 15 exons spanning 11.5kb and to date 265 residues of the murine promoter region have been published (48). Transcriptional start site mapping using primer extension and S1 nuclease mapping suggests there is more than one site but the major start site occurs 90 nucleotides upstream of the AUG start site. The first and last exons code for 5' and 3' untranslated regions of the *Nramp1* mRNA with the 3' end containing ~ 600 nucleotides. Interestingly 8 of the predicted 12 TM domains are encoded within single exons, and the majority of the transport motif (1.5.2) is also encoded by a single exon (49). Analysis of the areas surrounding the transcriptional start sites suggests that there are no classical TATA or CAAT sites, which are associated with RNA polymerase II transcription in many eukaryotic genes. Identification of two consensus intiator elements –5 and –15 residues upstream of the major transcriptional start site would seem to fulfil this role

however (50). In addition motifs that have been reported to be important in interleukin-8 receptor initiator element expression are present and include a GC-region and Sp1 site overlapping a AP-2 recognition site (51). Among the 265 nucleotides of the *Nramp1* promoter that aaa

Figure 1.6.1

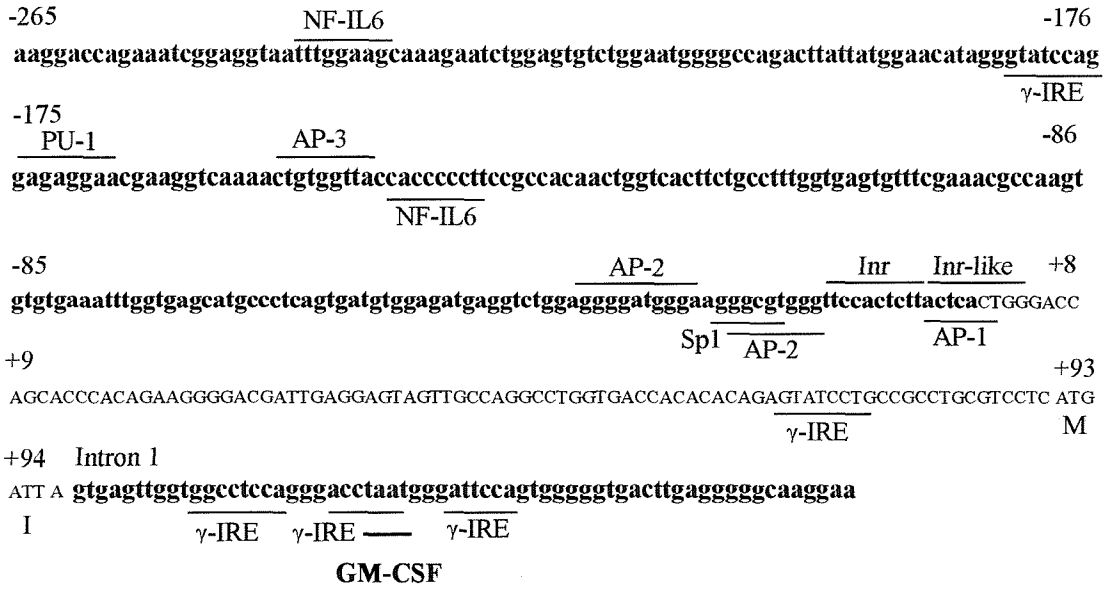

Figure 1.6.1. The Nramp1 promoter region: Sequence is shown up to –265 bp from the major transcriptional start site. Lower case bold letters display the promoter region and then later intron 1. Uppercase letters show exon I. Putative transcription factor recognition sites are underlined, those above the sequence indicating the sense direction (i.e. the sequence shown) those below, the anti-sense direction. Recognition sites for AP-1, AP-2 and AP-3 are also shown and may affect constitutive and/or inducible expression of *Nramp1*. Figure adapted from Wyllie *et al.* (52).

have been sequenced are a number of other potential transcriptional regulatory sites. Of particular interest is a binding site for the PU.1 transcription factor, -175 nucleotides from the major transcriptional start site, these sites have been proposed to be important in macrophage gene expression (53) and are found in other macrophage specific genes including the MCSF receptor (54).

Several studies have provided evidence for the induction of *Nramp1* mRNA by IFN-γ and LPS. This has been shown in macrophage cell lines J774a.1 and RAW264.7 (49), but also in isolated splenic macrophages from both resistant and susceptible mice (55). In accordance with these observations within the currently sequenced promoter lies a number of IFN-γ inducible associated sequences, -183, +70, +118 +127, +128, and LPS (NF-IL6) inducible sequences at positions –144 and –243 immediately upstream from the major transcription start site. Brown *et al* (55) also noted that GM-CSF (granulocyte macrophage colony stimulating factor) could regulate *Nramp1* mRNA expression for which there is a CATTW recognition site in intron 1. GM-CSF like PU.1 is also important for macrophage specific responses.

1.6.1 Disease Susceptibility And Human *NRAMP1*

The human *NRAMP1* gene, located on chromosome 2q35, has a cDNA length of ~ 2 kb and a genomic length of 14 kb, containing 15 exons (56). *NRAMP1* like *Nramp1* is believed to encode a polytopic membrane protein with 10-12 TMD. The overall identity with mouse Nramp1 is 88%, with highest regions of conservation overlapping TMD 1 and 3. As in mouse Nramp1, human NRAMP1 possesses the structural transport motif, an SH3 domain characteristic of signaling proteins, and a total of 5 sites for PKC. In addition, analysis of the 5' promoter region of *NRAMP1* has identified inducible promoter region elements for IFN-γ, suggesting it may be under inflammatory control like murine *Nramp1* (1.6).

There are nine sequence variants in the *NRAMP1* gene (57), of these: three variants are located in introns; one 4-bp deletion in the 3′ UTR (TGTG); and one (microsatellite) in the 5′ region (promoter) of the gene. The remaining four variants

are in the coding region, two are silent substitutions (274 C/T, 823 C/T) and two are missense mutations (A318V, D543N).

Weak linkage has been found using markers for *NRAMP1* to leprosy and TB in Vietnam and Brazilian families, respectively (58). Case-control studies using polymorphisms of *NRAMP1* however, have shown strong linkage to TB in the Gambia. R.Bellamy *et al.*(59) studied TB patients comparing them to healthy controls ethnically matched. They found that subjects heterozygous for two *NRAMP1* polymorphisms in intron 4 (G to C substitution) and the 3' untranslated region of the gene were over-represented. In addition individuals expressing both alleles were four times more likely, compared to other allele combinations, to associate with TB. The fact that these patients can be heterozygous for one of the alleles and be susceptible suggests the susceptible allele is dominant. This is not the case in mice where the resistant allele is dominant. No functional data are available on the action of these alleles although the discrepancy between mice and man may reflect a difference in *NRAMP1* action. Perhaps absolute amounts and total activity of *NRAMP1* are important; this is purely hypothetical however and based on the belief that the above mutations will cause atypical regulation of *NRAMP1* expression. Alternatively it has been suggested that incomplete linkage disequilibrium between the typed polymorphisms and an unknown mutation affecting function may be obscuring the actual pattern of dominance. Lastly it is possible that homozygotes for NRAMP1-variant alleles are underrepresented among adults due to a higher death rate amongst children infected with Mtb. This supports the theory that a spectrum of *NRAMP1* expression coincides with the severity of disease but this has not been observed in mice. In fact severity of infection in *Nramp1* resistant/susceptible heterozygote mice

is the same as that of homozygous resistant during Mtb infection (60). In addition control of Mtb by *Nramp1* seems distinct from that of *NRAMP1 (20)* (1.6.2).

A polymorphism in the promoter of *NRAMP1* encodes a putative Z-DNA forming GT dinucleotide repeat with four alleles: (1) $t(gt)_5ac(gt)_5ac(gt)_{11}g$; (2) $t(gt)_5ac(gt)_5ac(gt)_{10}g$; (3) $t(gt)_5ac(gt)_5ac(gt)_9g$; and (4) $t(gt)_5ac(gt)_9g$. These alleles are interesting, as luciferase reporter assays have shown them to vary the level of promoter activity alone and in response to lipopolysaccharide (LPS) (61). In the absence of exogenous stimuli, alleles 1, 2, and 4 are poor promoters but allele 3 drives high expression. Addition of LPS has no effect on alleles 1 and 4 but causes significant reduction in expression driven by allele 2 and enhances expression driven by allele 3. The study by R.Bellamys group showed linkage to allele 1 and in addition a study in Japan (62) occurring in populations from Tokyo and Osaka showed strong linkage to the promoter alleles 1 and 2 and significant protection, from TB, with allele 3 that drives high expression.

Since the cloning of *NRAMP1* studies have identified it as a possible susceptibility gene in juvenile rheumatoid arthritis and rheumatoid arthritis(63-66). Studies were initiated due to the effect of *Nramp1* on macrophage activation, reports suggesting increased TNFα and MHC II expression upon macrophage activation compared to macrophages from susceptible mice (67). This was relevant as rheumatoid arthritis is associated with an over activation of the immune system with many macrophages infiltrating the synovial membrane. In particular association with allele 3, that causes high-level expression of *NRAMP1*, is causative of susceptibility. This creates the possibility that promoter alleles of *NRAMP1* have been selected for in the population due to a balance between alleles of infection susceptibility and resistance to autoimmune disease and *vice versa*.

1.6.2 TB, the *Nramp1* susceptibility *NRAMP1* resistance conundrum

Although studies have shown that *Nramp1* can control TB susceptibility in mice (68;69) these studies have either used isolated macrophages or less virulent strains of Mtb (Erdman). However studies by Medina and North suggest that *Nramp1* has no role in resistance to the more virulent H37Rv (Human Mtb isolate) (70) which is not the case in humans (60;71;72). The high degree of nucleotide sequence conservation and structural motifs between human and mouse *Nramp1* strongly suggests that the proteins have similar functions. However, several key differences exist: First, all human *NRAMP1* genes sequenced so far have a glycine at position 105 in TMD 2 (73). This suggests that substitutions for glycine in TMD 2 are not tolerated in human *NRAMP1* and also that the mutation(s) causing susceptibility are different in mouse versus human *NRAMP1*; Second, although both human and mouse *Nramp1* are expressed in macrophages (31) (73) there is divergence in the tissue site between the two species. Strong expression of human *NRAMP1* was found in polymorphonuclear leukocytes (neutrophils) and macrophages of the lung (73). The latter finding is very relevant to TB, since the host cell for Mtb is the alveolar macrophage (20). This could be the reason for the difference in murine and human models as very little and no mRNA is detected in murine alveolar macrophages (20) and neutrophils, respectively. If this is not the case then it is unlikely differences are due to protein function due to the high homology between the two, but instead in differences between human and mouse models of TB infection. In light of this it has been suggested that the discrepancy may well be due to use of an unnatural mouse pathogen (H37Rv) (20).

1.7 Localisation Of Nramp1

Nramp1 contains localisation motifs in both its N-terminal and C-terminal domains. These consist of a consensus YXXZ motif (tyrosine motif), where X

corresponds to any residue and Z to a hydrophobic residue. This motif is involved in endosomal targeting (74) and a number of localisation studies have shown that Nramp1 is no exception (47). These studies used antibodies against the protein to show its co-localisation with markers for both lysosomes and late endosomes. It has also been shown that infection with *Leishmania major* leads to movement of Nramp1 to the phagosomes containing them (24). This is good evidence for a direct involvement of Nramp1 mediated bacteriostatic/bactericidal activity, discussed later (1.8.2).

M.avium infection can arrest phagosome maturation (75) in *Nramp1* mutant BALB/c mice. The pH of phagosomes containing live *M.bovis* is significantly more acidic in *Nramp1* resistant macrophages than in Susceptible (76). Collectively this suggests that Nramp1 may overcome pathogen infection by allowing maturation of the vesicles containing them. This could happen via direct attack on the bacteria reducing their inhibitory capabilities, or through increased vesicle fusion and recruitment/activation of bactericidal artillery.

1.8 Function

1.8.1 *Nramp2*

Nramp1 was the first member of the *Nramp* gene family to be cloned and identified, but its biochemical function still remains unclear, unlike its fellow family member *Nramp2*. Most studies to identify the biochemical function(s) of members of the *Nramp* family have focused on Nramp2 that has been easier to clarify. The first evidence that *Nramp1* could function as a divalent-cation transporter transpired from studies using its yeast homologue SMF1 (suppressors of mitochondrial import function), which showed that SMF1 could transport Mn^{2+} (77). Since this original

finding research in to *Nramp1* function has yielded conflicting results, not seen in functional studies of *Nramp2*. By expressing *Nramp2* in *Xenopus laevis* oocyte it was recognized as an important regulator of iron homeostasis and also as a broad range divalent metal ion transporter capable of transporting Fe^{2+}, Mn^{2+}, Zn^{2+}, Co^{2+}, Pb^{2+} and Cd^{2+}, but also that the protein transport activity was pH-dependent (78). These functional studies were used to identify rat mRNA/cDNA that modulates iron uptake in *Xenopus* oocytes in pursuit of proteins important for iron homeostasis, subsequently identifying Nramp2's ability to enhance ^{55}Fe uptake 200-fold. This protein turned out to be that causing anemia in Belgrade rats, a study undertaken separately, and brought about by the identification of *Nramp2* serendipitously as a byproduct of positional cloning for the gene that causes microcytic anemia in *mk* mice (79). Since then, *Nramp2* has been shown to be able to transport Fe^{2+} and Mn^{2+} in yeast and HEK293T cells (77;80). Gunshin and colleagues also claimed to demonstrate evidence proving that *Nramp1* could transport Fe^{2+} in *Xenopus* oocytes, but with less efficiency than *Nramp2* (78). *Nramp2* is expressed ubiquitously in all tissues but in particular the kidney and intestine (81). It is now believed to act at the intestinal brush border leading to apical membrane absorption of Fe^{2+} from the intestinal lumen into enterocytes. From here the iron transits, presumably through the labile iron pool, to the basolateral membrane where it may be transported by ferroportin1 (82) into the plasma. Once across this membrane the ferrous iron needs to be oxidised to its ferric state to allow binding by plasma transferrin. The protein believed to accomplish this is hephaestin, a copper oxidase (83). *Nramp2* is also believed to effect intracellular transport of iron a result of studies on *mk* mice and Belgrade rats. These studies not only identified a problem in iron absorption from the gut but also in the ability of these animals to utilise iron that was directly injected into

the blood stream (84). Consistent with these observations *Nramp2* is expressed on early and late endosomal/lysosomal (85;86) compartments where it is thought to transport iron released from transferrin into the cytoplasm.

1.8.2 *Nramp1*

One of the earlier suggestions proposed involving *Nramp1* in macrophage iron metabolism was that of Kuhn and colleagues (87). The group found lower cellular iron levels in IFN-γ treated resistant macrophages compared to iron levels in macrophages possessing susceptible *Nramp*1. It was also demonstrated that larger amounts of iron were taken up by isolated phagosomes obtained from resistant macrophages, based on these observations they considered that *Nramp1* may transport iron into phagosomes, where, together with a low pH, iron catalysed Fenton/Haber-Weiss reactions produced reactive oxygen species (ROS) to kill invading microorganisms:

$$H_2O_2 + O_2^{\bullet -} \xrightarrow{Fe^{2+}/Fe^{3+}} HO^- + HO^{\cdot} + O_2$$

In the same paper greater levels of intra-phagosomal iron were reported after the addition of this cation *in vitro* to resistant macrophages, less iron being incorporated into susceptible macrophages. Kuhn *et al.* have recently demonstrated that phagosomal uptake of iron induced by *Nramp1* is pH dependent. The investigators explored this using RAW264.7 cells expressing resistant *Nramp1*(88) and found that treatment of macrophages with lysomotropic (concentrating in lysosomes) agents such as chloroquine and ammonium chloride effectively attenuated uptake of iron into phagosomes. The group also found that phagosomal iron content increased in the

presence of cytokines involved in macrophage activation during inflammation, very suggestive of a natural role of iron in bacterial attack.

Zwilling and colleagues, also of which Kuhn is a part, have used isolated macrophages from resistant and susceptible mice to test the effect of iron overload on *M.bovis* infection (89). They demonstrated that resident resistant macrophages could no longer attenuate bacterial growth upon addition of iron. This effect could be reversed if resistant macrophages were previously stimulated with IFN-γ - perhaps due to stimulation of *Nramp1* expression by this cytokine increasing the levels of Nramp1 and therefore the macrophages' ability to withstand greater iron burdens. As susceptible (G169A) Nramp1 is not functional this effect would not be expected to occur in susceptible *Nramp1* allele containing macrophages, and did not. Furthermore ROS radical scavengers were able to abrogate bacterial death in both resistant and susceptible macrophages. Based on this observation the group again suggested that Fe^{2+} was enhancing phagosomal Fenton/Haber-Weiss chemistry resulting in increased *M.bovis* antimicrobial activity in resistant macrophages.

Fleming *et al.* remarked when studying the role of *Nramp2* in the Belgrade rat that *Nramp1*, given its specific expression in cells of a haematopoetic lineage, may be involved in senescent erythrocyte recycling by macrophages (90). Perhaps supportive of this observation our group showed that COS-1 cells ectopically expressing *Nramp1* have reduced cellular iron load compared to controls (43); also consistent with Kuhn and colleagues (87).

Gomes and Appelberg studied the in vivo effects of iron overload upon infection resistance of congenic resistant and susceptible mice (91). They found that feeding mice with iron-dextran, to cause iron overload, abolished the differences in *M.avium* growth in infected organs seen between resistant and susceptible control

mice. They concluded from these observations that Nramp1 antimicrobial function was hindered by excessive iron, and suggested that Nramp1 inhibits microbial growth through the removal of iron from their microenvironment starving them of an essential cation. Chronic iron overload leading to abrogation of *Nramp1* function is consistent with Kuhn and coworkers but the study by Gomes and Appelberg doesn't address the augmentation that small amounts of iron have upon *Nramp1* function.

Interestingly our group has shown that macrophages constitutively expressing resistant *Nramp1* have greater IRP2 (iron response protein 2) binding activity. Such a phenomenon would occur if levels of the labile iron pool were reduced decreasing the rate of IRP2 degradation, an observation directly suggesting that cytoplasmic iron levels are reduced perhaps due to sequestering within an internal vesicle (92).

Recently Jabado *et al.* used resistant peritoneal macrophages to demonstrate a pH-dependent Mn^{2+} transport activity for Nramp1(93). They did this in a novel way by using a divalent cation sensitive fluorophore, fura6, and covalently attaching it to zymosan particles. After phagocytosis of these particles microfluorescence imaging was used to investigate the movement of Mn^{2+} cations across intact and live cell phagosomes. Using this method the group was able to show that Mn^{2+} was removed from phagosomes of resistant macrophages faster than from susceptible counterparts, in addition this process was pH sensitive. This group like Gomes and Appelberg concluded that Nramp1 extrudes essential divalent cations from the phagosomal space reducing bacterial growth.

More recently Goswami *et al.* have studied the transport activity of *Nramp1* within *Xenopus* oocytes, demonstrating that Nramp1 could indeed transport Mn^{2+} but also that this process was bi-directional and affected by pH strongly suggesting that *Nramp1* codes for an anti-porter. As this was the case the group concluded that

Nramp1 was more likely to transport divalent cations from the cytoplasm, high pH to the low pH environment of the vesicle; a process dependent on the pH gradient (94). This result is consistent with the inability of *Nramp1* expression to complement SMF1/2 hypersensitivity phenotypes in yeast (77), whereas Nramp2's symport activity could.

In summary the discrepancies between group observations are not easily accounted for but are likely to reflect the diverse range of experimental conditions employed; no specific standard has been set. It would appear however that *Nramp1* induces transport of divalent cations into phagosomes (the bactericidal hypothesis) but other conditions may lead to their removal (bacteriostatic hypothesis).

1.8.3 PKC Activity and *Nramp1*

Olivier *et al.* have shown that PKC activity is increased in macrophage cell lines from congenic mice with a resistant *Nramp1* background compared to susceptible (95). This was displayed as an increase in basal PKC cytosolic activity and increased membrane translocation upon PMA and *M.avium* treatment. In addition PKC isolated from resistant and susceptible macrophages showed differing sensitivity to diacyglycerol (DAG) activation; resistant macrophages showed a 50% better response to DAG. The resistant *Nramp1* allele can therefore directly/indirectly modify PKC in a way that allows increased activation. PKC activity can be modified in a number of ways (96) although direct activation depends on the presence of DAG and Ca^{2+} second messengers. Recently it has been shown that newly synthesized PKC needs to undergo phosphorylation by PDK-1 on a loop located outside the active site, known as the activation loop (97). PDK-1 activates its substrate kinases by two mechanisms, direct or indirect. For Akt/PKB and the atypical PKCζ, phosphorylation

at the activation loop serves as a direct 'On/Off' switch for catalytic activity. Once phosphorylated by PDK-1, these kinases are directly activated. In contrast, phosphorylation at the activation loop of conventional PKC isozymes does not result in activation but primes PKC for subsequent activation. Specifically, the PDK-1 phosphorylation triggers two C-terminal autophosphorylation reactions required to generate a catalytically competent stable mature PKC. However, this species is maintained in an inactive conformation by its pseudosubstrate sequence (97). Relief of auto-inhibition and subsequent phosphorylation of substrates results from binding its lipid second messenger, DAG, at the membrane. This pathway is unlikely to be involved, as membrane binding of PKC in resistant and susceptible resting macrophages is the same. However, this does not exclude an increase in the activation of atypical PKCs.

Another modification can occur through interaction with oxidative radicals [98-99]. It is thought this transpires through oxidation of the N-terminal regulatory domain of PKC, the mechanism involving the active attack of zinc fingers that are cysteine rich (98). The regulatory domain is involved in DAG and Ca^{2+} binding required for activation (99) but when oxidised these moieties become redundant, PKC activity increasing (98). In fact many groups have identified oxygen and nitrogen radicals as activators of PKC and PKC dependent pathways (100-104).

Lafuse and colleagues have published evidence that PKC is involved in the stabilisation of mRNA in resistant macrophages (105). They originally identified that stability of mRNA from IFN-γ stimulated resistant and susceptible macrophages differed when treated with the immune suppressant corticosterone. Susceptible mRNA stability of a number of genes including *Nramp1* was greatly reduced but seemingly unaffected in resistant macrophages. The genes they assayed included

MHC II, TNF-α and iNOS all of the products of which have been reported as increased in resistant macrophages by other groups (95;106;107). These observations were addressed in a later paper by the Zwilling group illustrating that iron modulates the stability of *Nramp1* mRNA (89) and also that *Nramp1* decreases cellular iron levels. Specifically iron was shown to decrease the stability of *Nramp1* mRNA during IFN-γ stimulation whereas iron chelation increased it. As mentioned (1.8.2) Kuhn and co-workers demonstrated *Nramp1* mediated increases in isolated phagosome iron levels but also showed the involvement of radicals in *Nramp1* anti-microbial mechanisms. This led the group to hypothesise that iron transported into phagosomes is involved in Fenton/Haber-Weiss reactions and production of toxic radicals that actively attack the pathogen. To this end a recent report from the group has shown the involvement of radicals in the stability of *Nramp1* mRNA (105). Here radicals have been shown to be the cause of increased mRNA stability in *M.avium* infected resistant compared to susceptible macrophages. They have also shown that iron chelation decreases mRNA stability in resistant macrophages which is in stark contrast to their previous findings. The explanation for this was gross differences in experimental protocol between the papers. Previously they had stimulated with IFN-γ simultaneously with iron chelation treatment overnight. In the recent study however they activated macrophages overnight with *M.avium* then chelated iron 30 minutes before actinomycin D treatment and assessment of mRNA stability. The reason given involved the chronic effect of iron chelation on other genes whereas recently the investigators looked at an acute effect of the treatment on *Nramp1* mRNA stability.

Lafuse *et al.* investigated the effect of radical inhibitors upon *Nramp1* mRNA stability showing they decreased the stability of *Nramp1* mRNA from infected resistant macrophages to levels seen in susceptible macrophages(108). Interestingly

this paper also showed the involvement of PKC, effects consistent with the PKC activity observed by Olivier *et al.* (above). Specifically the classical PKC inhibitor (PKCα,β,γ), GÖ6976, reduced resistant mRNA stability to levels seen in susceptibles. Menadione, a superoxide generator, also increased resistant *Nramp1* mRNA stability and this effect was blocked by PKC inhibition. Measurement of the activity of particulate PKC demonstrated a time dependent increase above that seen in susceptible macrophages upon *M.avium* and menadione treatment. These results are very similar to those in the Olivier paper two years previously and are consistent with an *Nramp1* effect on PKC. Unfortunately Lafuse and colleagues did not carry out studies on basal PKC activity and mRNA stability. It would have been interesting to see if radicals were involved here also.

Between the Olivier and the Zwilling groups papers however it appears that PKC activity is increased in particulate fractions upon *M.avium*/BCG uptake and that this is perhaps an effect of radicals working via a PKC dependent pathway. The way in which this occurs may be through the classical PKCs α,β and γ (108) and perhaps could be a direct result of increased respiratory burst and iNOS activation seen in resistant macrophages (95;109).

1.8.4 NO and *Nramp1*

The effect of *Nramp1* and the role of nitric oxide in bactericidal activity are complicated. Although it appears that iNos activity is increased in resistant mouse macrophages not everybody concludes that this controls bacterial growth. Liew *et al.* (110) found that resistant macrophages from congenic mice and a number of inbred mouse strains produced more NO and had greater NO synthase activity than their susceptible counterparts. This was seen in response to IFN-γ or TNF-α upon

Leishmania major infection and was also correlated to the increased resistance seen in *Nramp1* resistant macrophages. Arias *et al.* (69) who investigated the effects of NO and resistance saw similar results upon infection of macrophages with the Mtb strain H37Rv. This group identified differences in [^{3}H]-uracil incorporation into Mtb that had been phagocytosed by macrophages from resistant and susceptible mouse strains. Resistant macrophages had an increased capacity to reduce this and also produced more NO. Interestingly IFN-γ treatment of macrophages and subsequent addition of N(G)-monomethyl-L-arginine (N(G)MMA), a nitric oxide synthase inhibitor, abolished the macrophages ability to kill. This is in conflict to the results produced by Brown *et al.* (67) (111) who showed that *M.avium* growth although differentially controlled in resistant/susceptible macrophages, as seen by other groups, was not effected by decreased NO production through the action of corticosterone. This was only the case in resistant macrophages however, as treatment of susceptible macrophages with the glucocorticoid attenuated further their ability to stop *M.avium* growth. Interestingly consistent with a number of groups, including Brown *et al.*, is an increase in iNOS mRNA in resistant macrophages (112). This may be due to changes in mRNA stability (1.8.3). In fact the increased iNOS mRNA found in resistant macrophages could be an affect of iron on the transcription factor NF-IL6 that binds to and activates the iNOS promoter. NF-IL6 is itself up regulated in iron deplete conditions suggested to occur during *Nramp1* expression (1.8.2).

1.9 Aims

The primary aim of this study was to characterise *Nramp1* activity in a non-invasive way. This was achieved by the use of *Nramp1* stably transfected RAW264.7 and L1 3T3 fibroblasts. These cell lines were used in the investigation of *Nramp1* effects on cell iron distribution, analysing a protein regulated by iron and also cellular processes affected by this cation.

Primary bone marrow macrophages isolated from a number of inbred strains of mice, both *Nramp1* resistant^{Gly169} and susceptible^{Asp169}, were used in the study of *Nramp1* mRNA and protein regulation by iron and radicals. In doing this it was hoped that characterisation of *Nramp1* expression would provide insights and support for its function and direction of cation transport.

Finally three putative PKC phosphorylation sites in the N-terminal domain of Nramp1 were mutated. This was done to investigate the possible action of these phosphorylation sites in relation to Nramp1 function and also its localisation in the cell; assays set up for wildtype *Nramp1* and also comparison of localisation between PKC mutant and wildtype fluorescently labelled *Nramp1* in microscopy studies were used.

CHAPTER 2

Materials And Methods

2.1 Materials

2.1.1 Chemicals

Chemicals were purchased from Sigma Chemical Company, Poole,U.K. unless otherwise stated. Cell culture requirements, Penicillin/ Streptomycin, Glutamine, Media etc were obtained from Life Sciences Gibco BRL. Radioactive isotopes were obtained from ICN Biochemicals, Thane U.K. All materials and chemicals were stored and handled as per manufacturers' instructions.

2.1.2 Water

Deionised water for general use was produced by reverse osmosis using a purite R1500 system. Further purification through a purite DC8 deioniser produced ultra high quality (UHQ) water. For RNA manipulation UHQ water was further treated with Diethyl pyrocarbonate (DEPC). DEPC was added to the UHQ water to a concentration of 0.01%, after mixing the water was allowed to stand overnight prior to autoclaving.

2.1.3 Sterilisation

Heat stable materials were sterilised by autoclaving at 15 psi for 15 minutes. Heat labile solutions were sterilised by filtration through a 0.22μm filter (Millipore).

2.1.4 Bacterial culture media

Luria-Bertani (LB) medium

LB broth is an all-purpose bacterial culture medium.

10g NaCl

10g Tryptone

5g Yeast extract

These were dissolved in 1 litre of deionised water and then autoclaved. For solid medium (LB agar) 1.5-% (w/v) purified agar was added prior to autoclaving.

Ampicillin and kanamycin

Ampicillin and kanamycin were added to culture medium to select for bacteria containing plasmids encoding ampicillin or kanamycin resistance. Ampicillin was made as a stock solution of 50mg/ml in water; filter sterilised and stored in aliquots at -20^0C. Kanamycin was made as a stock of 15mg/ml in water; filter sterilised and stored in 1ml aliquots at -20^0C. Unless otherwise stated the working concentration of Ampicillin was 100μg/ml and kanamycin 30μg/ml.

2.1.5 Cell culture medium

RAW 267.4 cell lines and L1 3T3 fibroblasts were cultured in Dulbecco modified Eagles medium (DMEM) containing 10%(v/v) Myoclone foetal calf serum (FCS) 2mM L-Glutamine, 10 units/ml penicillin with 100mg/ml streptomycin and 20mM HEPES buffered saline (tissue culture grade). These cells were cultured on Nunc 75cm^2 flasks and centrifuged in polypropylene Falcon tubes to reduce adhesion of cells to the plastic.

L-929 cells were cultured as above.

2.1.6 Cell Lines and mouse strains

L-929

Morphology: fibroblast-like

Species: mouse, C3H/An male 100 days old; **Tissue**: connective;

Split confluent cultures 1:5 to 1:10 using trypsin; after 2-3 days monolayer is confluent; split 2-3 times a week; seeded out initially at about 1.0-2.0 x 10^6 cells/25 cm^2. ***RAW 264.7***

Morphology: macrophage/mouse monocyte macrophage

Species: Balb/c mouse

Established from ascites of a tumour induced in a male mouse by intraperitoneal injection of Abselon Leukaemia Virus. Confluent cultures were split 1:2 to 1:6 depending on frequency of use . Cells were removed mechanically by scraping.

Receptors: Immunoglobulin and complement products.

L1 3T3

Morphology: Fibroblast

Mouse Swiss NIH embryo contact inhibited

Confluent cultures were split 1:2 to 1:6, depending on frequency of use, with trypsin/EDTA.

Mouse strains

Homozygous resistant *Nramp1*^{gly169}

- CBA
- DBA/2
- MF1
- C3H

Homozygous susceptible *Nramp1*^{Asp169}

- Balb/c
- C57BL6
- DBA/1

Heterozygous *Nramp1*$^{gly169/Asp169}$

- F1 descendants of CBA/C57BL6 cross.

2.1.7 Cell treatments

Details of final concentrations and length of treatment are given in relevant result sections. All solutions were dissolved in serum free DMEM unless otherwise stated.

Ferric ammonium sulphate (FAS): 100mM

Defferoxamine meysolate (DES): 10mM

Sodium nitroprusside (SNP): 100mM

Murine recombinant Interferon γ (IFN-γ) in water : 25 units/ml final concentration

Lipopolysaccharide (LPS): 50ng/ml final concentration

Murine superoxide dismutase (SOD): 10μg/ml

Murine catalase: 100mg/ml

Hemin: 10mM in DMSO

Paraquat: 100mM

SIN-1: 100mM

Bisindolylmaleimide I hydrochloride (Calbiochem): 1mM

Zymosan: 100mg/ml in PBS

2.1.8 Crystal violet stain

This stain was prepared as required. 1g of crystal violet was dissolved in 40mls of methanol. The volume was then made up to 200mls with water and the stain was filtered through 3MM Whattman paper.

2.1.9 SDS Page

SDS page gels were made freshly from stock stacking and resolving buffers.

X2 Stacking Buffer (200mls)

6.04g Tris, pH 6.8

0.2% SDS

X2 Resolving Buffer (200mls)

14.52g Tris, pH 8.8

0.2% SDS

% SDS page gels used (10mls)

Reagent	4%	10%	12%
Stacking Buffer	5 mls	-	-
Resolving Buffer	-	5 mls	5 mls
Protogel 30% Bis acrylamide	1.3 mls	3.3 mls	2.6 mls
Water	3.6 mls	1.6 mls	2.3 mls
10% Ammonium per-sulphate	100 µl	100 µl	100 µl
TEMED	10 µl	10 µl	10 µl

Ultra pure protogel 30% w/v acrylamide, 0.8% w/v bis-acrylamide was from national diagnostics, Hull, England.

Sample loading buffer X2

100mM Tris-HCl (pH 6.8)

20% Glycerol (v/v)

200mM β-mercaptoethanol (v/v)

4% SDS (v/v)

0.2% Bromophenol blue (w/v)

X10 SDS-PAGE running buffer

250mM Tris base

1.92M glycine

1% SDS (w/v)

2.1.10 Western blotting

Western transfer buffer

1 part methanol

4 parts SDS-PAGE running buffer (1x final)

2.1.11 Antibody detection

Antibodies used

Nramp1 antibody was that used in other studies (113) and was directed toward the first 1-82 amino acids of the N-terminal region or an additional antibody raised to the first 54 amino acids of the N-terminal domain.

Murine PKCβI and PKCα antibodies were from SantaCruz.

All primary antibodies were detected using goat anti rabbit antibody.

Phosphate buffered saline (PBS)

Prepared from tablets as per manufacturers instructions

PBS/Tween

0.05% Tween 20 (v/v) in PBS

Blocking agent

10% Milk powder (w/v) in PBS/Tween

Antibody diluent

5% Milk powder (w/v) in PBS/Tween

2.1.12 Plasmid preparation

10-500ml Bacterial Cultures

10ml – Macherey-Nagel nucleospin plasmid kit

250-500ml – Macherey-nagel nucleobond PC 500 kit

Plasmids were isolated as per manufacturers' instructions

Agarose gel

1% electrophoresis grade agarose(w/v)

100mls 1xTBE

10µl Ethidium bromide

X5 TBE (1 litre)

54g Tris

27.5g Boric acid

20mls 0.5M EDTA, pH 8.0

Agarose loading buffer (X6)

0.18% Bromophenol blue (w/v)

0.18% xylene cyanol FF (w/v)

60mM EDTA, pH 8.0

18% Ficoll type 400 (w/v)

2.1.13 Nitrite measurement

Greiss reagent

1% sulphanilamide (w/v)

0.1% N-(1-naphthylethyl)enediamine hydrochloride (w/v)

2.5% orthophosphoric acid (v/v)

2.1.14 Northern blotting

All materials used were soaked overnight in 0.1% SDS and rinsed in 0.01% DEPC treated water prior to use. All solutions were made using DEPC treated water.

Hybridisation Solution

5x SSPE v/v

20X SSC

175.3g NaCl

0.5% SDS w/v

10% Dextran Sulphate w/v

1/100 salmon sperm DNA

88.2g NaCitrate

pH 7.0

MOPS (5X) running buffer

0.1M MOPS (pH 7.0)

40mM Sodium acetate

5mM EDTA (pH 8.0)

20X SSPE (1 litre)

175.3g NaCl

27.6g $NaH_2PO_4.H_2O$

7.4g EDTA

pH 7.4

RNA loading buffer (x2)

50 % glycerol

1mM EDTA (pH 8.0)

0.25% bromophenol blue

0.25% xylene cyanol FF

Washing Solution

1X SSC

0.1% SDS

1% RNA Gel

2.475 g agarose

165 ml water

49.5 ml 5x MOPS

45 ml formaldehyde

2.1.15 Chloramphenicol acetyltransferase (CAT) assay

Running solvent

95% chloroform (v/v)

5% methanol (v/v)

2.1.16 RNA Extraction

RNA Extraction Buffer	*Proteinase Digestion Buffer*
0.14M NaCl	0.2M Tris.Cl (pH 8.0)
1.5mM $MgCl_2$	25mM EDTA (pH 8.0)
10mM Tris.Cl (pH 8.6)	0.3M NaCl
0.5% Nonidet p-40 (NP-40)	2% SDS
1mM dithiothreitol	
20mM Vanadyl ribonucleoside complex	

2.1.17 Nuclear fast red

Dissolve 5 g aluminum sulfate $\{Al_2(SO_4)_3 \cdot 18\ H_2O\}$ to 100 ml distilled water by heating the solution and then add 0.1g nuclear fast red. Then cool down and filter.

2.1.18 Fluorescently tagged fusion proteins

EGFP-Nramp1 – Nramp1, accession number X75355, was cloned from the start codon to the stop codon into pEGFP-N3 (clontech) using EcoRI and BamHI restriction sites added using PCR.

DsRed-Nramp1 – As above but the PCR product was cloned into pDsRed2 (clontech)

EGFP-Nramp2 – Nramp2 was also cloned from its start codon to its stop codon into pEGFP–N3.

2.2 Methods

2.2.1 Cell culture

Cells were passaged or harvested for experiments by removing them from the Plastic with a cell scraper or trypsin (2.1.6), centrifuging at 1000 rpm for 10 minutes

in polypropylene Falcon tubes, resuspending in fresh media for counting and then diluted to the appropriate numbers for the experiment and incubated at 37°C in an atmosphere of 5% CO_2. Counting was done using trypan blue exclusion and a haemocytometer (grid count x10^4 x dilution factor = cell number /ml). Transfected cell lines were selected by the addition of 500μg/ml Geneticin (G418) and passaged in G418 for one week every month.

2.2.2 Isolation and culture of mouse bone marrow macrophages

Femurs were isolated from mice and the bone marrow flushed out using a 1ml syringe containing DMEM. Cells were pooled from multiple animals, resuspended and plated onto triple vent bacterial petri-dishes (Greiner) and grown in culture medium (2.1.5) in the presence of 10% L-cell conditioned media (the media from which L-929 cells have been grown) that contains granulocyte colony stimulating factor (GM-CSF); in addition to serum (2.1.5) etc. After incubation for 5 days an additional 10% v/v of L-cell soup was added. Precursor cells were allowed to mature and differentiate for a further 4 days at which point any cells left floating were washed off using pre-warmed serum free DMEM. Adherent cells were used as macrophages and shown to express macrophage antigens Nramp1 and iNOS and were phagocytic. Cells were used in experiments after 2 days rest.

2.2.3 Transfection of cell lines

Calcium phosphate transfection of L1 3T3 fibroblasts

1. Fibroblasts were plated out to a density of 0.5 x 10^6 cells/90mm tissue culture dish in culture medium (2.1.5) and incubated overnight at 37°C in an atmosphere of 5% CO_2.

2. The following morning the medium covering the cells was replaced with 5ml DMEM pre-warmed to room temperature and the plates then kept in the incubator for 3-4h.

3. DNA to be used for transfection was precipitated from alcohol but then allowed to dry in a tissue culture cabinet before being resuspended in the appropriate volume of sterile water to a final concentration of 1μg/μl. Aliquots of DNA were stored at –20°C.

4. For each transfection 2 microcentrifuge tubes were labelled A and B. 250μl of 2x HBS (HEPES buffered saline) was added to tube B. Into eppendorf A 31μl 2M $CaCl_2$ was added and the appropriate volume of DNA this was then made up to 250μl by the addition of sterile water. The contents of tube A was added to tube B dropwise without mixing and incubated at room temperature for 10-15 minutes to allow a fine precipitate to form.

5. The 500μl of the $CaPO_4$ precipitated DNA was added to the 5ml of medium covering the cells, drop wise. The cells were incubated at 37°C for 4h.

6. After 4h the medium from the cells was removed and the cells washed once with 5ml PBS before the addition of 6ml of pre-warmed culture medium (2.1.5).

Electroporation of RAW 264.7 cells and L1 3T3 fibroblasts

RAW cells were harvested and counted as in 2.2.1, and resuspended to a concentration of $1x10^7$ cells/ml. 0.5ml of this was transferred to a Bio-Rad gene pulser cuvette, 0.4cm gap between electrodes, and 10μg of DNA added. The cells were allowed to stand for 5 minutes before electroporating at 950μF, 350v using a Bio-RAD capacitance extender plus and gene pulser II. Cells were then resuspended in 12 ml of culture medium (2.1.5) and transferred to a $75cm^2$ flask.

Fibroblasts were treated as above but resuspended to a concentration of $1x10^6$ cells/ml and electroporated at 450μF and 500v.

2.2.4 Culture of stable transfectants

Two days after transfection (2.2.3) 500μg/ml G418 was added. Cells were then cultured in the presence of G418 for the duration of cloning and selection. Once it was clear clones were growing, cells were harvested counted and serial dilutions were made onto 96 well plates, 200μl culture medium/well. Cells were plated to 1,5 and 10 cells/well on three 96 well plates respectively. These cells were allowed to grow for ~ 2 weeks at which point wells containing cells were harvested and transferred to $25cm^2$ flasks. Clones were tested for expression by, from a single clone, western blotting.

2.2.5 Protocols for cell growth measurement

Cells were counted in triplicate using a haemocytometer (grid count $x10^4$ x dilution factor = cell number /ml) and trypan blue exclusion as a measure of cell viability. The cells were added to a 96 well plate in 200μl of media, using $100x10^3$ cells in row 1, $50x10^3$ cells in row 2, 10 $x10^3$ in row3, 5 $x10^3$ in row 4 and 1 $x10^3$ in row 5, row 6 contained 200μl of media only. This plate was used to produce a standard curve. $1x10^3$ cells in 200μl media were placed in the remaining wells for tests one plate was used per day of culture. Readings were made by emptying the media from the plates and gently tapping onto a paper towel before adding 200μl of crystal violet stain per well. The plates were incubated at room temperature for 10 minutes, the stain decanted, and then they were washed in three changes of water and dried. The absorbed stain was resolubilised in 200μl methanol. The plates were agitated carefully; each plate was read on a MRX microplate reader (Dynex) at 570nm. A standard curve was plotted from the

known cell number against OD_{570nm}. Sample cell numbers were obtained by reference to this standard curve. 12 wells were routinely used per cell line and treatment and averages taken from the mean of these results.

[^{3}H]- thymidine uptake

Cells were plated out to a density of 25 x 10^3 /well in triplicate in a 96 well plate with 200µl of media/well. These cells were left overnight or treated with ferric ammonium sulphate where indicated. The following morning [methyl-^{3}H] thymidine (ICN) incorporation was allowed to occur for four hours (1µCi/well) before cells were washed three times using PBS and harvested. This was done by scraping the wells twice with 100µl of 0.1% SDS PBS and adding this to 3mls of Optiphase 'Hisafe' 3 liquid scintillation cocktail (Wallac). Incorporation of ^{3}H-thymidine was measured using a Beckman 6500 multipurpose scintillation counter. Readings were averaged according to cell number controls (above) and statistical analysis carried out.

2.2.6 Plasmid preparation

Unless otherwise stated all plasmids were maintained in JM109 cells frozen at –70°C in 25% glycerol in LB broth. Cultures from frozen stocks were streaked out onto LB plates containing 100µg/ml ampicillin or 30µg/ml kanamycin and cultured overnight at 37°C. A single colony was picked from this culture and inoculated into a 250ml conical flask containing LB medium with selecting antibiotic and cultured with agitation at 37^{0}C overnight. At this point plasmids were extracted using a nucleobond PC 500 kit (Macherey-Nagel). The optical density of the preparation was determined at 260nm and 280 nm from a diluted sample. Diagnostic digestions were used to confirm the identity, integrity and purity of the plasmid. 1µg of the plasmid was made up to 8µl with water

1µl of the appropriate 10X enzyme buffer and 1µl of enzyme were added and incubated for 1 hour at 37°C. 2µl of agarose gel buffer was added and the reaction mixture was separated according to size by electrophoresis in an agarose gel at 100v constant current for 1 hour in the presence of 1x TBE. If needed the plasmid was reprecipitated and resuspended to 1µg/µl using sterile water in cell culture conditions then stored at -20 °C prior to use.

2.2.7 Isolation of insert or vector DNA

Isolation of cut plasmid DNA was done using gel extraction. After pilot digests (10µl volumes) the DNA (2.2.6) digestions were scaled up to 100µl to allow sufficient quantities of DNA to be prepared for cloning purposes. At this point the cut DNA was run in an agarose gel (2.2.6) and the appropriate DNA band removed by excision using a razor blade. DNA was then purified using a Macherey-nagel nucleospin extract kit.

2.2.8 Transformation of competent *E. coli*

For transformation JM109 cells were bought in from Promega and cells transformed as per manufacturers' instructions.

2.2.9 Protein estimation

Unlysed eukaryotic cells, following washing to remove serum proteins, were resuspended in 100-400µl PBS. 3µl of the cell suspension was removed and added to 100µl of PBS (phosphate buffered saline) containing 0.1% SDS in a 96 well plate. This was repeated in triplicate for each sample. A standard curve was prepared with a range of BSA concentrations between 0 and 20µg, each standard was added to 100µl 0.1% SDS PBS. Protein estimation was achieved using the micro BSA protein assay reagent

kit (Pierce). Samples were treated according to the manufacturers' instructions. The absorbance at 562nm was measured using a Dynex MRX microplate reader. The standards were used to prepare a standard curve and the protein contents of samples were estimated by reference to this curve.

2.2.10 SDS-PAGE

SDS-PAGE fractionates polypeptide-SDS complexes by electrophoretic molecular sieving in polyacrylamide gels according to molecular size assuming a linear non-structured conformation. Boiling in SDS and β-mercaptoethanol, which disrupts secondary and tertiary structures and also inter- and intra-chain disulphide bonds respectively, denatures the proteins. The resulting polypeptide chains have approximately equal charge to mass ratios and are separated solely on the basis of molecular size

All glass plates and spacers (1.5mm) were cleaned and degreased with absolute ethanol. The apparatus was assembled according to the manufacturers' instructions (Bio-Rad). SDS-PAGE was performed using the discontinuous buffer system method of Laemmli (1970), with 10% separating and 4% stacking acrylamide gels, unless otherwise stated.

All buffers and solutions were prepared using deionised water. Polymerisation of acrylamide to form gels was catalysed by free radicals from N,N,N'N'-tetra-methylenediamine (TEMED) generated by the action of the initiator ammonium persulphate (APS). The 10% separating gel and 4% stacking gel mixes were prepared as described (2.1.9) The 10% separating gel was poured and allowed to polymerise allowing room for the 4% stacking gel to be poured on top. The stacking gel was poured and the well-forming comb carefully inserted and the gel allowed to polymerise.

The required volume of 1x running buffer was diluted in water immediately prior to use. Once the acrylamide within the 4% stacking gel had polymerised the comb was removed. Both outer and inner reservoirs were filled with x1 running buffer. Air bubbles that had formed within the sample wells were removed and the samples were carefully layered within the wells. Samples were in SDS sample buffer at 2mg protein/ml, and were passed repeatedly through a syringe (25GA5/8 needle), to shear DNA. This was done to avoid aggregation of Nramp1 protein as it is highly hydrophobic and heating can cause this (114), 10-15µl /track was loaded. Electrophoresis was carried out at 35mA constant current per gel.

2.2.11 Western blotting

After SDS PAGE the glass plates were separated, small plate down most and the stacking gel was cut away. The gel was soaked in blotting buffer until needed. A piece of Immobilon-P membrane the same size as the gel was cut and soaked in blotting buffer. 6 pieces of Whatman paper (6 x 10 cm) were cut and moistened in transfer buffer and 3 stacked on the dry graphite electrode of the semi-dry blotter (Bio-rad) and the membrane placed on top of the Whatman paper. The gel was placed on the membrane, 3 pieces of Whatman paper were stacked on top and the assembled stack rolled with a glass pipette to remove air bubbles and excess buffer. Paper towel was used to dry the electrode. The assembled blot was run for 1-hour 100mA/membrane constant current.

Antibody detection

The following procedure is for western blotting of Nramp1 protein. Detection of specific proteins on Western blots was by immune detection using specific antibodies. Post transfer the blot was incubated in blocking agent at room

temperature for 60 minutes. The blot was then incubated in primary antibody for 1-hour 1:1000 dilution in antibody diluent with agitation at room temperature. It was then washed for 5 minutes x3 in PBS/Tween. Following this the blot was incubated 1:10,000 (in antibody diluent) in horseradish peroxidase (HRP) conjugated goat anti-rabbit secondary antibody for 45 minutes. The blot was then washed x3 in PBS/Tween and once in water prior to detection using enhanced chemiluminescence (ECL) reagent (Amersham) as per manufacturers' instructions.

Detection of mouse PKCβ1 and PKCα was identical but samples were boiled for 5 minutes before gel loading and primary antibody (Santa-Cruz) was diluted 1:500 in antibody diluent.

2.2.12 Chloramphenicol acetyltransferase (CAT) assay

Cell extracts were prepared by harvesting cells, washing x2 in PBS then resuspending the pellet in 50μl 0.25M Tris (pH 7.8). The cells were lysed by freezing in liquid nitrogen for 2 mins thawing at 37°C for 2 mins for a total of 3 times. The resulting lysate was heated to 65 °C for 5 mins to inactivate proteins less stable than CAT, which interfere with the assay. After pulsing in a microfuge the supernatant was removed to a clean eppendorf tube and a sample removed for protein estimation to allow normalisation for CAT determination. For each sample 10μg of protein was placed in an eppendorf and the volume made up to 25μl with 0.25M TRIS (pH 7.8). A master mix was made for all samples of; 20μl of 4mM Acetyl CoA, 1μl ^{14}C Chloramphenicol, 70μl 1M Tris pH 7.8 and 91μl of this master mix added to each sample and incubated at 37 for 1 hour. The tubes were then pulsed in a microfuge and 500μl ethyl acetate added then vortexed for 30 seconds and centrifuged for 2 minutes at 13000 RPM to allow separation of the two phases. The ethyl acetate (top layer) containing the

Chloramphenicol and acetylated derivatives were removed to a clean labelled microfuge tubes. The ethyl acetate was evaporated in a Speedi-vac on a low drying rate for about 20 mins. Each sample was resuspended in 15µl ethyl acetate and spotted onto a thin layer chromatography (TLC) plate, 1cm apart and 1cm above the base, drying between applications to keep the sample loading area small. When loading was completed the plate was dried and carefully placed in TLC tank containing running solvent just sufficient to touch the bottom of the TLC plate. The samples were allowed to run until the solvent front had reached the top of the plate. The plate was then, removed, air dried and exposed to film in an autoradiography cassette at room temperature, using the 1st exposure to estimate optimum exposure. Percentage conversion was calculated through exposing a phosphoimager screen (Molecular dynamics) and calculating emissions as per manufacturers' instructions.

2.2.13 Northern blotting

Total mRNA Extraction

Macrophages were washed twice using cold PBS before being removed from plates using a policemen. Cells were then pelleted at 3000 rpm for 5 minutes at which point the PBS was removed by aspiration and the pellets resuspended in 200µl of RNA extraction buffer (2.1.16). Vandyl ribonucleotide complex and DTT were added just before use. Extracts were incubated on ice for 5 minutes before being pelleted at 12000 rpm at 4^0C for 2 minutes. The supernatant was then removed and added to 200µl of proteinase digestion buffer containing freshly added proteinase K (200µg/ml). Samples were then incubated for 2 hours at 37^0C before protein was extracted using phenol: chloroform and mRNA ethanol precipitated in three volumes of ice-cold ethanol. Phenol, chloroform and ethanol used for mRNA extraction were separated from that

used for DNA. mRNA pellets were resuspended in DEPC treated water and mRNA concentrations measured using a spectrophotometer at 260nm.

Blotting

3μg of each sample in an equal volume of RNA sample buffer was loaded. The RNA was subsequently fractionated by electrophoresis in a 1% RNA agarose gel in 1X MOPS buffer for 3 hours at 100 volts. The gel was removed and the RNA transferred to nitro-cellulose (Hybond-N) by capillary elution with 10mM NaOH. The blot was dried at 60°C for 1 hour. The cDNA probe for hybridisation was prepared using a prime-a-gene labelling system (Promega). 100-200ng cDNA (1-2μl vol.) were used. After 1 hour of incubation the reaction was stopped by addition of: 10μl 0.5M EDTA (pH 8.0), 10μl 10% SDS and 70μl water. The labelled probe was separated from unincorporated nucleotides by passage through a sephadex G50 column and then denatured by boiling for 5 minutes in the presence of 100μl salmon sperm DNA. The blot was pre-hybridised at 65°C for 30 minutes in hybridisation buffer prior to addition of 100μl of the labelled probe. The blot was then incubated overnight at 65 °C and washed X2 in washing buffer for 20 minutes and then 10 minutes. The blot was wrapped in cling film and exposed to film in an autoradiography cassette at -70 °C with an intensifying screen. Alternatively the membrane was incubated with a phosphoimager screen and bands quantitated using the STORM phospho-imager system.

2.2.14 Measurement of nitric oxide production

Nitric oxide production was determined by measuring the accumulation of nitrite, the stable end product of nitric oxide. Supernatants from 48-hour cultures of cells were removed and 100μl of supernatant mixed with 100μl of Griess reagent in a microtitre plate. Standards were prepared using 0-200μM sodium nitrite. After 15

minutes incubation at room temperature, the absorbances were read at 570nm on a plate reader (MRX) and the test values calculated with reference to the standard curve prepared using the (0-200μM) sodium nitrite standards.

2.2.15 Quantification

The strength of signal on autoradiographs produced after Western Blot analysis was measured using the Phoretix software from Non-Linear Dynamics LTD. UK.

2.2.16 Oligo Annealing

Equal concentrations of oligos were heated to 100°C for two minutes, allowed to cool to 65°C, and left at this temperature overnight. The annealed oligos were then run out on a 1.5% agarose gel containing 0.01% ethidium bromide and excised under a UV light. Following this the oligos were electroeluted using viscing tubing, phenol:chloroform extracted and precipitated with one volume of isopropanol and 10% 3M Na Acetate pH 5.2 before being resuspended in 15μl of water.

2.2.17 Prussian blue

This method detects the ferric iron loosely bound to protein complexes; ferric iron in the presence of an acidic potassium ferrocyanide solution forms an insoluble bright blue pigment.

Slides were washed twice with PBS before being placed in a mixture of 25ml of 2% hydrochloric acid and 25ml of 2% potassium ferrocyanide combined immediately before use. This was left for 10 minutes before slides were washed with PBS. Nuclei and membranes were counterstained with nuclear fast red for 5 minutes (2.2.18).

2.2.18 Nuclear fast red staining

Stains nuclei red and background stains membranes pink.

1. The cells were fixed in 75% ethanol for 30 seconds at +4°C.
2. They were washed twice with ice-cold PBS.
3. Stained with nuclear fast red for 30-60seconds.
4. Rinsed in PBS.
5. Dehydrated
    a. 70% ethanol for 30sec.
    b. 95% ethanol for 30sec.
    c. 100% ethanol for 30sec.
6. Xylene diped for 30 secs.
7. Second xylene diped for 30 secs.
8. Air-dryed for at least 20 minutes.

2.2.19 PNGaseF treatment of cell extracts

PNGaseF (New England Biolabs) was used as per manufacturers guidelines using 20μg of total protein extract.

The following inhibitors were added to make a new denaturing buffer, which was used as above, to reduce protease digestion:

- 2mM DTT
- 1mM PMSF
- 100μl of α-aprotinin to 10mls of denaturing buffer
- 1% β-mercaptoethanol
- 0.5% SDS

Membrane extraction

Cells were harvested and pelleted in a centrifuge at 1200 RPM for 10 minutes in a 50ml falcon tube. The media was aspirated off and the pellet resuspended in 5 ml of homogenisation buffer (10mM Tris-HCL, pH 7.4, 1mM EDTA containing 100x dilution of 1mg/ml leupeptin, 100x dilution of α-aprotinin, 200μM PMSF, made just before use). This suspension was then passed up/down a 10ml syringe fitted with a large bore needle 20 times, but kept on ice. The samples were subsequently spun in 50ml Oakridge tubes in a pre-cooled centrifuge for 20 minutes at 12000 xg. The supernatant was removed and spun in 13ml Oakridge tubes in a 70.i Ti rotor in a Beckman centrifuge at 50000xg for 30 minutes. The supernatant was aspirated off and the pellets resuspended in 100μl of TNE (10mM Tris-HCL pH7.4, 150mM NaCl, 1mM EDTA). This suspension was then tested for protein concentration before use.

2.2.20 Cell staining and preparation

Cells were allowed to grow on glass cover slips before being washed x2 in PBS and then fixed in 4% paraformaldehyde in PBS for 20 minutes. This was followed by x2 washes with PBS and quenched with 100mM glycine in PBS for 30 minutes, before x2 washes in PBS. The cells were then post-fixed in methanol for 30 minutes before washing/permeablised in 0.05% Nonidet in PBS. Cells were subsequently blocked in 10% normal goat serum for 1 hour, 1 in 200 dilution, followed by 2 hours incubation in an affinity purified rabbit polyclonal C-terminal Nramp1 antibody (1/200 dilution) (45). These cells were then washed x2 using 0.05% Nonidet in PBS before being incubated with a 1 in 200 dilution of Alexa Fluor 488 goat anti-rabbit IgG (Molecular probes) for 1 hour.

Cells were visualised using a Zeiss Axioplan 2 digital microscope and Zeiss AttoArc HBO 100W epifluorescence unit. Pictures were analysed using metamorph 2 imaging software.

2.2.21 Confocal microscopy

Cells were transfected using electroporation as in 2.2.3. 80 µl from the electroporation was then added to Falcon 35 x 10 mm polystyrene tissue culture dishes in a total of 2mls of DMEM plus serum. These cells were grown for 24-48 hrs before being washed x3 using DMEM/F-12 without phenol red, but containing 10%(v/v) Myoclone foetal calf serum (FCS) 2mM L-Glutamine, 10 units/ml penicillin with 100mg/ml streptomycin and 20mM HEPES buffered saline (tissue culture grade). 2mls of this media was then added to the cells before being used for confocal microscopy. Cells were warmed using a heated stand and maintained in an atmosphere of 5% CO_2 during microscopy. Media was constantly circulated using a Gilson minipulse 3 pump system at a setting of 5.

Imaging was performed on a Bio-Rad MRC-1024ES confocal scanning laser microscope system using a krypton/ argon laser and LaserSharp version 3.2 software (Bio-Rad). 605DF32, 522DF32 band pass filters were used for photomultiplier tubes 1 and 2, respectively. Laser power was set to 30% on all lines 488 (EGFP), 568 (DsRed, LysoTracker and TRITC–transferrin). All cells were imaged using a x63/1.4NA PlanApo objective. Photomultiplier tube 3 was used for transmission imaging. All other settings are as in the text. Images were analysed using metamorph 2 imaging software and annotated using Corel photo-impact software.

2.2.22 Primers and PCR

PCR

50µl reaction mixture total volume.

H_2O	-	41.1µl
10x pfu buffer	-	x1 final (5µl)
dNTPs	-	25nm Final (0.4µl)
p-nut DNA template	-	0.25µg
GFP muts	-	125ng
GFP CHAS	-	125ng
Pfu polymerase	-	0.5 µl added after initial strand separation and annealing

Conditions:

94°C	-	5 min	30 cycles of:		
54°C	-	1 min	94°C	-	1 min
	-	add enzyme	50°C	-	1 min
68°C	-	2 min	68°C	-	2 min

Statistical analysis

All statistical analysis was carried out using Student's T-test with minimal confidence intervals of $p<0.05$.

Chapter 3

Regulation Of *Nramp1* Expression

3.1 Introduction

The way that gene products are regulated is related to their function in the cell and can occur at transcription, post-transcription, translation or post-translational levels. mRNAs encoding proteins involved in iron homeostasis often have characteristic stem loop structures known as the iron response element (IRE) in their 5' or 3' untranslated regions. The most well characterised genes undergoing this kind of post-transcriptional modification are the mRNAs encoding ferritin and the transferrin receptor. Other mRNAs containing IREs include: IREG1; Nramp2 splice variant and erythrocyte 5-aminolevulinate synthase (eALAS), these proteins are involved in iron export, import and production of haem, respectively(115). Regulation of these gene products by iron regulating proteins IRP 1/2 is naturally related to their role in iron homeostasis, but IREs have also been found in mammalian mitochondrial aconitase enzyme mRNAs (115) that do not directly regulate iron levels but link cellular energy requirements with this.

Ferritin is essential for storage of iron and consists of two polypeptides, H and L, or heavy and light ferritin chains. The proportion of these chains in the ferritin molecule dictates its ability to store iron through rate and duration of storage. H ferritin contains ferroxidase activity and allows faster storage of iron, but L-ferritin, although incorporating iron more slowly holds onto it longer (115). The relative proportions of these polypeptides in the ferritin molecule are believed to affect a cell's

ability to store iron. Both H and L-ferritin mRNAs contain 5' IRE elements that bind iron response proteins one and/or two (IRP1 and IRP2). These proteins are essential to iron regulation and react to cellular iron levels through assembly or disassembly of an iron sulphur cluster (4Fe-4S) within IRP1 or through protein stability, reliant on oxidation and ubiquitation for IRP2 (116). Both proteins respond to iron excess through decreased mRNA binding activity and iron depletion through increased mRNA binding. Binding of IRPs to the 5' end of ferritin mRNAs blocks their translation through steric inhibition of the 43S preinitiation complex (117).

Unlike ferritin, the transferrin receptor mRNA contains five IREs in its 3' untranslated region. Transferrin is essential for intercellular iron transport and binds to the cell surface by the transferrin receptor and by receptor mediated endocytosis is internalised. The endosome thus formed is acidified leading to release of iron from the transferrin and the apo-transferrin transferrin receptor complex is released to the cell exterior through transferrin receptor recycling. Iron released from transferrin is subsequently 'pumped' into the cytoplasm by Nramp2 (1.8.1), a protein divalent cation symporter. The transferrin receptor therefore controls the levels of iron entering the cell, dependent upon IRP1/2 IRE binding activity. In iron excess IRP fails to bind to the transferrin receptor mRNA, resulting in its rapid breakdown. This is believed to be the result of endonucleolytic cleavage at a site known as the rapid turnover determinant (115). So two major protein determinants of iron regulation within the cell are regulated by their own substrate. The way in which these two proteins are regulated also reflects the action they have on cellular iron. Ferritin is increased during iron replete conditions and the transferrin receptor decreased reducing iron induced toxicity. These two events regulate levels of iron within the labile iron pool, the pool of iron sensed by IRPs. In iron deplete conditions transferrin

receptor expression is up regulated and ferritin down regulated reflecting the cells need for more iron. This process brings about homeostatic control of iron levels.

Nramp2 also contains a putative IRE in its 3' untranslated mRNA depending on the splice variant. In addition, *Nramp2* expression is up regulated by iron during iron deficiency in mice (118). This is another example of regulation reflecting protein function, Nramp2 being required at the intestinal brush border to increase iron uptake during deficiency. No such classical IRE exists within *Nramp1*, but data do suggest *Nramp1* is regulated by iron through mRNA stabilisation (89;105). Results show *Nramp1* mRNA from susceptible^{Asp169} (S) macrophages had a shorter half-life compared to resistant^{Gly169} (R) macrophage *Nramp1*. This difference could be reversed with desferoxamine. They also showed that addition of iron to the medium decreased *Nramp1* mRNA stability in both R and S macrophages; the effect more pronounced in S macrophages. Lastly, resting macrophages showed differences in the average half-life of mRNA, R macrophages again much more stable. The group concluded that Nramp1 must be involved in cellular iron distribution with iron being transported by Nramp1 into intracellular vesicles (89), demonstrated by increased radioactive iron uptake into isolated phagosomes of R macrophages (87). Recently data suggest it is the action of radicals and PKC that cause the increased stability of *Nramp1* mRNA in R macrophages(108). The increased oxidants in activated *Nramp1* R macrophages presumably being those from increased respiratory burst and NO production that are associated with this allele (109;119). These results necessitate that *Nramp1* mRNA is controlled negatively by iron, but positively by radicals. This is interesting, as iron excess could catalyse radical production by Fenton chemistry. *Vice versa* addition of both superoxide and nitric oxide, induced during macrophage activation and moieties that can potentially interact with IRP1 increasing its binding

activity, could increase the labile iron pool through decreased storage and increased uptake of this cation(115). In view of these results however it would appear that both iron and radicals could act independently on *Nramp1* mRNA stabilisation.

The aim of the following work was to characterise semi quantitatively changes in Nramp1 protein expression under varying conditions of iron and oxidative stress treatments. This was done in a number of inbred mouse strains from both resistant and susceptible *Nramp1* backgrounds. In addition, amounts of *Nramp1* mRNA were evaluated. Finally, characterisation of Nramp1 expression would provide insights and support for its function and direction of cation transport.

3.2 Results

3.2.1 The Characterisation Of Nramp1 Antibodies

To investigate factors regulating Nramp1 protein, western blotting was carried out on extracts from murine primary bone marrow macrophages (PBM). The antibodies used in these experiments were polyclonal and raised to the first 54(N) and 82(B) amino acids of the Nramp1 N-terminal sequence. B antibody has been successfully used in detection of Nramp1 transfected into COS-1 cells (43) and also in detection of *Nramp1* transfected into RAW264.7 cells (RAW) (113). To confirm that the antibody could detect Nramp1 in PBM western blots of both RAW transfected cells (4.2.11) and PBM were probed and compared for characteristic Nramp1 staining; consisting of a lower 45kDa discrete band and a higher molecular weight diffuse band, 90-100kDa. Nramp1 from CBA PBM is recognised by B antibody (fig.**3.2.11**, lane **3**) but interestingly its mobility is distinct to that of characteristic Nramp1 from *Nramp1*^{Gly169} sense transfected RAW cells (37), lane **2**: the high MW protein, 90-100kDa in 37s (*Nramp1*^{Gly169} sense stably transfected RAW264.7 cells), appearing higher in the gel

showing it migrates at a slower rate. Also of interest is the possible heterogeneity among mouse strains, as Nramp1 from PBM of MF1 mice (4.2.12) does not display such a significant difference.

Figure 3.2.11

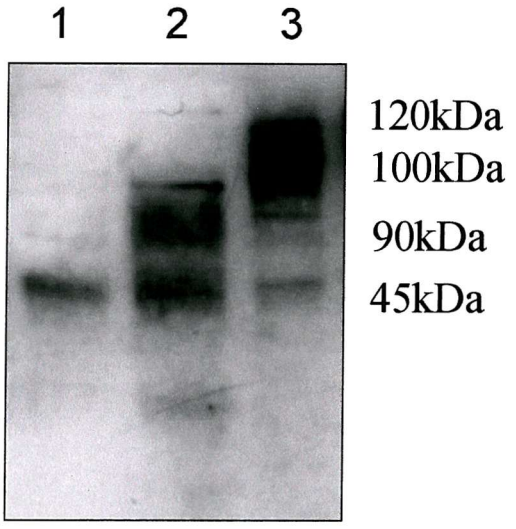

Figure 3.2.11. Pattern of Nramp1 staining after western blotting of PBM and RAW264.7 macrophages: Protein extracts from (**1**) *Nramp1* Gly169 anti-sense transfected RAW cells, 21, (**2**) *Nramp1* Gly169 sense transfected RAW, 37 and (**3**) bone marrow macrophages from $CBA^{Gly169/Gly169}$ mice were analysed by western blotting. The membrane was then probed for Nramp1 expression (2.2.11). Sizes of the Nramp1 polypeptides are indicated on the left. Blot of a typical experimental outcome.

The 45kDa band migrates to a similar point in *Nramp1* Gly169 anti-sense transfected RAW cells (21) (lane **1**), 37s (lane **2**) and also PBM (lane **3**).

N antibody recognises a smaller part of the Nramp1 N-terminal domain but still recognises western blotted Nramp1 typical of studies using B antibody and was the antibody used in further experiments.

3.2.2 Regulation Of Nramp1 Protein Expression By Iron

Regulation of *Nramp1* mRNA by iron and IFN-γ/LPS has already been documented (105), but changes in the level of protein have not (48). To this end PBM from a number of inbred strains of mice were used to study regulation.

As IFN-γ and LPS potently stimulate *Nramp1* mRNA expression, an observation that is consistent with putative inducible sites found within the promoter sequence (1.6), they were tested first in examination of Nramp1 regulation. The action of these two compounds together induced both low MW (45kDa) and high MW (90-100kDa) Nramp1, and as such were used as a base line for iron modulation. Iron was introduced to PBM as ferric ammonium sulphate, a ferric iron donor, and was removed by chelation using desferoxamine. Individually these compounds have been used successfully to regulate *Nramp1* mRNA stability(89). During the course of western blotting, interpretation of regulation was assumed to be a consequence of differential Nramp1 expression and not of changes in immune-reactivity to a pool of pre-existing Nramp1 after treatment. Onward modulation of protein will be referred to as a change in expression.

Regulation of Nramp1 protein occurs primarily at the 45kDa polypeptide band (low MW). This can be seen as strong induction in both IFN-γ/LPS and iron treated cells, lanes **2** and **4** compared to lane **1**, in all mouse strains (fig.**3.2.21 (a)**); this band is responsive in both homozygous R and S mouse PBM. As has been reported before no 90-100kDa (high MW) Nramp1 protein is detected in S mice(113) although there is non-specific staining in C57BL6. The regulation of high MW (HMW) Nramp1 polypeptide is consistent with but often less stark than that of low MW (LMW) Nramp1 polypeptide in R macrophages at 24 hours. Figure **3.2.21** lane **1** compared to **4** in (**a**) for both C3H and CBA extracts.

Figure 3.2.21

(a)

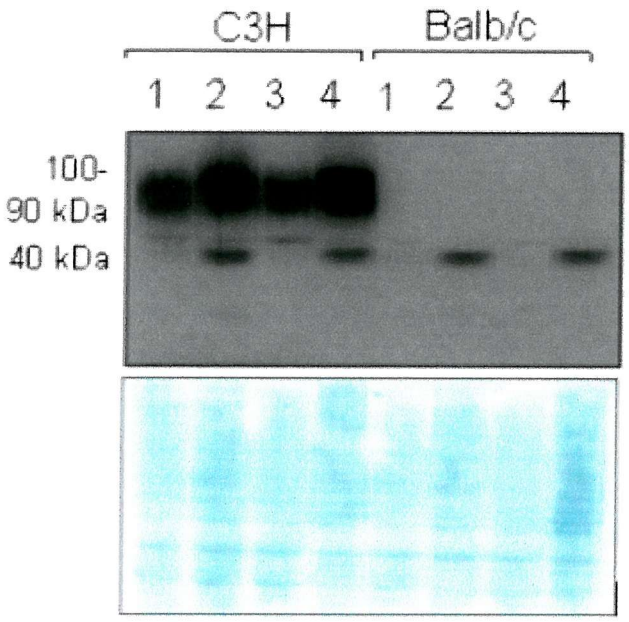

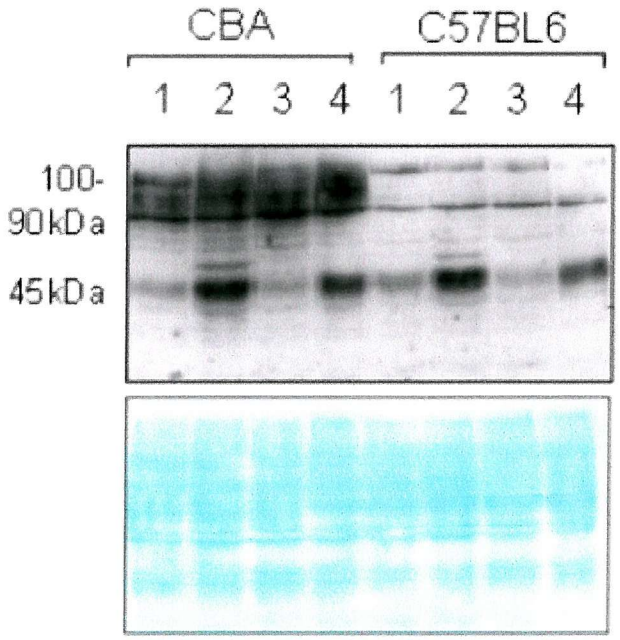

(b)

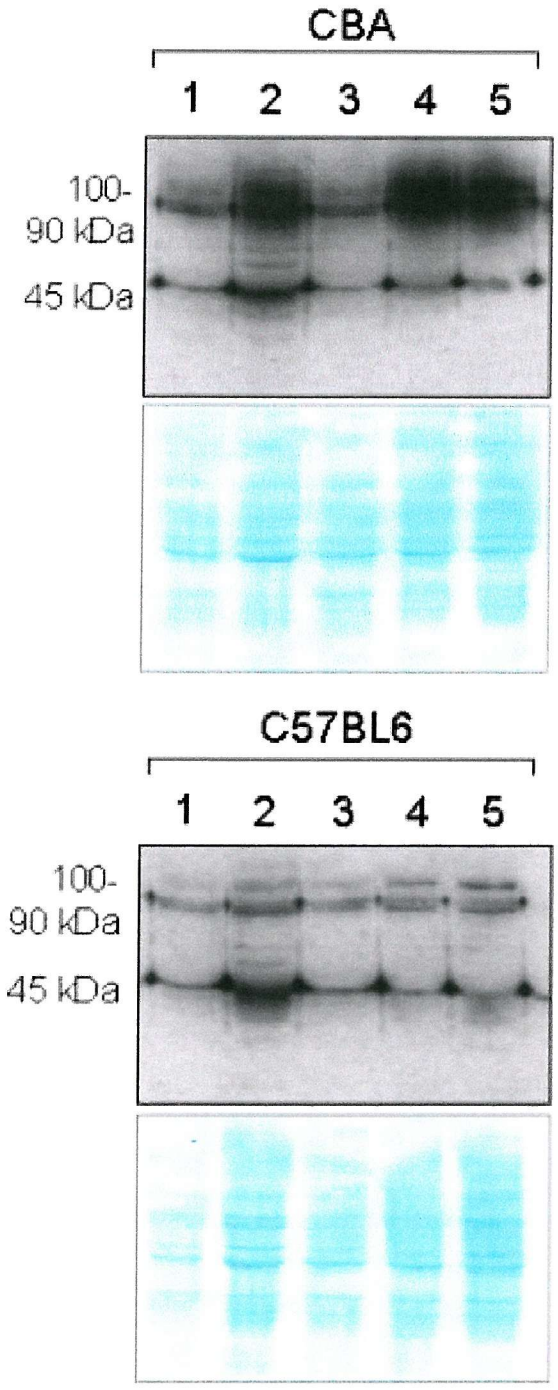

Figure 3.2.21. Iron induces Nramp1 expression in murine PBM. PBM were cultured as in methods (2.2.2). These cells were treated for 24 hrs (**a**) or 48hr (**b**) with control media (**1**), IFN-γ and lipopolysaccharide (**2**), 100 μM desferoxamine (Des) (**3**), 100 μM ferric ammonium sulphate (FAS) (**4**), and 500μM sodium nitroprusside (SNP) (**5**)((b) only). Membranes are shown as protein loading controls. PBM from two R (CBA, C3H) and two S (C57BL6, Balb/c) strains of mice were tested corresponding to the two major allelic forms. Blots for CBA and C57BL6 PBM were repeated at least 3 times.

48-hour iron treatment, lane **4** (fig.**3.2.21** (**b**)), results in much greater levels of HMW protein compared to control, lane **1**, in CBA extracts; suggesting a consistent stimulus is required to maintain PBM HMW Nramp1 expression. Unlike HMW Nramp1, LMW protein is largely absent by 48 hours, lane **4** of both CBA and C57BL6 murine extracts (**b**); implying PBM become insensitive to the iron treatment over a chronic time period. This does not occur during IFN-γ/LPS treatment, lane **2**, which shows prolonged expression of the LMW band. Treatment of macrophages with desferoxamine, lane **3**, revealed no enhanced protein expression compared with controls, lane **1** (fig.**3.2.21**) in all mouse strains tested. The reason there is no decrease in expression is not known. Lane **5** (fig.**3.2.21** (**b**)) shows changes in Nramp1 expression with sodium nitroprusside (SNP) treatment, a donor of nitrosonium ions. This effect is referred to in 3.2.3.

Presence of a possible 65kDa inducible band can be seen in IFN-γ/LPS induced CBA and C57BL6 (fig.**3.2.21** (**a**), lane **2**) PBM extracts lying just above the 45kDa band. IFN-γ induction of this polypeptide band has been shown in N11 cells (45) using a C-terminal Nramp1 antibody. The size of the band in figure 3.2.21 was not accurately determined and does not always show induction by IFN-γ. This can clearly be seen in the C3H macrophages, figure **3.2.21** (**a**), where this band appears in lanes other than IFN-γ + LPS.

Iron regulated Nramp1 expression was repeated at least three times in CBA and C57BL6 PBM but also in two other mouse strains of both R and S origin (C3H and Balb/c) signifying this cation's role in Nramp1 expression.

3.2.3 Radical Regulation Of Nramp1

As discussed, studies of *Nramp1* mediated changes in PKC activity and the stability of *Nramp1* mRNA have identified radicals as important mediators (1.8.3).

For this reason it seemed necessary to investigate the effect that radicals have upon Nramp1 expression. To this end compounds able to generate nitric oxide derivatives or oxygen radicals within cells were assessed for their ability to induce Nramp1 (fig.**3.2.31**).

Figure 3.2.31

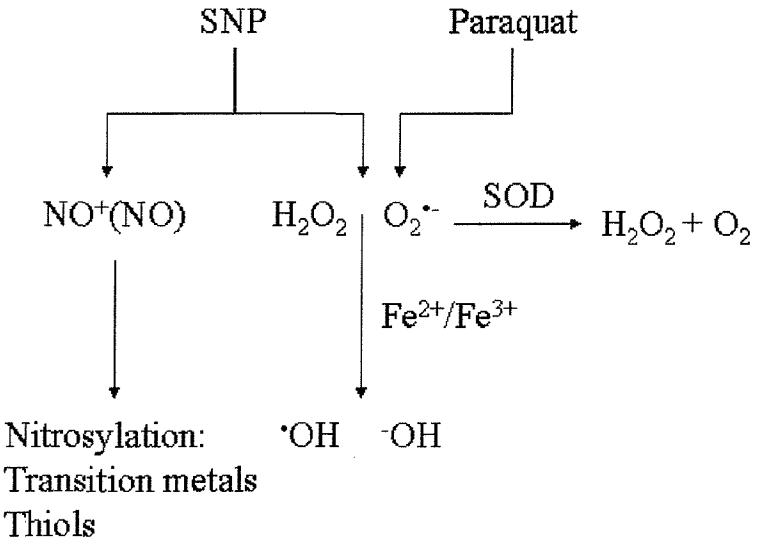

3.2.31. Action of compounds used to induce Nramp1 expression. SNP = sodium nitroprusside, SOD = superoxide dismutase.

Sodium nitroprusside (SNP) was the first compound to be used in these experiments, producing nitrosonium ions (NO^+) and in the presence of reducing agents able to release nitric oxide. Figure **3.2.32** shows the induction of Nramp1 protein over 24 hours, like iron treatment SNP causes induction of 45 kDa (LMW) Nramp1, lane **3** compared to lane **1**. In addition the HMW diffuse band is increased (lane **3**) above that of the control (lane **1**).

Figure 3.2.32

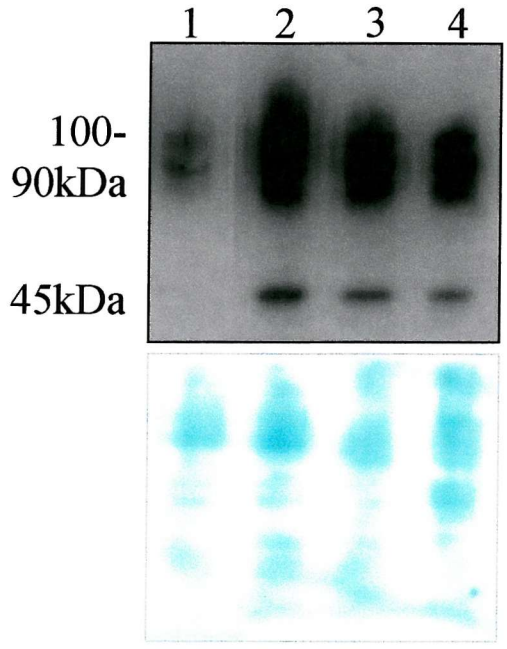

Figure 3.2.32 Radical regulation of Nramp1 in mouse PBM. MF1 PBM were treated for 24 hours in the presence of: control media (**1**); IFN-γ + LPS (**2**); 500μM SNP and (**3**) 100μM paraquat (**4**). Cells were harvested for western blotting and run on an 8% gel. The stained membrane shows the protein loading. Blot showing a typical experimental outcome.

Induction also follows the same pattern of LMW Nramp1 up-regulation followed later by persistent HMW Nramp1 expression and lower levels of LWM at 48 hours, figure **3.2.21(b)** lane **5**. Interestingly it should be noted that control levels of Nramp1 expression were variable between experiments but lower levels coincided with a greater responsiveness to treatment.

SNP is also able to produce superoxide and hydrogen peroxide (fig.**3.2.31**). In addition to this it contains Fe^{2+} (120) and in the absence of controls any one or

combination of these factors could be inducing Nramp1 expression. In order to ascertain which radical(s) were capable of induction other compounds were used. To this end the effect of paraquat on Nramp1 regulation was investigated. Paraquat is a superoxide ion donor (fig.**3.2.31**) and was therefore useful in determining the role of this moiety. Figures **3.2.32**, lane **4** compared to lane **1**, and **3.2.33** show that paraquat is able to induce Nramp1 protein expression in both MF1 and CBA PBM, respectively. This observation indicates that the presence of nitric oxide is not needed for superoxide to induce expression but does not dismiss a role for this molecule in regulatory effects. It should be noted that the reason for the absence of LMW Nramp1 in figure **3.2.33** is not known.

Finally the use of superoxide dismutase, a superoxide scavenger, in treatment of PBM leads to reduction in the expression of Nramp1 compared to control untreated cells, lanes **1** and **2** figure **3.2.34**. This coincides with both a decrease in LMW and HMW Nramp1 polypeptide bands. Cells are still responsive to IFN-γ/LPS and iron, lanes **3** and **4** respectively.

Figure 3.2.33

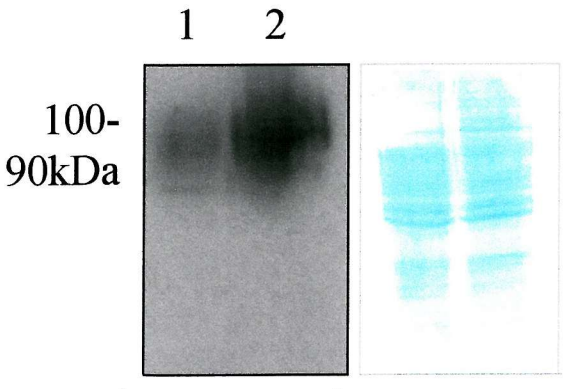

Figure 3.2.33 Superoxide augments Nramp1 protein expression. PBM were harvested and cultured as in methods. Cells were then treated with control media (**1**) or 100μM paraquat (**2**) for 24 hours at which point cells were harvested for western blotting. Macrophages from CBA mice were used. Amido black stained membranes are shown as loading controls.

Figure 3.2.34

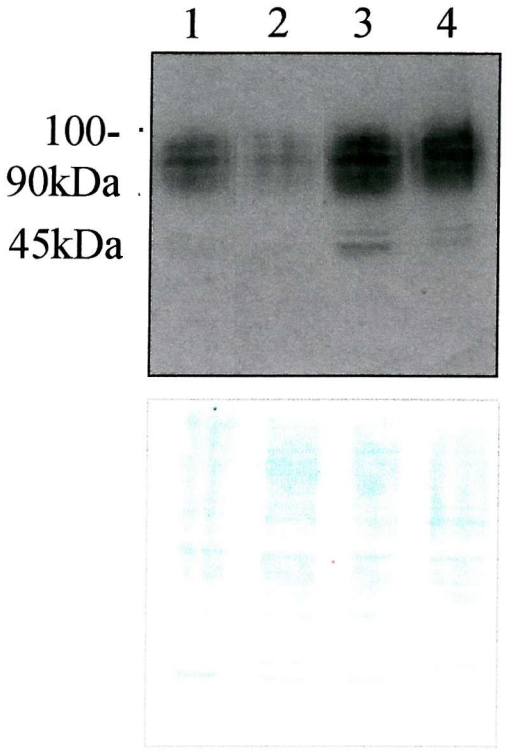

Figure 3.2.34. Superoxide dismutase blocks expression of Nramp1. PBM from MF1 mice were treated for 24 hours with control media (**1**), superoxide dismutase (1μg/ml) (**2**), IFN-γ + LPS (**3**) and 100μM FAS (**4**). Cells were harvested and analysed by western blotting for Nramp1 expression. Amido black stained membrane shows comparable loading.

The treatment of macrophages with hydrogen peroxide showed that this molecule has no role in the regulation of Nramp1 protein expression (not shown).

3.2.4 Regulation Of *Nramp1* mRNA By Iron

Results in our laboratory have shown that not all macrophage cells express *Nramp1 in vivo*, cells of the liver and spleen, Kupffer cells and splenic macrophages, and inflammatory macrophages in a haemorrhagic brain lesion model do, whereas the resident macrophage cells of the brain, gut, kidneys and lung do not (121). Factors regulating *Nramp1 in vitro* may be our key to understanding the differential regulation of *Nramp1 in vivo*. One common factor in the differential regulation of *Nramp1* is iron. Kupffer cells and splenic macrophages are involved with RBC iron salvage/recycling and the specific role of these cells could be the key factor.

Therefore *Nramp1* regulation by iron and haem derived products was also evaluated at the level of *Nramp1* mRNA.

Treatment of PBM with IFN-γ + LPS or FAS for 24 hours showed that both caused accumulation of *Nramp1* mRNA, figure **3.2.41** lanes **2** and **4** compared to control lane **1**, as observed for LMW/HMW Nramp1 protein. There appears to be no expression of mRNA in resting macrophages, lane **1**, suggesting that Nramp1 protein still remaining at this point is not newly synthesised but that lingering after transcription has stopped; also implying that Nramp1 protein is not rapidly degraded over 24 hours and therefore quite stable for this length of time. However like its protein, levels of *Nramp1* mRNA in resting cells are also variable (fig.**3.2.42**, lane **1**). Desferoxamine has no effect on mRNA accumulation lane **3**, figure **3.2.41**.

Figure 3.2.41

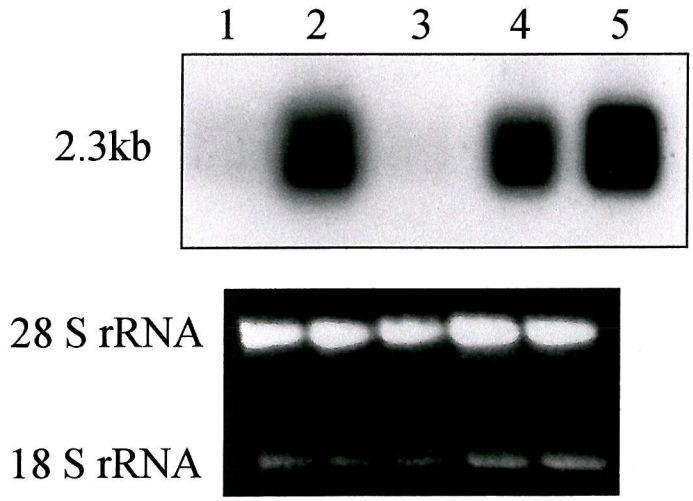

Figure 3.2.41 Induction of *Nramp1* mRNA in murine PBM. Whole cell RNA was harvested from PBM as described in methods and 3μg analysed using Northern blotting. Cells were treated for 24 hrs with the following: Control media (**1**); IFN-γ + LPS (**2**); 100 μM Des (**3**); 100μM FAS (**4**) and 500μM SNP (**5**). 1μg of sample RNA was run separately and stained with ethidium bromide to allow visualisation of 28S and 18S rRNA. This was used as a loading control. Blots were repeated at least a total of three times between murine PBM. Blots were prepared as in (2.2.13).

Figure 3.2.42

(a)

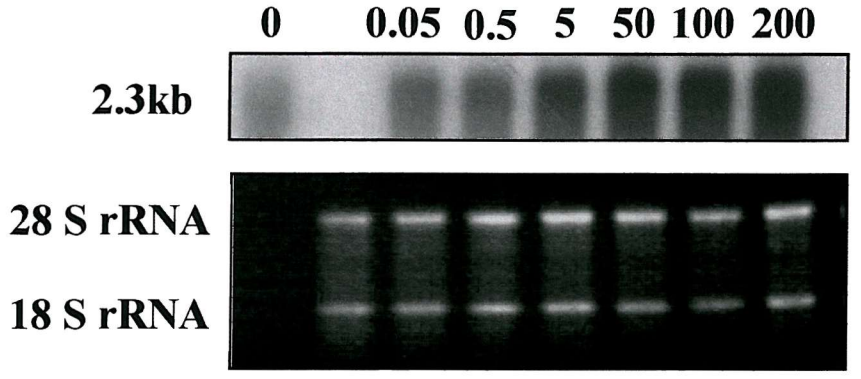

(b)

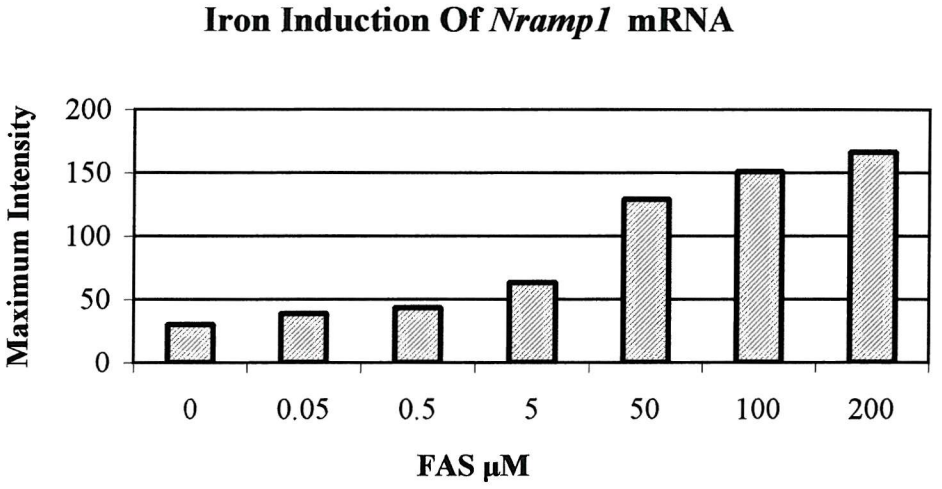

Figure 3.2.42. Augmentation of *Nramp1* expression is sensitive to low [FAS]. C57BL6 PBM were harvested and cultured as described in methods. Cells were incubated for 24 hrs with increasing [FAS], 0 - 200 µM. **(a)** 3µg of total cell RNA used for Northern blotting and probed for *Nramp1*. An ethidium stained gel is shown as a loading control (1µg RNA loaded). **(b)** Graph showing measured intensities for *Nramp1* mRNA expression with increasing [FAS] (2.2.15). Example from one of two repeats showing similar results.

Figure 3.2.43

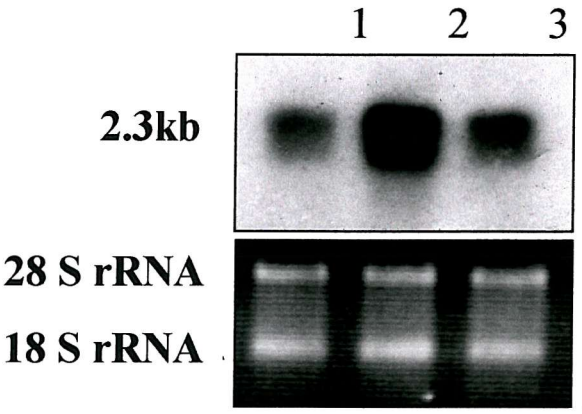

Figure 3.2.43. Iron chelation blocks *Nramp1* mRNA induction by FAS. Total cell RNA was harvested for Northern blotting from C57BL6 PBM as described in methods. They were then treated for 24 hrs with: 100 μM desferoxamine (**1**), 100 μM FAS (**2**) and 100μM Desferoxamine with 100μM FAS (**3**). An ethidium stained gel is shown as a loading control (1μg RNA loaded).

Figure **3.2.42** shows that *Nramp1* mRNA induction is sensitive at concentrations lower than 100μM FAS, stimulation occurring after 24 hours treatment with as little as 0.5μM, but 5μM causing a 2 fold increase and 100μM a 5 fold increase.

To demonstrate that iron was the influencing factor in FAS induction, cells were incubated in the presence of both desferoxamine and FAS. The presence of an iron chelator should remove any inducing effects of iron released from FAS. This does occur and is clearly represented in figure **3.2.43**; lane **1** shows desferoxamine treated cells, lane **2** FAS treated, and lane **3** both desferoxamine and FAS where induction is abrogated.

Lastly it should be noted that SNP is also a powerful promoter of *Nramp1* mRNA accumulation over 24 hours, figure **3.2.41** lane **5**, consistent with its ability to induce Nramp1 protein over this time period.

3.2.5 Hemin And *Nramp1* Regulation

Macrophages of the reticuloendothelial system are responsible for approximately 80% of effete red blood cell (RBC) recycling (122). Studies of iron overloaded congenic *Nramp1* R and S mice showed that differences in *M.avium* growth between the two strains were abrogated in the liver and spleen. In addition to this comparison of *Leishmania donovani* growth in liver, spleen, and peritoneal macrophages from R and S mice show significant differences in growth in all the tissues except spleen (123). These results imply that iron concentrations determine closely the ability of *Nramp1* to fight infection and also raise the possibility that removal of iron from macrophages of the liver and spleen is the primary action of *Nramp1* but consequently aids in infection resistance. Spleens of *Nramp1* S inbred mice are enlarged compared to R mice (121) and differences in iron distribution within the spleens of iron-loaded mice are clearly visible. This may reflect an inability of macrophages from S mice to recycle RBC iron leading to greater infiltration of macrophages into the spleen to cope. In light of these studies and also that *Nramp1* likely encodes an iron transporter (like its close homologue *Nramp2*) the possibility of regulation of *Nramp1* in response to RBCs or metabolites of RBC breakdown seemed likely. To test this the haem analogue, hemin, was used in the analysis of Nramp1 protein and mRNA regulation.

Figure 3.2.51

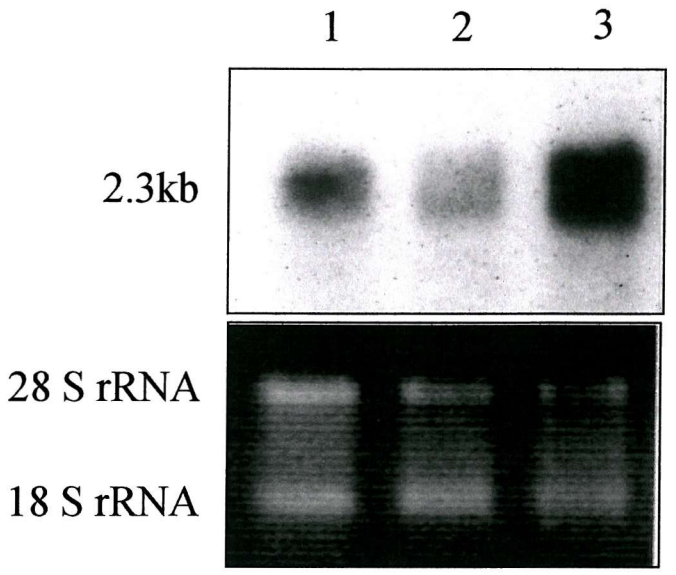

Figure 3.2.51. The haem synthetic analogue, hemin, promotes *Nramp1* expression. C57BL6 PBM were harvested and cultured as described in methods. Cells were treated for 24 hrs with control media (**1**), 0.1% DMSO (the solvent for hemin) (**2**), and 10μM hemin (**3**). Total cell RNA was harvested and used for Northern blotting. An ethidium stained gel is shown as a loading control (1μg RNA loaded).

Figure **3.2.51** lane **3** compared to lane **1** shows that hemin is able to up-regulate *Nramp1* mRNA expression over 24 hours. Interestingly the DMSO control, lane **2**, reduces the expression of *Nramp1* mRNA and this may be due to its ability to act as a radical scavenger (124).

3.3 Discussion

Over 24 hours iron was shown to cause increases in both *Nramp1* mRNA and protein. Additionally it was found that superoxide is an important mediator of Nramp1 protein induction as it was able to augment expression; *vice versa* removal of superoxide from resting PBM abrogated Nramp1 expression. Lastly hemin, a synthetic analogue of haem, is able to increase levels of *Nramp1* mRNA over 24 hours indicating that metabolites of RBC breakdown may also regulate expression.

Comparison of Nramp1 polypeptides by western blotting suggests that there is heterogeneity within a single cell, and also between cell lines and PBM. This has been reported for other glycosylated proteins and can be a result of developmental stage, nutritional changes, enzymatic equipment or genetic background (125).

Use of an additional unreported anti-Nramp1 antibody to the first 54 amino acids of the N-terminal sequence has shown similar affinity to that used in previous studies. This antibody was able to detect Nramp1 identical to that seen in RAW264.7 cells (113) by the previous antibody but also Nramp1 polypeptides in murine PBM. Employing this antibody produced the first western blot extracts showing IFN-γ/LPS up-regulation of Nramp1 polypeptide expression in PBM. HMW Nramp1 polypeptide is absent from western blots using S or functionally null PBM. However the LMW band is present and shows identical regulation to R PBM extracts. In addition iron is able to up-regulate expression of both HMW and LMW polypeptide bands in R PBM. By 48 hours if no stimulus is present levels of HMW Nramp1 drop, as is seen in untreated and desferoxamine treated PMB (fig. **3.2.21 (b)** lanes **1** and **3**). Although time points past 48 hours have not been investigated it appears that iron may only have a transient effect on protein induction; alternatively it may reflect chronic regulatory changes to proteins involved in iron homeostasis abrogating iron

induced Nramp1 expression. This is manifested as a decrease in levels of LMW Nramp1 after 48 hours of incubation in iron, a process that does not occur in IFN-γ/LPS treated cells that still display good induction of this band at 48 hours. The early increase and later decrease of LMW Nramp1 with sustained levels of HMW suggests that the 45kDa (LMW) band could be a precursor to the 90-100kDa (HMW) Nramp1. This is supported by the reconstitution of a single band upon removal of carbohydrate from Nramp1 (chapter 5, fig.5.3.1). However studies using ^{35}S-methionine labelled proteins and immune-precipitation of Nramp1 are needed to confirm this.

The high levels of Nramp1 protein expression in untreated PBM at 24 hours may be a result of GM-CSF induced up-regulation, a peptide used to cause differentiation of bone marrow precursor cells to PBM. This peptide is able to augment *Nramp1* expression (55) and may be responsible for the changeable levels of residual protein; although cells are washed and allowed to rest for two days without GM-CSF the heavily glycosylated Nramp1 protein may require extensive processing for its removal. In addition differences between western blots may reflect the amounts of GM-CSF used to treat precursor cells. The source of GM-CSF used in these experiments is from the media incubating L-929 cells (2.2.2) and variability between batches may reflect differences in residual Nramp1 expression later.

Like Nramp1 protein it is shown here that over 24 hours of iron treatment PBM respond by accumulating *Nramp1* mRNA. This is not consistent with other groups (89) where iron was shown to decrease *Nramp1* mRNA stability in both R and S macrophages, but more so in S. This last observation does not translate to protein regulation, as both S and R PBM seem equally capable of increasing LMW Nramp1 expression under iron treatment. Decreases in *Nramp1* mRNA stability therefore

have little effect on accumulation of *Nramp1* mRNA and protein over 24 hours of iron treatment.

The labile iron pool concentration, which is the concentration of chelatable iron within the cell, has been estimated to be ~ 10^{-8} M [185] and is believed to allow cell signalling through changes in its size. The concentration of transferrin in media is around 30-40μM and its iron saturation around 30-50%. The dissociation constant of the transferrin receptor for diferric transferrin is ~ 0.1-1nM and therefore the transferrin receptor will always be saturated. Addition of 100μM FAS to cells will lead to iron saturation of cells in excess of physiological boundaries. This iron is unlikely to be taken up through the transferrin receptor pathway as it is already saturated although studies have shown a number of other pathways that are involved in uptake of low molecular weight iron compounds. These include active transport of transferrin iron across the plasma membrane, an effect that seems dependent on radical formation and independent of transferrin receptor, and also non-specific uptake involving pinocytosis (126). Knowing that excess iron would cause radical production and also that these radicals have the potential to induce *Nramp1,* lower concentrations of iron were tested for their ability to induce mRNA. There are moderate differences in both 50 and 500nM FAS incubations leading to an increase in *Nramp1* mRNA. These concentrations are only 0.5 and 5 times greater than the estimated concentrations of intracellular labile iron pool, respectively. The actual amount seen by the cell however will probably be less due to the potential of serum proteins and biological membranes to bind iron (52). This may therefore represent a more physiological change in iron concentration such as that seen by splenic macrophages during iron recycling of effete RBCs (122).

Superoxide anion from paraquat is able to induce Nramp1 protein expression alone and superoxide dismutase is able to reduce Nramp1 expression in resting R PBM – an effect possibly due to the phagocytosis of SOD and subsequent effect on intracellular redox activity, although no data exist for this theory. However, there is a tenuous link with other groups where it has been noted that radicals are able to increase the stability of *Nramp1* mRNA (105). In addition to this the nitric oxide donor SNP is able to induce *Nramp1* mRNA and protein expression. However in the absence of controls or compounds exclusively releasing NO it is not possible to say if NO plays a pivotal role in *Nramp1* regulation.

The way in which iron and superoxide mediate induction of *Nramp1* mRNA or protein is not known. The regulation by other groups would suggest that stability of *Nramp1* mRNA is the influencing factor. These results are consistent with the superoxide effects seen here but the opposite to those seen for iron. If mRNA stability was solely responsible for changes in Nramp1 protein expression then iron should reduce it. The opposite actually occurs iron-causing accumulation of *Nramp1* mRNA and protein; in this circumstance it would appear necessary to have increased rates of *Nramp1* transcription. For this to transpire there must be regulatory sites within the promoter that can sense changes in iron load.

Using TRANSFAC (127), examination of *Nramp1*'s promoter sequence up-stream of that published (un-published by our group) highlights a number of interesting regulatory elements. Of these there are two antioxidant response elements (ARE), which are located 3868-3878bp upstream of the ATG codon and in intron 2, 757-767bp. This is particularly interesting as not only does Nramp1 respond to superoxide stress it is also protective against oxidative stress in RAW264.7 cells stably transfected with *Nramp1*^{Gly169} (4.2). In addition recent characterisation of the

orthologous *Nramp1* in prokaryotes (128). ARE elements bind Nrf1/Nrf2 (NF-E2 related factor 1/2) which heterodimerise with small Maf proteins and possibly Jun and Fos (129) to regulate the induction of detoxifying genes (130;131). Nrf2 itself is found in macrophages and is bound to a protein called Keap1 (Kelch-like ESC-associated protein 1) that retains it in the cytoplasm until an appropriate oxidative signal causes release of Nrf2 allowing its translocation to the nucleus. It has been postulated that critical cysteine residues in Keap1 sense oxidative changes and allow release of Nrf2 (132). If this occurs then NO may also be able to interact here through modification of thiols (133). As well as this, ARE elements are important sites for the hemin responsiveness of haem oxygenase I (134), therefore ARE sites may be an interface for multiple signals culminating in *Nramp1* regulatory events.

Interestingly iron can effect the formation of dinitrosyl iron complexes and S-nitrosothiols that have been reported to be involved in storage and transport of NO (135). This would lead to release of free NO, which is able to interact with free thiol groups and could provide a common link between iron and possibly nitric oxide induced *Nramp1* expression, although this requires further investigation.

Our group has attempted to regulate levels of *Nramp1* mRNA through addition of RBCs to RAW264.7 cells but have found total levels of its mRNA to be insensitive to not only these but also iron alone. This cell line, however, does remain responsive to IFN-γ and LPS (48). The reason for this is unknown but analysis of an unpublished extended part of the *Nramp1* promoter suggests that there are 6 non-canonical putative c-myc sites (**1-3** CACATG, **4** CACTTC, **5** CATTTG, **6** CATTGT). As these cells are dividing unnatural interaction of transcription factors with the promoter may be occurring leading to the unresponsiveness seen. RAW264.7 cells

incubated with heat-treated RBCs clearly showed that they could erythrophagocytose (fig.**3.3.1**) suggesting this was not the cause of the insensitivity seen.

Figure 3.3.1

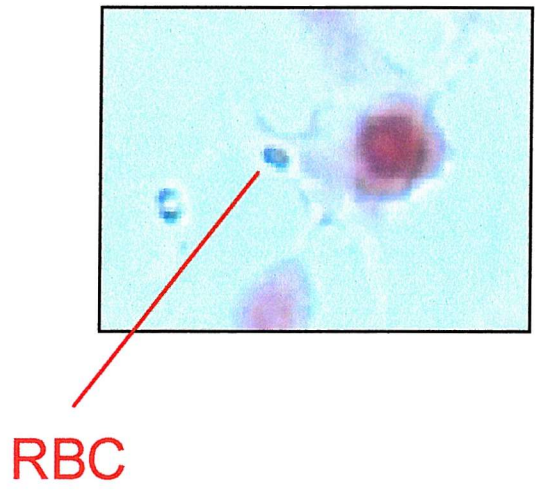

Figure 3.3.1. RBC uptake by RAW264.7 cells: RAW 264.7 cells were incubated with ~ 3 RBC/cell for 3 hrs. Cells were then fixed and stained with the membrane/nuclear stain neutral red. RBCs were visualised with the iron stain, Prussian blue. (x100 magnification oil immersion). Result shows a typical experimental outcome.

Although not shown in RAW264.7 macrophages our group has shown enhanced expression of Nramp1 protein in isolated splenic macrophages during the addition of RBCs (121). If this is the case it is supportive of a role in which *Nramp1* aids erythrocyte iron recycling. Numerous studies have shown that expression of *Nramp1* in cell lines or IFN-γ activated *R* mouse macrophages have decreased total cellular iron levels (43;113;136). Up-regulation of *Nramp1* during RBC breakdown may aid in release of iron from the cell.

Haem is broken down by haem oxygenase-1 (HO-1) into bilirubin, CO and ferrous iron (fig.**3.3.2**). HO-1 is located on the endoplasmic reticulum and once iron is released it is believed to enter the labile iron pool.

Figure 3.3.2

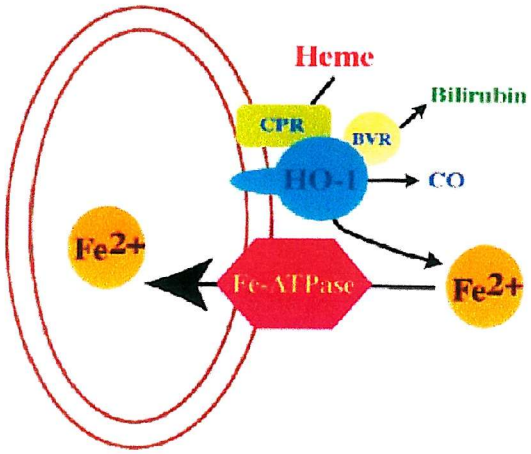

Figure 3.3.2. The breakdown of haem and release of iron: The diagram is adapted from Baranano *et al.* (137). HO-1 is located on the endoplasmic reticulum and together with other enzymes breaks down haem into bilirubin, carbon monoxide and ferrous iron. The recently identified p-type iron ATPase (Fe-ATPase) is involved in transport of ferrous iron into the lumen of the ER

Here the newly characterised Fe-ATPase (137) transports iron into the ER perhaps for recycling. At this point however Nramp1 may also take iron and transport it into the lumen of late endosomes and lysosomes for recycling. The presence of two transporters performing this function implies that they are degenerate and perhaps the lack of a strong phenotype in *Nramp1* KO mice is because of this. These mice show no obvious abnormalities but study of serum iron levels or tissue iron loads have not been reported (138). The fact that bacteria rapidly proliferate in the liver and spleens of *S* mice, areas of RBC recycling, would suggest that these tissues are particularly prone. If *Nramp1* is indeed redundant then a phenotype may only present under stress, such as infection or iron overload; observable facts (1.4 & 1.8.2).

The direction of Nramp1 transport is still an active topic and groups have produced evidence for both directions. On the one hand: members of the Zwilling

group and Blackwell group(67;89;94;136;139) have shown that *Nramp1* expression increases phagosomal iron concentration and uptake into *Xenopus* oocytes, respectively. This would suggest Nramp1 transports divalent cations into intracellular vesicles; on the other hand Gros and colleagues and Gomes and Appelberg have shown that *Nramp1* causes removal of divalent cations from phagolysosomal lumens, and iron overload eliminates differential infection susceptibility between R and S mouse strains, respectively (91;93). These results suggest Nramp1 acts to remove divalent cations from the pathogens vicinity. The regulatory data presented in this chapter show that *Nramp1* expression is increased during iron incubation. If cation transport were from the vesicle lumen to the cytoplasm *Nramp1* would be positively regulated by its own substrate leading to a continual feedback loop. This seems unlikely especially as Nramp1 expression decreases during 48 hours of iron incubation. If instead Nramp1 retains iron within an intracellular vesicle then it would negatively regulate its own expression, presumably the more logical conclusion.

In summary it has been shown that *Nramp1* mRNA and protein expression are increased by iron, and protein by superoxide. The identification of two putative ARE sites within Nramp1's sequence may be the target of these two moieties, but also a possible target of hemin which can also augment accumulation of *Nramp1* mRNA. It is suggested that *Nramp1* may act to increase the efficiency of senescent erythrocyte iron recycling.

Chapter 4

Nramp1 and Cellular Iron Distribution

4.1 Introduction

As discussed in the introduction many groups have been interested in trying to identify the main substrate(s) for Nramp1. Through the identification of *Nramp2* and subsequent studies using this protein it is now firmly believed that Nramp2 is a divalent cation transporter with preference for ferrous iron (1.8.1). The close sequence identity between *Nramp1* and *Nramp2* led to the natural conclusion of a similar transport activity for *Nramp1*. It has not been until recently that direct evidence for this exists in *Xenopus laevis* oocyte studies and a novel approach using zymosan covalently labelled with a fluorescent probe (fura6) effected by divalent cation concentrations(93;94). These two studies themselves conflict, one showing Nramp1 acting as an antiport the other as a symport (1.8). There is also uncertainty as to the natural substrate for *Nramp1*.

In order to identify if *Nramp1* is able to modulate iron status RAW264.7 and L1 3T3 fibroblasts were stably transfected with plasmid encoding wildtype sense $Nramp1^{Gly169}$ or anti-sense $Nramp1^{Gly169}$ as a control. These constructs are the same as those reported previously (113), producing constitutive expression through β-actin promoter activity. The cell line RAW264.7 was originally immortalised from Balb/c macrophages that are homozygous S and therefore carry non-functional protein (138); parental L1 3T3 cells (from Balb/c mice) do not express *Nramp1*. These lines were used to study the effect of *Nramp1* on cellular iron distribution. As Nramp1 is

expressed on internal membranes its ion transport activity would either increase or decrease the availability of cations/iron within the labile iron pool. Non-invasive indicators of iron within this pool were used. Studies on transcriptional activation of PKCβ show that it is up regulated in iron replete conditions (140). If PKCβI levels are modulated by *Nramp1* expression it would provide evidence of changes in cytoplasmic iron.

Cytoplasmic levels of iron also regulate cellular growth; the rate-limiting step in DNA synthesis is performed by ribonucleotide reductase, which removes the 2'-hydroxyl group on the ribose moiety of ribonucleoside diphosphates and triphosphates replacing them with a hydrogen atom. Studies have shown that this enzyme works through a radical dependent mechanism that itself relies on iron in the protein's catalytic centre. Iron chelation studies on cells suggest that the ribonucleotide reductase iron ion is freely removable and depletion of the labile iron pool is sufficient to do this (141). This in turn decreases cell proliferation (142). If Nramp1 reduces cytoplasmic iron levels this should be reflected by a change in cell proliferation.

Lastly the resistance of expressing lines to paraquat-induced stress was investigated. Paraquat is a generator of intracellular superoxide radicals and in the presence of trace amounts of free iron superoxide and hydrogen peroxide can lead to the production of hydroxyl radical and hydroxyl anions, otherwise known as the Haber-Weiss reaction.

Haber-Weiss Reaction

$$O_2^{\bullet-} + H_2O_2 \xrightarrow{Fe^{2+}/Fe^{3+}} O_2 + {}^{\bullet}OH + OH^-$$

Hydroxyl radicals are highly reactive and can cause radical chain propagation leading to damage far in excess of the initial reaction. They can cause damage to proteins, lipids and DNA making them extremely cytotoxic. In light of this the hypothesis formulated was that if *Nramp1* expression depletes cytoplasmic iron levels then paraquat should be less harmful to these cells as radical catalysed reactions will no longer occur in the vicinity of major cellular events, like translation.

4.2 Results

4.2.1 Expression Of *Nramp1* In RAW264.7 And L1 3T3 Fibroblasts

Figure **4.2.11** shows the expression of Nramp1 protein in L1 3T3 and RAW264.7 cell lines. RAW264.7 cells originate from Balb/c mice that are homozygous for S and figure **4.2.11** (**b**) shows parental **RAW** (un-transfected) and anti-sense *Nramp1*^{Gly169} stably transfected RAW264.7 cells (**21**) contain no HMW 90-100kDa Nramp1 protein, but low levels of the 45kDa LMW band. Sense *Nramp1*^{Gly169} transfected RAW cells, lines **32** and **37**, show expression of both the HMW and LMW polypeptide bands. L1 3T3 fibroblasts contain no HMW/LMW polypeptide (fig.**4.2.11** (**a**) **AS3/AS7**) in accordance with the tissue specific expression of *Nramp1*. Expression of the HMW and LMW bands can clearly be seen in stably sense *Nramp1*^{Gly169} transfected 3T3 lines **S4** and **S7** suggesting *Nramp1* is undergoing the correct posttranslational modifications in this cell type. Below each western blot amido black staining of the membranes confirms comparable loading.

Often constitutive protein expression promotes levels of proteins that are non-physiological and direct abnormal function. To ascertain if *Nramp1* expression in these cell lines was physiologically relevant protein extracts from IFN-γ treated

Figure 4.2.11

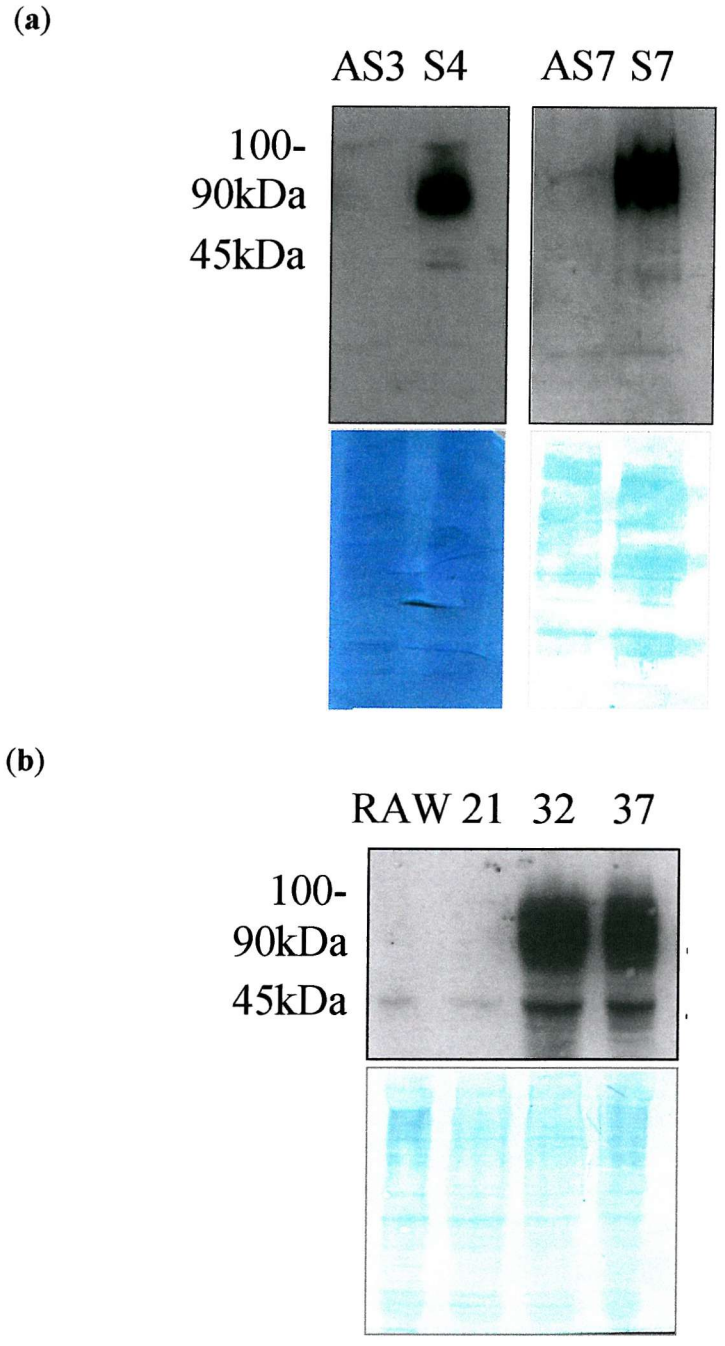

Figure 4.2.11. Nramp1 expression in L1 3T3 and RAW264.7 cells stably transfected with *Nramp1*^{Gly169} sense and anti-sense constructs. Western blots showing: **(a)** L1 3T3 fibroblast cell lines S4 and S7 expressing sense *Nramp1*^{Gly169}, AS3 and AS7 expressing anti-sense *Nramp1*^{Gly169}. **(b)** RAW264.7 cell lines 32 and 37 express sense *Nramp1*^{Gly169}, 21 expresses anti-sense *Nramp1*^{Gly169}. RAW is an un-transfected parental RAW264.7 cell line.

Figure 4.2.12

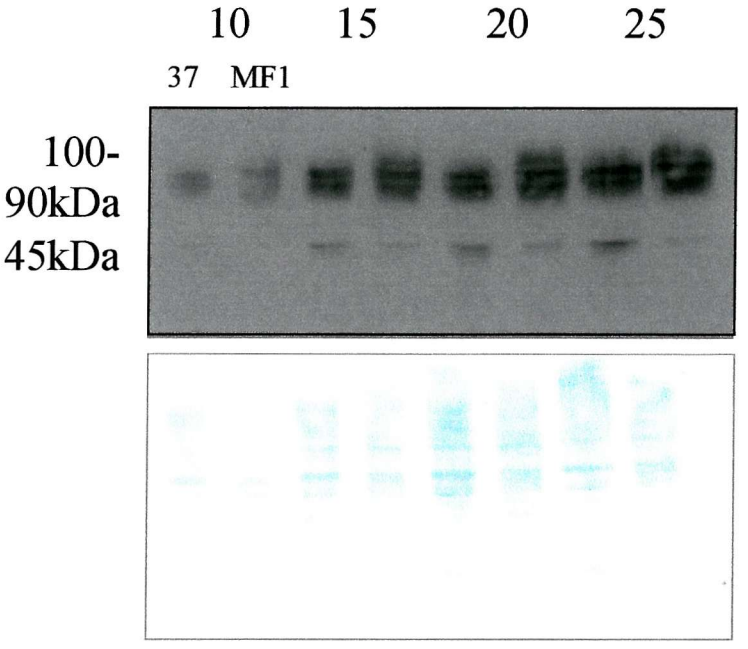

Figure 4.2.12. Comparison of Nramp1 immune reactivity from 37 and murine PBM extracts: From left to right lanes come in pairs 37 then MF1, with 10, 15, 20, 25 μg of protein loaded. MF1 PBM were stimulated overnight with IFN-γ. Amido black stained membrane shows loading.

MF1 PBM were analysed by western blotting against 37 cell extracts at a range of protein amounts. Figure **4.2.12** shows that the natural expression of Nramp1 during IFN-γ treatment in MF1 PBM is comparable to the protein levels of artificaially constituitively expressed Nramp1 in the 37s. The similarity of Nramp1 expression in these cells suggests that possible overexpression of Nramp1 and subsequent indirect repression of other proteins within the 37s is minimal. Other results (not shown) verify expression in 3T3 cells to be comparable or less than RAW cell transfectants.

4.2.2 Effect Of *Nramp1* Expression On PKCβI Protein Levels

To investigate whether PKCβI protein levels were responsive to iron in RAW transfectant lines, cells were serum-starved for 24 hours in the presence of a range of

FAS concentrations, a ferric iron donor, and extracts analysed using western blotting for PKCβI expression. Figure **4.2.21** demonstrates that PKCβI protein expression is modulated with iron during serum starvation, reaching maximal induction at around 100 μM FAS. These effects are consistent with those seen by Orlando *et al.* (140) showing modulation of PKCβ mRNA, and allowed the further use of PKCβI protein as an iron sensor in *Nramp1* expressing lines.

Figure 4.2.21

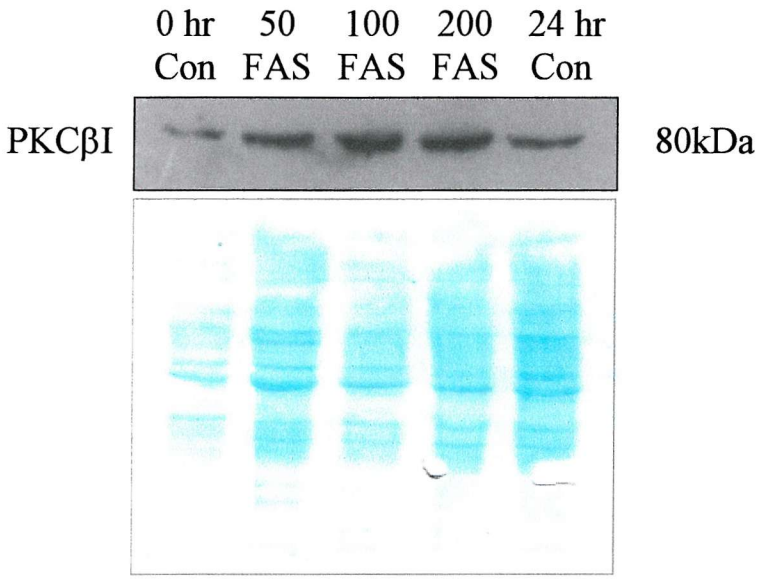

Figure 4.2.21. Regulation of PKCβI levels by iron: Western blot of PKCβI from RAW264.7 cell extracts. From left to right, 0 hr Con - control no treatment, 50, 100 and 200 FAS - cells were treated for 24 hours in the presence of 50, 100 and 200 μM FAS without serum. 24 hr Con - cells were serum starved for 24 hours.

Although PKCβI showed modulation by iron it was a primary goal to see if it was affected in the context of *Nramp1* expression. To do this *Nramp1* expressing lines were probed for PKCβI expression. Figure **4.2.22** shows that although lines expressing anti-sense *Nramp1* have detectable PKCβI expression (**21**, **AS7** and **AS3** -

controls), lines expressing sense *Nramp1* have reduced PKCβI levels (**37**,**S7** and S4 - controls). The weak expression in the sense lines can be augmented with iron (**37**, **S7** and **S4** - FAS), which does not occur in the anti-sense lines that show good expression with no treatment. S7s do not appear as responsive to iron treatment (**a**) although an independent cell line S4 (**b**) showed lower PKCβI expression, inducible with FAS.

Figure 4.2.22

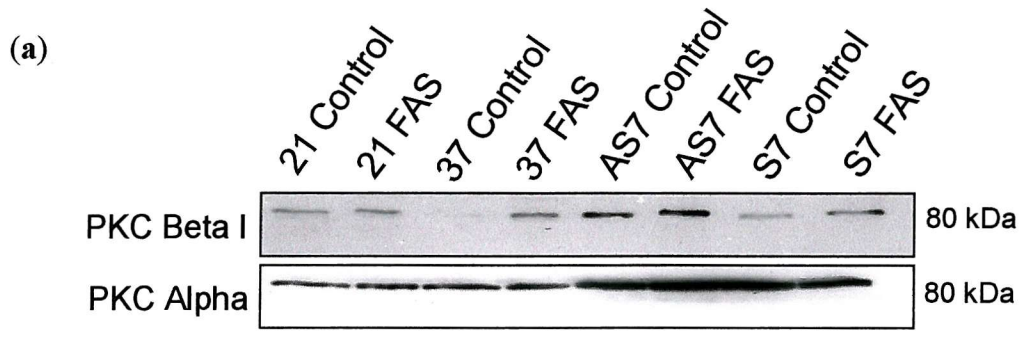

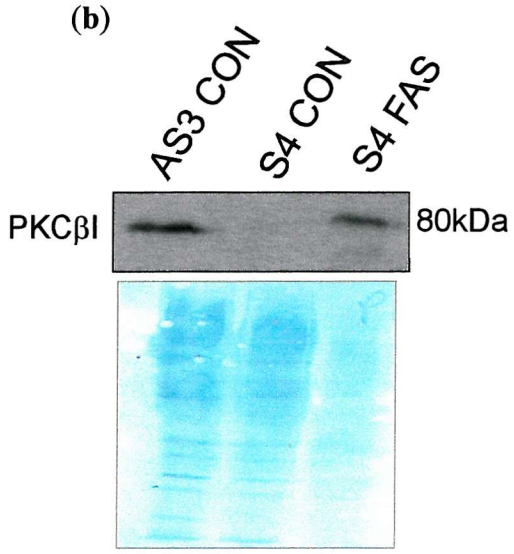

Figure 4.2.22. Expression of *Nramp1* depletes PKCβI levels, an effect reversed by addition of iron. (a) Cells were harvested for protein and western blotted using a PKC βI antibody (santacruz). Extracts were re-ran and probed with a control antibody, PKC α (santacruz). Cell lines were either untreated – control, or treated with 100μM FAS for 24 hours – FAS. (**b**) Cells were treated as in (a), the amido black membrane is shown as a loading control. 21/AS7/AS3 - anti-sense *Nramp1*^{Gly169} lines, 37/S7/S4 – sense *Nramp1*^{Gly169} lines.

Staining a parallel blot with PKCα that is not iron-regulated and appears not to be influenced by *Nramp1* expression revealed comparable loading (fig.**4.2.22 (a)**).

4.2.3 Cell Growth

Cells were first tested for their responsiveness to iron deprivation by growing them (2.2.5) in the presence of desferoxamine for four days at which point they were counted. Figure **4.2.31** demonstrates the effect of iron deprivation on RAW and fibroblast transfectant lines, growth being completely abolished in all lines. This is in accordance with other published reports (142). The difference in cell numbers between untreated RAW and fibroblast lines is likely to be a result of cell contact growth inhibition. This will occur more rapidly in 3T3 fibroblasts, as they are ~ 2-3 times wider than their RAW counterparts.

Figure 4.2.31

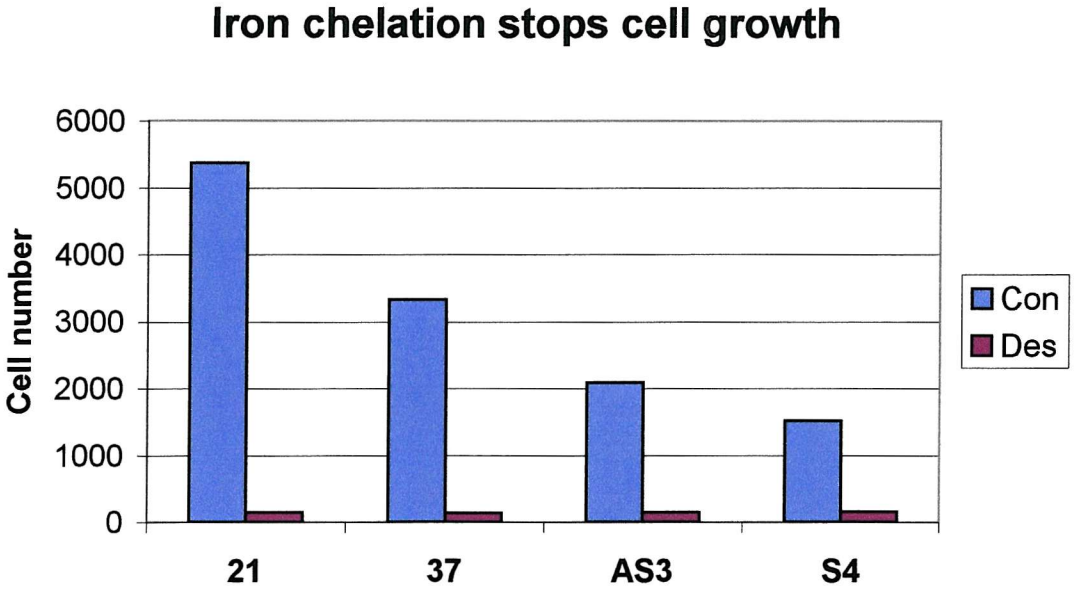

Figure 4.2.31. Iron chelation abolishes cell growth. Cells were plated onto a 96 well plate as in methods (2.2.5) and either treated with 100μM desferoxamine (Des) or control media. Cells were grown for four days before counting. Error bars are not shown but are within 10% of total values.

Showing that iron deficiency is able to stunt cell growth the next step was to examine the effect of *Nramp1* on growth. Figure **4.2.32** is a graph of several separate experiments amalgamated and used to investigate the growth of untreated and iron treated *Nramp1* sense and anti-sense expressing RAW lines. Interestingly addition of iron to the media leads to an increase in growth in all lines suggesting that the iron content of the serum limits proliferation. This was useful in assaying *Nramp1* effects however as it allowed observation of differences between baseline growth and that occurring upon the addition of iron. Using this it is obvious that expression of *Nramp1* attenuates growth even in the presence of iron. The differences between 100μM/200μM FAS treatment of expressing and non-expressing lines is statistically significant using Students t-test. The variation in growth seems amplified upon iron treatment compared to that of controls, where the differences appear small, but *Nramp1* expressing controls show significantly less growth ($p < .05$).

The unforeseen problem with the above results is that while it appears *Nramp1* expressing lines grow slower it would also appear that iron is unable to reverse these effects. This could mean that the constitutive expression of *Nramp1* is the reason the cells are growing at as slower rate. Alternatively it could be that the concentrations of iron being used were toxic to *Nramp1* expressing lines. In pursuit of this difficulty RAW lines were incubated in a range of iron concentrations and the cells counted again after four days. Figure **4.2.33** is an example of a typical experiment and shows that varying iron concentrations do not reverse the effect of *Nramp1* expression. There is consistently about a 30% difference in growth between lines at any iron concentration. This implies that it may be the quantity of Nramp1 protein expression that is having the growth modulatory effect, but comparison of cell lines to mouse PBM would suggest that these levels were within a physiological range (fig. **4.2.12**).

Figure 4.2.32

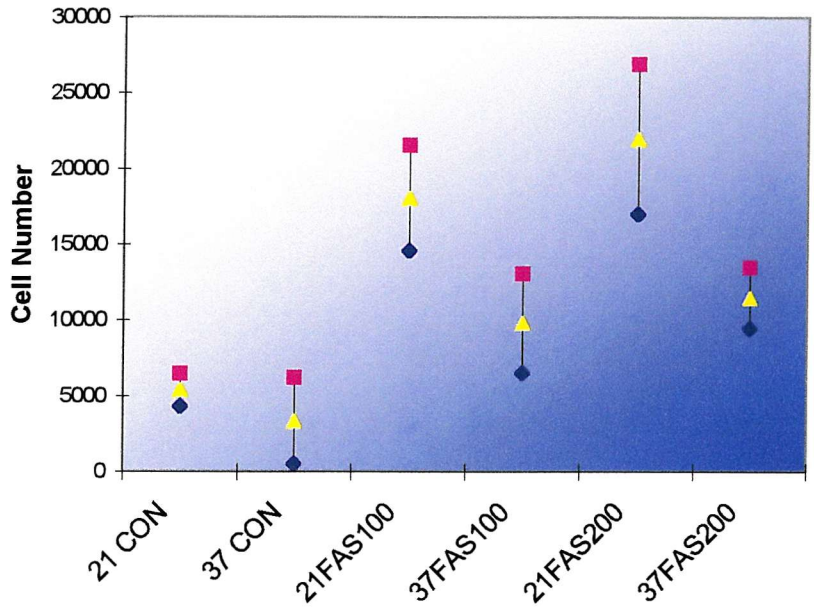

Figure 4.2.32. *Nramp1* expression reduces RAW cell growth. Cells were plated and counted as in methods (2.2.5). Above graph is from the amalgamation of three separate experiments, where plates have been counted on day four. Cells were either left or treated with 100/200μM FAS for the duration of the experiment.

To try and decipher if *Nramp1* could affect cell growth a different protocol was needed. One of the problems with the crystal violet assay is that it was a measure of changes over a long period of time. Also, due to the nature of the assay it is very difficult to get accurate readings of cell numbers below a confluency of ~5000 cells, which correlates to around day 3 and 4 of the assay. The reason for this is that background staining of wells can be variable even with thorough washing, causing a large increase in the standard deviation and making statistical analysis difficult. This can be seen by the large error bars in figure **4.2.32**, **37** control, which as a proportion to the actual number of cells is considerable.

Figure 4.2.33

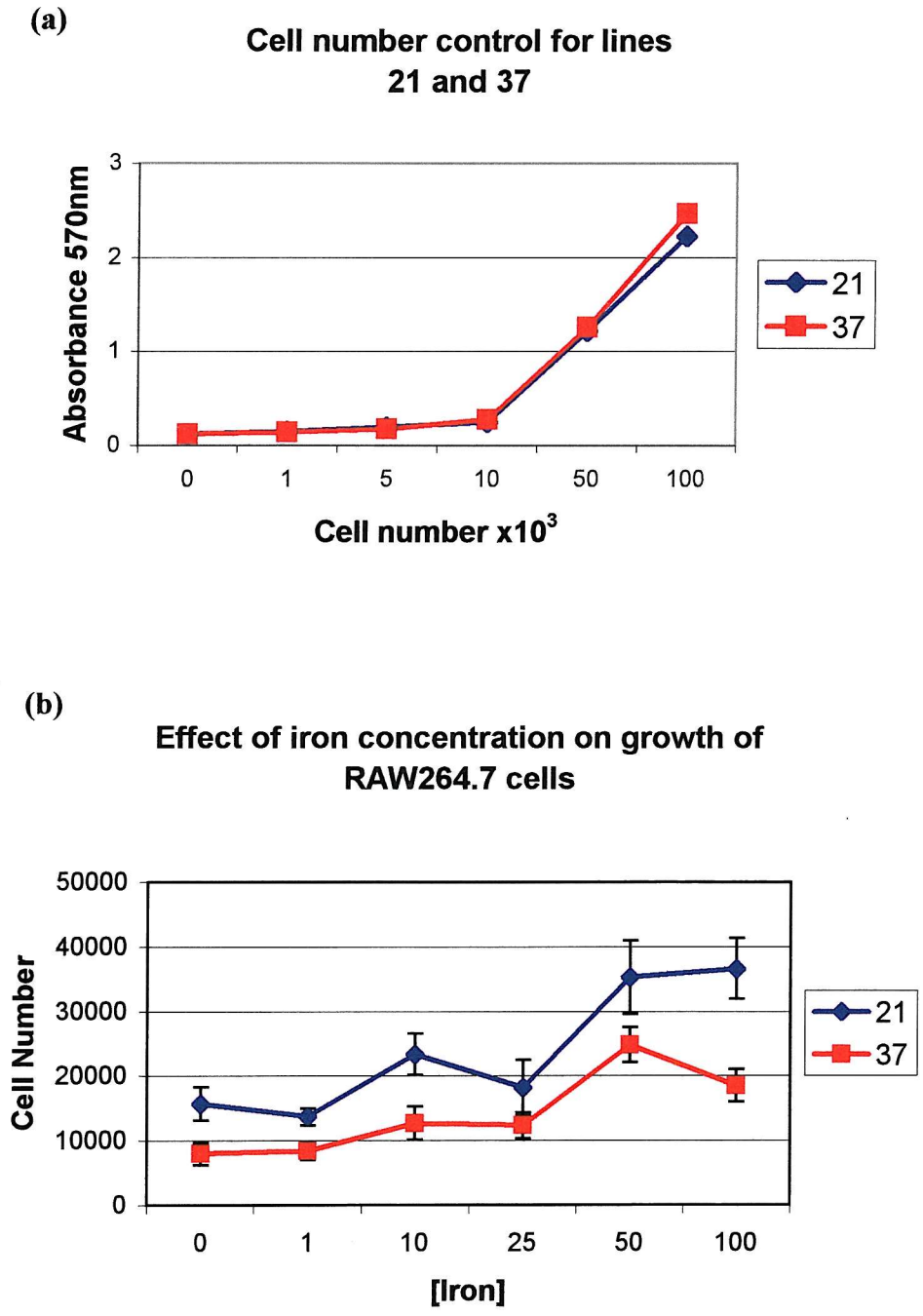

Figure 4.2.33. Chronic iron incubation does not reverse the growth inhibitory effects of *Nramp1*. (**a**) An example of a standard curve after cells have been counted (2.2.5). This is also used as a control to ensure similar cell numbers at the start of any experiment. (**b**) Cells were grown in the presence of FAS at 0, 1, 10, 25, 50 and 100μM for four days before harvesting. Data shows a typical experimental outcome.

The chronic nature of the above assay means the cells have a chance to equilibrate iron within the media through changes in levels of proteins involved in cellular iron regulation, so although a shift in cell growth occurs with addition of iron it is not possible to say if this is a functional effect of *Nramp1* or simply a result of its expression. Therefore the protocol chosen was to measure the incorporation of [^{3}H]-thymidine into cells. This assay has a number of advantages over the crystal violet assay. First, it allows direct analysis of DNA synthesis the rate of which is of primary interest. Second a 'snap shot' of this process is possible due to the sensitivity of the assay only requiring 4 hours of incubation to measure growth rates. Third, equal cell numbers can be plated immediately to a density producing a good signal. Fourth there are no chronic incubation times with excess iron, reducing any effects of equilibration or compensation.

4.2.4 [^{3}H]-Thymidine Incorporation Into Cell Lines

To ensure that the thymidine assay was producing the same growth differences seen in the crystal violet assay control work was done with untreated cells. Results in figure **4.2.41** show [^{3}H]-thymidine incorporation into four lines: **RAW**264.7 parental cells, **21**, **32** and **37** allowing analysis of two expressing and two non-expressing lines, respectively. Crystal violet assay was used to ensure similar numbers of cells between lines, fig.**4.2.41** (**a**). Thymidine incorporation is clearly reduced in expressing lines, fig.**4.2.41** (**b**), and this can be seen particularly with thymidine incorporation expressed in terms of the relative numbers of cells between lines, fig.**4.2.41** (**c**). This curve is a classic growth curve demonstrating that as cell numbers cause strain on the available space and nutrients little further growth can occur.

Figure 4.2.41

(a)

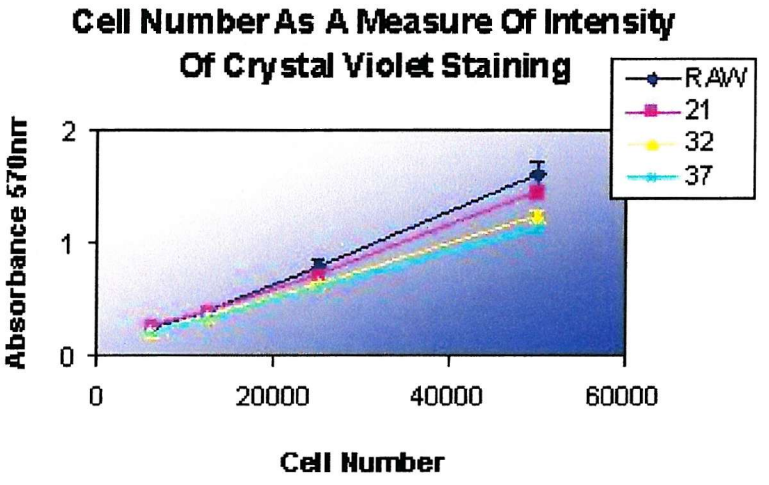

(b)

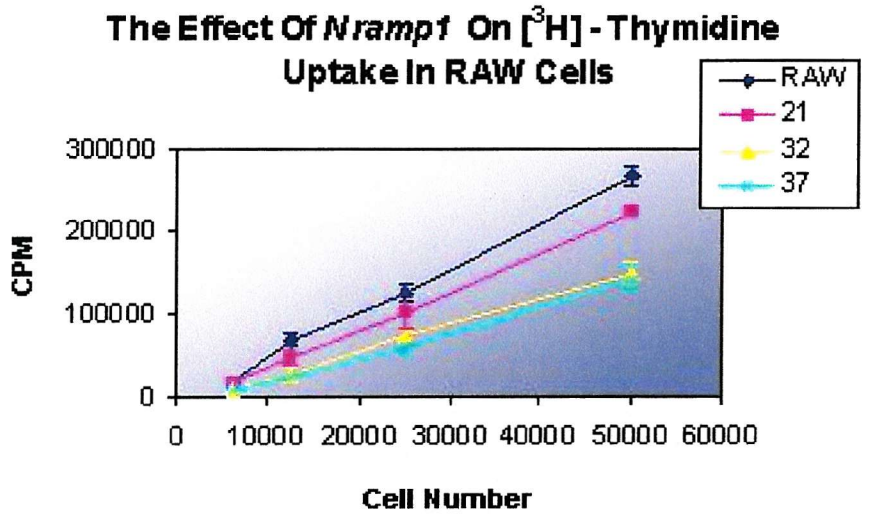

(c)

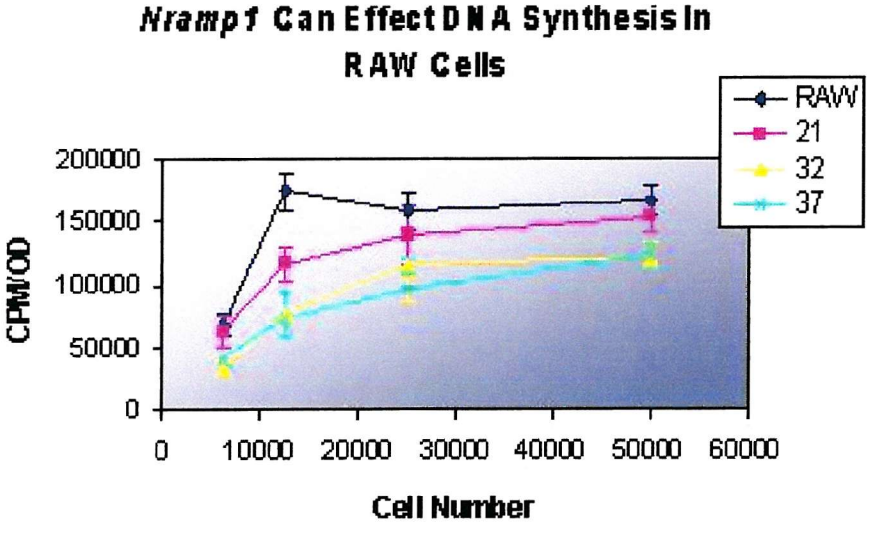

Figure 4.2.41. *Nramp1* reduces DNA synthesis in RAW cells. Cells were plated onto 96 well plates in triplicate at the following densities: 6.25 x 10^3; 12.5 x 10^3; 25 x 10^3 and 50 x 10^3. They were allowed to rest overnight before [^{3}H]-thymidine incorporation was measured (2.2.5). A second plate was set up for crystal violet assay (2.2.5) to allow comparison of cell numbers between the lines. **(a)** This graph shows the OD, from crystal violet assay, of each cell line at their varying cell densities. **(b)** [^{3}H]-thymidine incorporation of each cell line. **(c)** Shows the rate of [^{3}H]-thymidine incorporation per cell with increasing cell density. Data show typical experimental outcome.

Differences between non-expressing and expressing lines are all significant using Students t-test ($p<.05$).

Table 4.2.42 (a)

	RAW	21	37
Control	**99%** (+/- 7%)	**100%** (+/- 7%)	**85%** (+/- 7 %)
FAS	**100%** (+/-10%)	**94%** (+/- 7%)	**99%** (+/- 9%)

(b)

Lines Compared	Un-supplemented Media	Iron Supplemented media
RAW V 37	T = 3.1	T= 0.06
21 V 37	T = 5.3	T = 0.8

Table 4.2.1. Iron reverses attenuation of DNA synthesis caused by *Nramp1* expression. Cells were counted and plated in triplicate onto 96 well plates, 25 x 10^3 cells/well. They were subsequently left overnight with 200μM supplementation of FAS, after which [^{3}H]–thymidine incorporation was assayed (2.2.5). **(a)** Results are expressed as the % incorporation compared to the cell line with the greatest CPM/OD, which has 100% incorporation. **(b)** Differences in incorporation between lines were tested using the Students t-test, $p < 0.05$. T values greater than **1.86** indicate significantly greater growth of non-expressing *Nramp1* RAW lines, RAW and 21. Data is an amalgamation of three repeats.

The next step was to test the effect iron had on the growth of these lines. Interestingly this time iron was able to remove the growth deficit (table **4.2.1 (a)**) and differences between lines were no longer statistically significant (table **4.2.1 (b)**). The percentage differences in thymidine incorporation between expressing and non-expressing lines are lower than that seen during crystal violet analysis of cell growth (~16% compared to 25-30%). This is believed to occur as differences in cell growth will be amplified over the longer time period of this experiment whereas thymidine incorporation is measured between lines with identical cell numbers. Still it would seem that *Nramp1* has only an acute effect on DNA synthesis.

4.2.5 The Effect Of *Nramp1* Expression On Fibroblast Growth

The crystal violet assay was used to evaluate growth in L1 3T3 fibroblasts as cells show a dose dependent increase in growth following iron supplementation; 4 fold above control with 200μM FAS incubation (fig.**4.2.51**, **AS3**), an effect missing in *Nramp1*^{Gly169} transfected cell lines (fig.**4.2.51**, **S4** and **S7**). Differences between iron treated cells are obviously significant but Students t-test ($p < .05$) also shows control growth is significantly greater in AS3 compared to S4/S7 cell lines. The variation seems small in this graph due to the relatively larger growth of iron treated AS3s. Therefore fibroblasts and RAW264.7 cells would seem to handle iron in distinct ways highlighted by their differential ability to proliferate. S7 and S4 cell lines although displaying differences in their response to iron when regulating PKCβI (fig.4.2.22), do not continue this difference in growth assays.

Figure 4.2.51

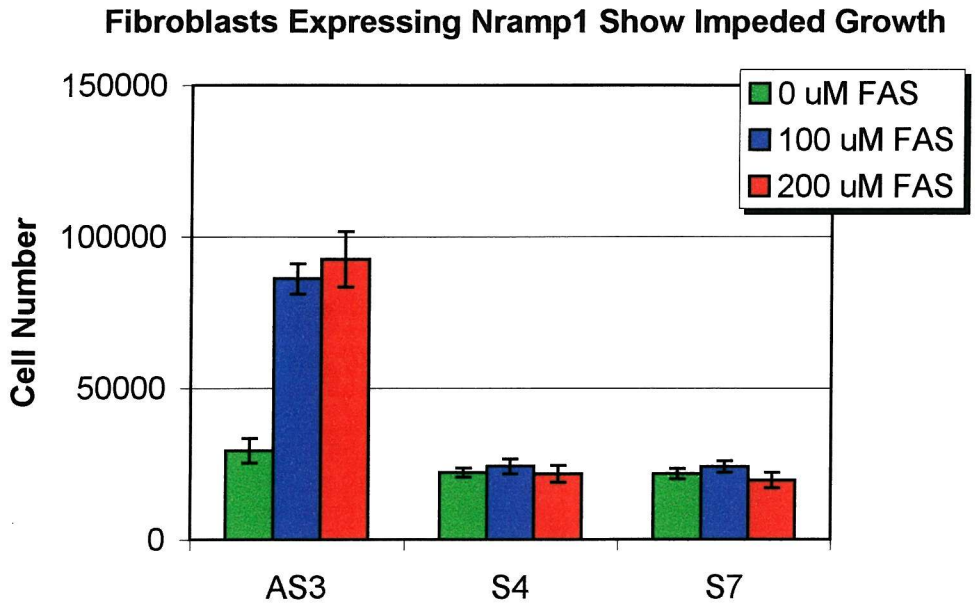

Figure 4.2.51. ***Nramp1*** **expression abrogates iron induced fibroblast growth**. Cells were grown for four days in media containing a range of FAS concentrations before cell numbers were assessed using crystal violet, 2.2.5. Results show a typical experimental outcome and are significant using a Students t-test ($p<.05$).

4.2.6 *Nramp1* protects against paraquat induced oxidative stress

As stated in the introduction (4.1) this experiment was set up to test for differences in the cytoplasmic iron pool through induced oxidative stress using a superoxide donator, paraquat. The results of these experiments suggest that *Nramp1* expressing lines have a higher tolerance for oxidative stress. This was demonstrated by a significantly better ability to grow after exposure to this compound (fig.**4.2.61 21/RAW** vs **32/37**). 32s and 37s were able to reasonably tolerate this even up to 1mM paraquat.

Figure 4.2.61

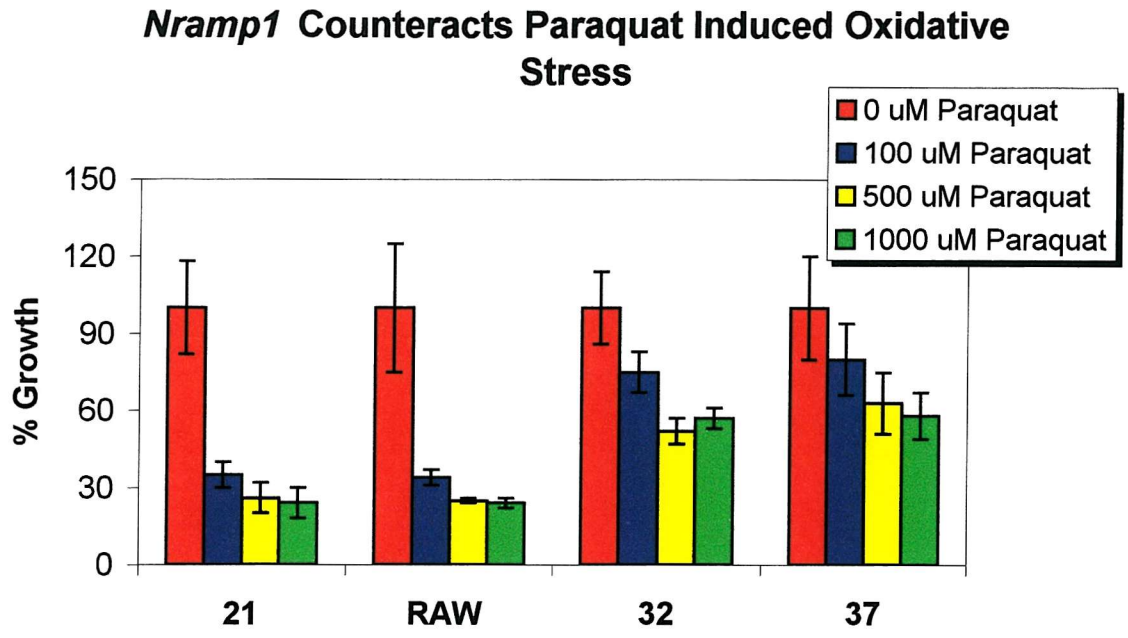

Figure 4.2.61. *Nramp1* expression counteracts paraquat induced oxidative stress. Cells were harvested and suspended, for 5 hrs, in media containing 0, 100, 500 or 1000 μM paraquat. They were then spun down and re-suspended in normal media before being plated onto a 96 well plate, 1000 cells/well 12 repeats. After 5 days in culture viable cell numbers were assayed using crystal violet staining (2.2.5). Results show a typical experimental outcome and are expressed as the % growth compared to un-treated cells. Results are significant using Students t-test ($p<.05$).

4.3 Discussion

The experimental designs employed in this chapter were chosen to test the cytoplasmic iron pool, non-invasively, for differences in *Nramp1* expressing and non-expressing cell lines. This was done using constitutively expressed *Nramp1* in RAW264.7 and L1 3T3 fibroblasts. The inherent problem with this study is that experiments were done using constitutive expression of *Nramp1* and no other lines were produced expressing constitutive protein as a control. This could be done using vectors containing the susceptible *Nramp1* sequence Asp169. In the absence of this

levels of protein were compared from the highest Nramp1 protein expressing line to IFN-γ treated PBM. These results suggested levels were similar between the two allowing a greater confidence in the viability of expressing lines.

Studies by Alcantara *et al.* (140) showed regulation of PKCβ mRNA by iron, but not PKCα, in HL-60, K562 and U937 cell lines. Here it is shown that PKCβI protein levels are regulated by iron in RAW264.7 and L1 3T3 fibroblasts. PKCβI is produced by alternative splicing of PKCβ mRNA producing two isoforms βII and βI (96). This study shows PKCβI protein is up-regulated in response to iron but no changes in PKCα expression were noted consistent with the Alcantara group. In addition PKCβI expression is clearly regulated in a way that is suggestive of decreased cytoplasmic iron in *Nramp1* expressing lines. Iron was also able to remove the apparent block in *Nramp1* expressing cells with increased expression similar to that in non-expressing lines. These results conflict with those produced by Olivier *et al.* (95) where immortalised macrophage lines from congenic *Nramp1* resistant and susceptible mice had no discernable difference in PKCβ protein expression. This may be attributable to differences in Nramp1 expression, as this group were using resting macrophages and although no western blot of Nramp1 was included expression levels will be lower than activated macrophages, resulting in a weaker *Nramp1* phenotype. The expression system in our study produced constitutive levels of Nramp1 comparable to an activated wildtype macrophage. In addition, regulation of wildtype *Nramp1* in immortalised cells has not been thoroughly investigated and levels will be very different depending on the time of immortalisation during differentiation of the macrophages. Early immortalisation would lead to very low levels of *Nramp1* expression as this gene is switched on during maturation (143). Finally the Olivier group was using antibodies to PKCβ and was therefore detecting both isoforms. It is

possible that that these two isoforms are regulated in an independent manner, minimising differences between cell lines.

The growth rate of cell lines was the next parameter tested, working with the hypothesis that effects on cytoplasmic iron may relate to the activity of ribonucleotide reductase, which requires iron for its catalytic activity. To this end cells were allowed to grow over four days before being counted using a crystal violet assay. *Nramp1* expressing RAW cell lines tested in this way showed a slower growth rate. Addition of iron produced similar growth deficits, but did cause increased growth in all lines. As this effect was a culmination of culture over four days it was impossible to say if growth differences were an effect of *Nramp1* function or simply its constitutive expression. Knowing that the cells were responding to iron from the PKCβI assays taking place overnight, a new assay was employed. Using tritiated thymidine it was possible to see a similar growth deficit, in four hours, in *Nramp1* expressing lines, but this time iron was able to reverse the effect. Interestingly fibroblast lines tested using crystal violet after four days growth showed a strong phenotype, *Nramp1* expressing lines unresponsive to iron. This may reflect differences in the way the two lines handle iron, for instance macrophages of the liver and spleen are responsible for >80% of iron recycling from effete red blood cells. Macrophages will therefore be geared towards the handling and release of iron. Fibroblasts on the other hand largely require iron for their own growth needs and may be less efficient at releasing it. Macrophages grown in culture over four days are as a result more likely to adjust to their iron surroundings quickly whereas fibroblasts may not, amplifying the effect of *Nramp1*. The results would suggest therefore, that Nramp1 is sequestering iron away from the cytoplasm reducing induction of PKCβI expression and also decreasing the rate of DNA synthesis where a likely target is ribonucleotide reductase.

Lastly it was shown that expression of *Nramp1* in RAW cells protects against oxidative stress. This would occur if levels of free iron in the cytoplasm were reduced decreasing Haber-Weiss reactions and radical chain propagation in the cytosol.

Together all three results suggest that *Nramp1* is effecting cellular iron distribution in a way that reduces levels of the metal in the cytoplasm. Whether this is a direct effect or through *Nramp1* modulation of another protein is impossible to say. However, because of the role other members of the *Nramp* family have in iron transport it is logical that Nramp1 could be directly affecting iron. In keeping with the evidence this would require Nramp1 to pump iron into an intracellular vesicle. Nramp1 localises to late endosomes and lysosomes and due to the dependence of the transporter on hydrogen ions, it would seem likely an antiport mechanism would be in operation; as has been shown for other divalent cations transported by Nramp1 in *Xenopus* oocytes (94). For a symport model to work hydrogen ions would have to be forced against the large concentration of hydrogen ions in the lumen of late endosomes and lysosomes, requiring energy. There is no literature to suggest Nramp1 or any other member of the Nramp family requires ATP for transport. Pointed criticism by groups against the antiport model manifests as the high homology between Nramp1 and Nramp2. *Nramp2* has conclusively been shown to code for a symport transporter, a discovery that has marked Nramp1 and led to the belief that it must transport divalent cations out of vesicles down a hydrogen ion gradient. The high homology does not necessarily dictate this to be true however, a phenomenon arising in the multidrug resistance transporter family. MDR1 is over expressed in most multidrug-resistance cell lines, and confers multidrug resistance when transfected and over expressed in otherwise drug-sensitive cells (144). However, although MDR2 shows 78% overall amino acid identity and has the same predicted

domain organization as MDR1, MDR2 protein does not confer multidrug resistance and functions as a phosphatidylcholine flippase (145). Nramp1 and Nramp2 have only 66% identity and ~77% similarity. As mentioned, Goswami *et al.* recently suggested the antiport model for Nramp1 after studies in *Xenopus* oocytes (94), and it would therefore appear that the high homology in the *Nramp1* family does not dictate functional identity, as in the MDR family.

Interestingly studies by Cabantchik and colleagues have demonstrated a sturdy link between levels of iron within the labile iron pool (LIP), ferritin expression, growth and oxidative stress(146;147). Ferritin over expression led to a decrease in the size of LIP and a subsequent attenuation in cell growth upon activation of H-ras compared to controls(146). In addition a separate paper by the group showed that over expression of H-ferritin could protect against oxidative stress through decreasing the labile iron pool(148). These data are consistent with the *Nramp1* effects above that may also precipitate due to a decreased LIP brought about by *Nramp1* expression.

In conclusion it is interesting to speculate on the role of *Nramp1* as a putative antioxidant protein. This has been reported for *S.typhimurium* and *E.coli Nramp* orthologues (128), and in reference to 3.3 TRANSFAC analysis of an extended part of the *Nramp1* promoter has identified putative antioxidant response elements (ARE) (unpublished). The results from this chapter also imply that *Nramp1* expression leads to depletion in the levels of the labile iron pool, possibly through sequestering iron within an internal vesicular system.

Chapter 5

Cellular Localisation Of Nramp1

5.1 Introduction

Chapter 4 examined processes that are established to be dependent on iron; radical production, cell proliferation and PKCβI transcriptional expression, furthermore chapter 3 demonstrated that *Nramp1* expression is regulated by iron and a synthetic analogue of a major product of erythrocyte breakdown, hemin. Our interpretation of these data was that *Nramp1* expression causes iron to be sequestered within an internal vesicular system. Unpublished results by our group have shown that *Nramp1* expressing RAW cells phagocytosing anti-transferrin immune-complexed ^{59}Fe-labelled transferrin release more ^{59}Fe than non-expressing lines during zymosan uptake (not shown). This is believed to occur as a result of lysosome fusion with the plasma membrane releasing iron to the extracellular media; zymosan induced exocytosis involves the de-acidification of lysosomes and has a partial requirement for PKC, otherwise little is known about the mechanism (149;149). In order to establish if Nramp1 was present on lysosomes secreted during zymosan uptake, linking it with iron release, Nramp1 was tagged with enhanced green fluorescent protein (EGFP). In addition to this fibroblasts are known to exocytose their lysosomes during treatment with calcium ionophore and were also used in study of Nramp1 movement.

Mouse *Nramp1* contains five consensus protein kinase C (PKC) phosphorylation motifs, S/T-X-R/K. Three of these are located in its predicted cytosolic N-terminal domain 1 between TM 6-7 and the last in the C-terminal cytoplasmic tail. Figure

5.1.1 shows a clustal X alignment of the N-terminal domain of vertebrate Nramp1. The highlighted residues indicate the consensus PKC motifs, and shows that the first PKC site in mice is not conserved with other species. The later two sites show 80-100% identity, suggesting that perhaps these two sites have the greater functional importance, or the first site specific to the function of Nramp1 in mice.

Analysis of this region suggests it could be a putative Src homology 3 (SH3) binding domain. It also shows structural homology to the proline rich region of microtubule-associated protein 4 (MAP4)(41). Indeed, Tokuraku *et al.*, demonstrated that NRAMP1 could bind α and β tubulin (41). This has lead to the speculation that Nramp1 could link and un-link from the microtubule system and to some extent control movement of Nramp1 positive vesicles, and its own movement around the cell. In fact serine phosphorylation in other proteins has been shown to effect their localisation (150). *Nramp1* contains putative localisation motifs that are consistent with its vesicular location, and during macrophage phagocytosis of particles Nramp1 rapidly translocates from a largely peri-nuclear region to the periphery of the cell (24). It is hypothesised that specific changes in the phosphorylation of the MAP4 like domain could control binding to microtubules, or another unknown protein, allowing Nramp1's rapid translocation.

The three serines critical for putative N-terminal phosphorylation were mutated to alanine through modification of their codons. This mutant construct (p-nut) was then stably expressed in RAW264.7 and L1 3T3 fibroblasts to examine its function and localisation. In addition an EGFP-p-nut construct was made in order to study its movement in parallel to studies undertaken for Nramp1 (above), discerning any differences between the two.

Figure 5.1.1

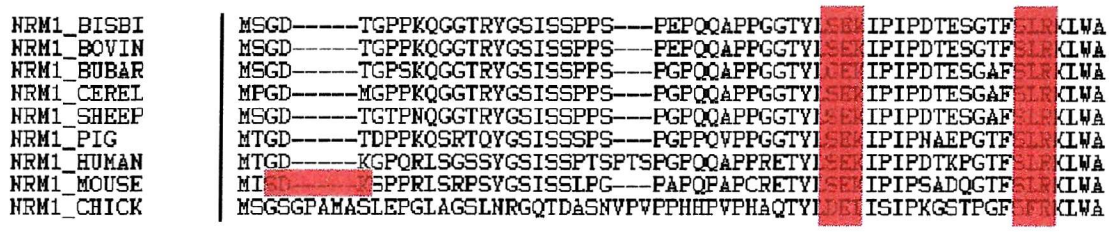

Fig.5.1.1. Clustal X alignment of vertebrate Nramp1 protein sequences: Alignment shows the N-terminal domain from each species. Highlighted residues show the homology between PKC phosphorylation motifs.

This study provides a link between lysosomes and secretion of iron that is modulated by *Nramp1*. In addition it is shown that both EGFP-tagged Nramp1 and p-nut chimeras are targeted in an identical manner both localising to vesicles that are described in the literature as containing this protein. Interestingly both chimeras also localise to vesicles containing zymosan suggesting phagocytosis is a general stimulus for Nramp1 movement, but also that removal of putative N-terminal PKC sites from *Nramp1* has no effect on targeting. Unexpectedly replacement of the N-terminal putative PKC sites leads to alternative glycosylation of this protein as demonstrated by SDS-PAGE and treatment with PNGaseF; this is discussed.

5.2 Results

5.2.1 The Construction Of A Phosphorylation Mutant Expression Vector

The three N-terminal putative PKC motifs were removed by substitution of the serine residue for structurally similar but non-modifiable alanine. This was achieved by synthesis of four unequally sized oligos replacing an alanine codon for that of

serine. The sequence is otherwise identical to that published previously (33) (GenBank Acc.No X75355) from 12 bp to an internal XmaI site, position 284-289 bp, in the murine *Nramp1* cDNA. The addition of a 5' SalI restriction site was required for subsequent cloning, as were the sticky ends for both the 5' SalI and 3' XmaI site formed after oligo annealing.

The oligos were annealed (fig.**5.2.11**) and purified by electroelution (2.2.16), however direct insertion of the oligo into the pHβA-1-neo expression vector containing wildtype *Nramp1* (p-wil) (151) could not be achieved. This is due to the presence of multiple XmaI sites in the vector sequence. Therefore cloning required an additional subcloning step into an *Nramp1* pBluescript SK (+/-) subclone that has a unique XmaI site. Figure **5.2.13** shows the construction of the vector diagrammatically and figure **5.2.12** (**a**) orientation digests. The 2203 bp *Nramp1* cDNA was ligated into the BamHI site of pBluescript and appropriate orientation clones selected with restriction endonuclease digestion using HindIII. Antisense orientation products generate a diagnostic fragment of approximately 700 bp, whereas sense fragments are approximately 1.5 kb. In order for subsequent cloning to work correctly the antisense orientation was required. Other digests were performed to double check correct insertion. These include:

- BamHI: 2.2 kb *Nramp1* insert drop out
- SmaI or XmaI: 300 bp drop out if in antisense orientation
- SalI: Linearisation

The above criteria were met for both clones tested. This allowed subsequent removal of the residues between the internal *Nramp1* XmaI site and a SalI site located in the pBluescript polylinker.

Figure 5.2.11

(a)

1S

5'**TCGAC**GAGGGAGCTAGTTGCCAGGCCTGGTGACCACACACAGAGTATC
CTGCCGCCTGCGTCCTC**ATG**ATT**GCG**GACAAGAGCCCCCCGAGGCTGAGC
AGGCCCAGTTATGGCTCCATTTCCAGCCTG 3'

2S

5'CCTGGCCCAGCACCTCAGCCAGCGCCTTGCCGGGAGACCTACCTG**GCG**G
AGAAGATCCCCATTCCCAGCGCAGACCAGGGTACATTC**GCC**CTGAGGAAG
CTGTGGGCGTTCACGGGGCCTGGTTTCCTCATGAGCATCGCTTTCCTTGA**C**
3'

3A

5'**CCGGG**TCAAGGAAAGCGATGCTCATGAGGAAACCAGGCCCCGTGAACG
CCCACAGCTTCCTCAG**GGC**GAATGTACCCTGGTCTGCGCTGGGAATGGGG
ATCTTCTC**CGC**CAGGTAGGT 3'

4A

5'CTCCCGGCAAGGCGCTGGCTGAGGTGCTGGGCCAGGCAGGCTGGAAAT
GGAGCCATAACTGGGCCTGCTCAGCCTCGGGGGGCTCTTGTC**CGC**AATCA
TGAGGACGCAGGCGGCAGGATACTCTGTGTGTGGTCACCAGGCCTGGCAA
GTAGCTCCCTC**G** 3'

(b)

Figure 5.2.11. p-nut oligo annealing. (**a**) Sequences of each synthetically made strand used in the synthesis of the PKC knockout (p-nut) are shown. **1S** and **2S** contain the coding strand, whereas sequences **3A** and **4A** encode the antisense strand. Residues highlighted in red show the position of the SalI motif. Residues highlighted in green show the position of the XmaI motif. Yellow highlighting indicates the position of the start codon and bold lettering the substituted alanine codons. (**b**) Diagram indicating how each strand interacts to form the required double stranded mutant insert.

At this point the mutant sequence (fig.**5.2.11 (a)**) was ligated into this site to produce a murine *Nramp1* sequence devoid of all 5' PKC sites. Figure **5.2.12 (b)** shows the cut pBluescript vector with the subsequent approximate 300 bp drop out and also the annealed mutant oligos. The slight size discrepancy is due to the addition of polylinker residues on the drop out which are not present in the mutant insert. In order to check for the correct mutant insert clones, diagnostic restriction included the use of XmaI and EcoRI (fig.**5.2.12 (c)**). In the mutant clones both XmaI and EcoRI sites will be removed from the pBluescript polylinker. Cutting with XmaI will not produce a 300 bp drop out, as only the *Nramp1* internal site will be present. In addition EcoRI will not linearise the plasmid if the mutant insert is present in the murine *Nramp1* cDNA. The addition of a 5' SalI restriction site was required for subsequent cloning, as were the sticky ends for both the 5' SalI and 3' XmaI site formed after oligo annealing. Clone 1 is the only clone to for fill these criteria. In addition a double digest using SalI and XbaI was used to check the whole *Nramp1* sequence was present. Presence of internal and polylinker XbaI sites should produce fragments of about 3kb, 1.5kb, and 670kb in the mutant clones. The smallest fragment will again be slightly bigger if the wildtype insert is present due to additional polylinker sequence. Figure **5.2.13** shows this cloning step diagrammatically.

Figure 5.2.12

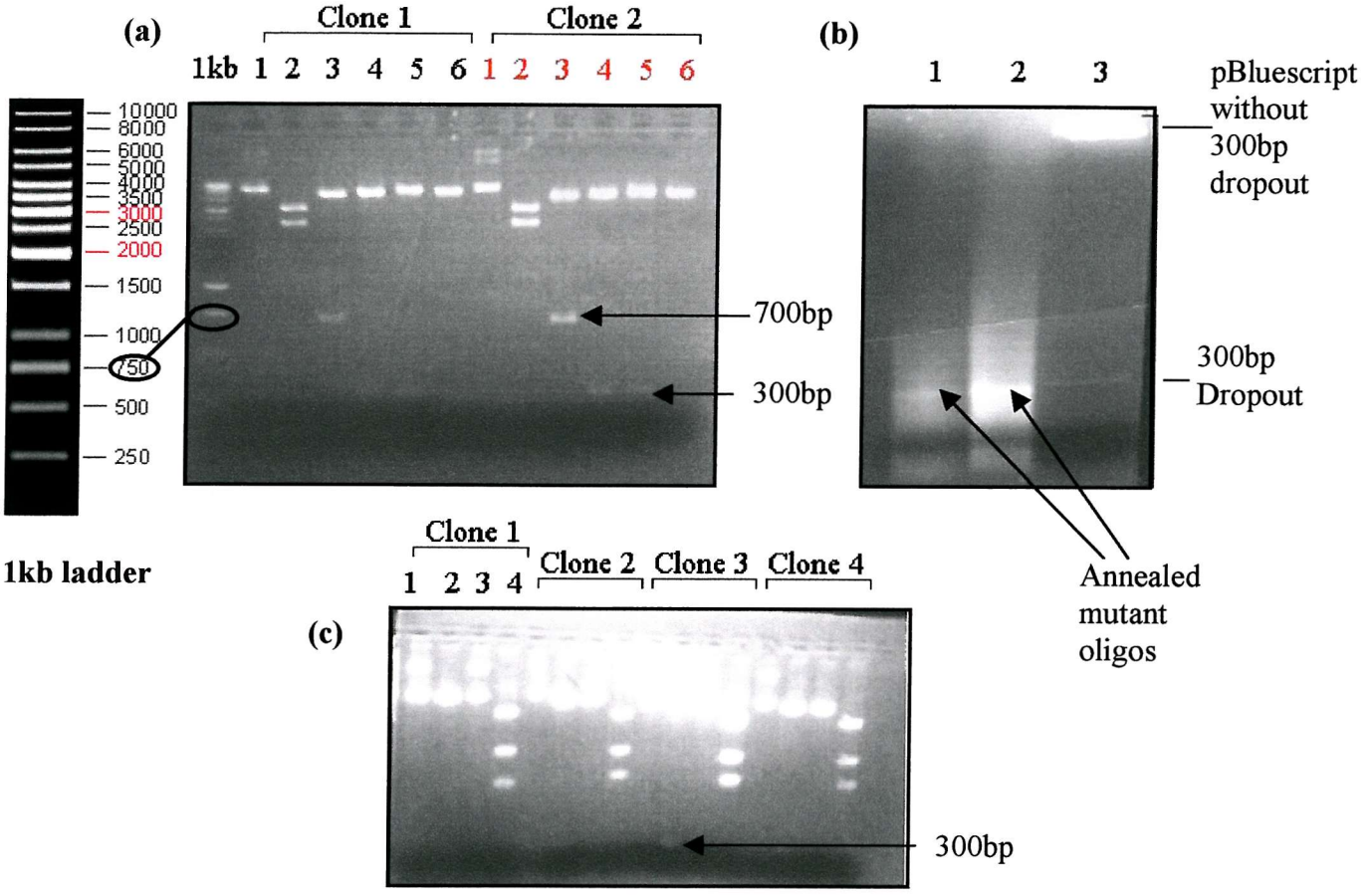

Figure 5.2.12. Cloning digests I.

(a) Digestion of clones with: (1) uncut (2) BamHI (3) HindIII (4) SmaI (5) XmaI (6) SalI.

	Uncut	BamHI	HindIII	SmaI	XmaI	SalI
Band size(s) from sense clones	~10.2kb	8kb 2.2kb	8.7kb 1.5kb	8.3kb 1.9kb	8.3kb 1.9kb	10.2kb
Band size(s) from antisense clones	~10.2kb	8kb 2.2kb	9.7kb 700bp	9.9kb 300bp	9.9kb 300bp	10.2kb

(b) **1** and **2** annealed oligos (**3**) XmaI/SalI plasmid showing drop out.

(c) **1** = uncut, **2** = SmaI, **3** = EcoRI and **4** = SalI/XbaI

	Uncut	SmaI	EcoRI	SalI/XbaI
Band size(s) with wildtype insert	~5.2kb	4.9kb 300bp	5.2kb	3kb,1.5kb, 720bp
Band size(s) with mutant insert	~5.15kb	5.15kb	~5.15kb	3kb,1.5kb, 650bp

Figure 5.2.13

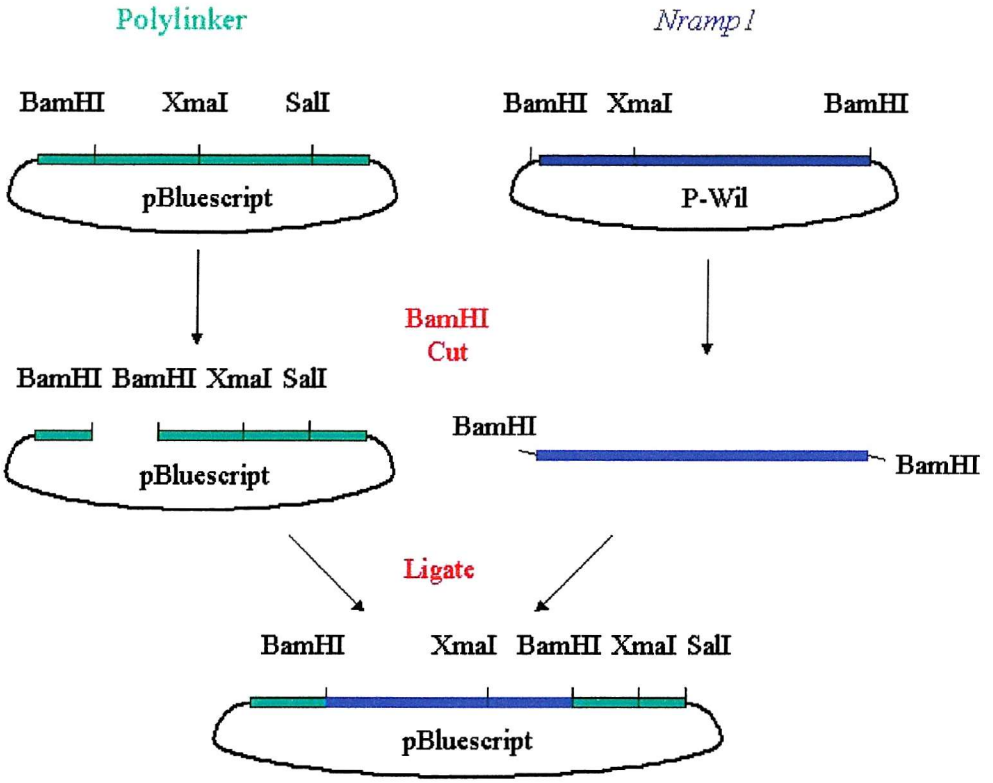

Figure 5.2.13. Cloning step I. Flow chart showing the cloning of wildtype Nramp1 from pHβA-1-neo (P-Wil) into pBluescript via a BamHI restriction site.

Once the mutant insert was present in pBluescript it was directionally subcloned into pHβA-1-neo via SalI and BamHI (fig.**5.2.15**). Diagnostic digests using BamHI and BamHI/HindIII double digests were performed to analyse clonal insertion. A BamHI single digest should only linearise (fig.**5.2.14 (b)**), which it appeared to do in every clone assuming the control plasmid was nicked. The double, BamHI/HindIII, digest should produce a drop out of about 1.5kb in positive clones (clone **3**, fig.**5.2.14 (c)**). Figure **5.2.16** shows the final cloning steps to form the p-nut mutant expression vector.

Figure 5.2.14

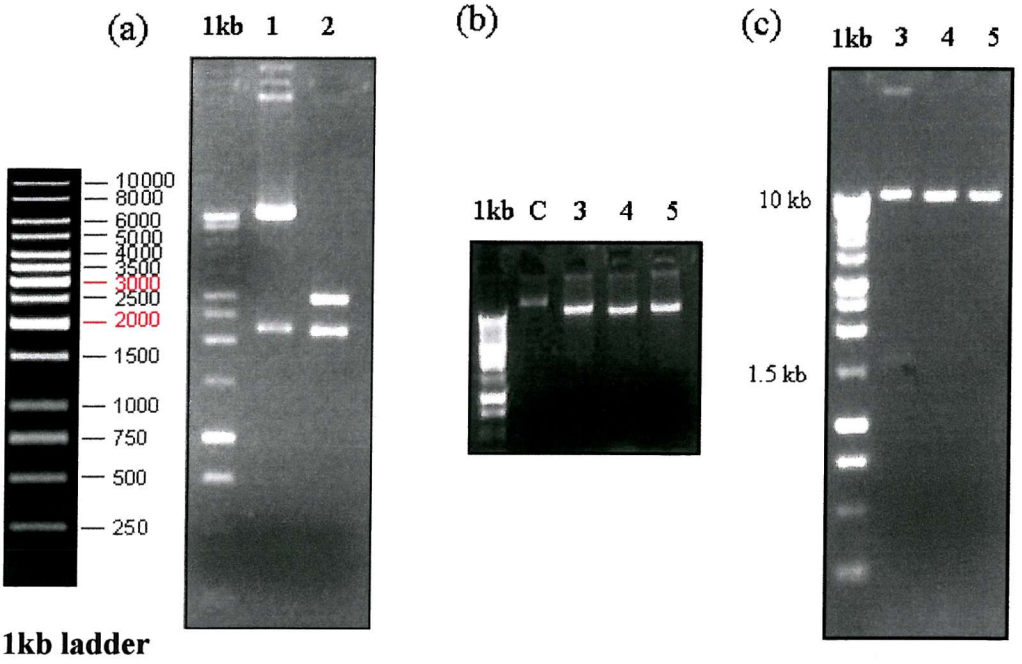

Figure 5.2.14. Cloning digests II. Restriction digests of clones. (**a**) (1) is pHβ A-1-neo wildtype vector cut with SalI and BamHI (2) is the mutant *Nramp1* in pBluescript cut with SalI and BamHI.

	pHβ A-1-neo cut with SalI and BamHI	**mutant *Nramp1* in pBluescript cut with SalI and BamHI**
Fragment size(s)	~10kb and 2.2kb	3kb and 2.15kb

(**b**) C = uncut vector, 3-5 = p-nut clones cut with BamHI. Ie after insertion of mutant insert into pHβ A-1-neo.

(**c**) Clones 3-5 were then cut with BamHI and HindIII to definitively show insertion.

	BamHI and HindIII
Size of bands with mutant insert	10kb and ~1.5kb
Size of bands without mutant insert	10kb

Figure 5.2.15

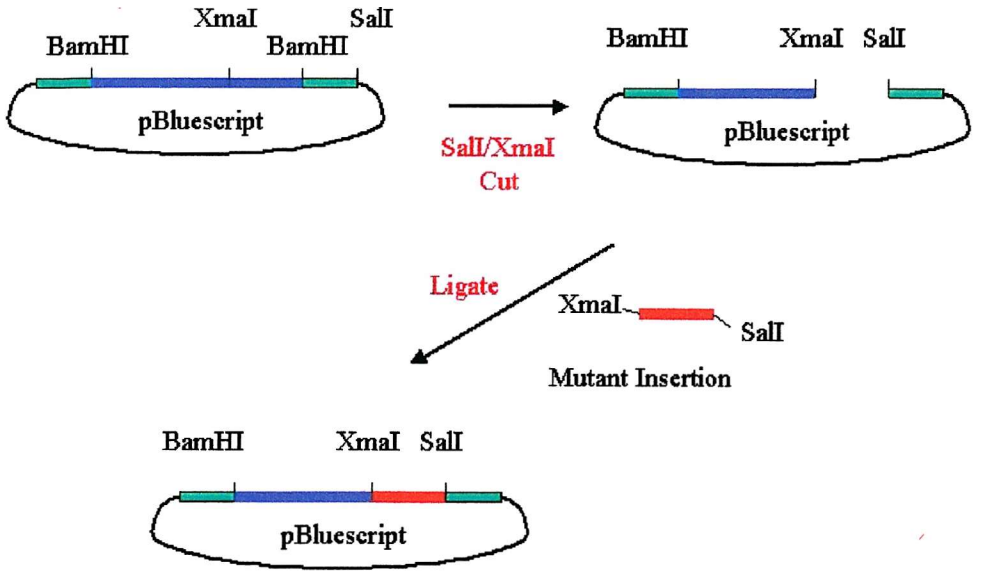

Figure 5.2.15. Cloning step II: Flow diagram showing the removal of a 5' part of the wildtype *Nramp1* sequence with subsequent insertion of a identical sequence; except for substitution of three serine codons for alanine (fig 5.2.11).

Figure 5.2.16

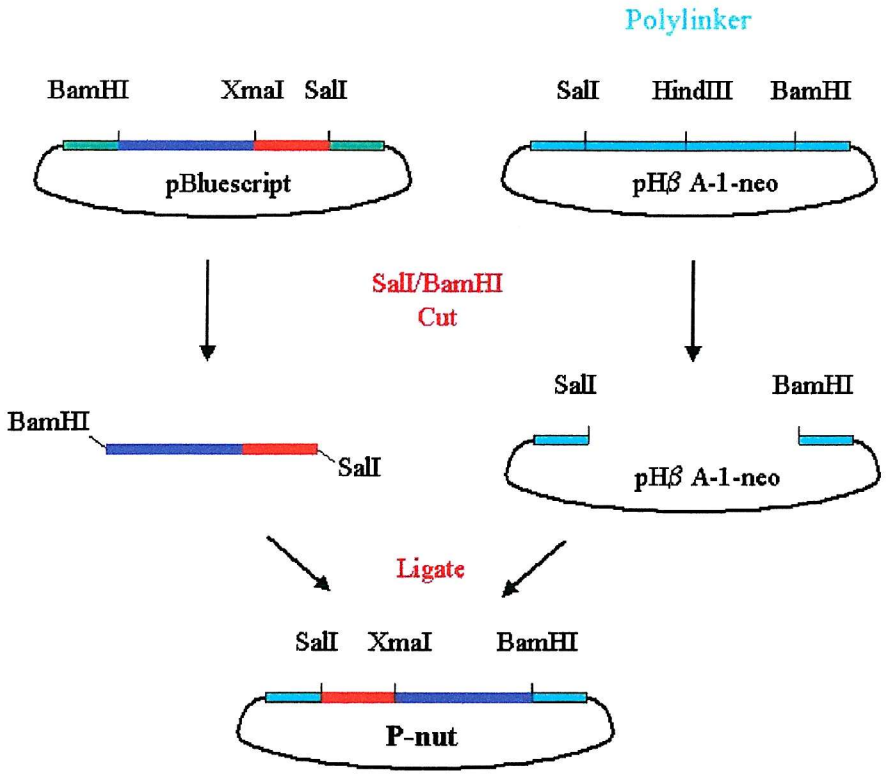

Figure 5.2.16. Cloning step III: Flow chart showing the cloning of mutant *Nramp1* into pHβA-1-neo to form the p-nut mammalian expression vector.

After cloning the p-nut construct was sent for sequencing (Oswel, Southampton). Figure **5.2.17** shows that all three serine codons in wildtype *Nramp1* were successfully mutated to alanine codons.

Figure 5.2.17

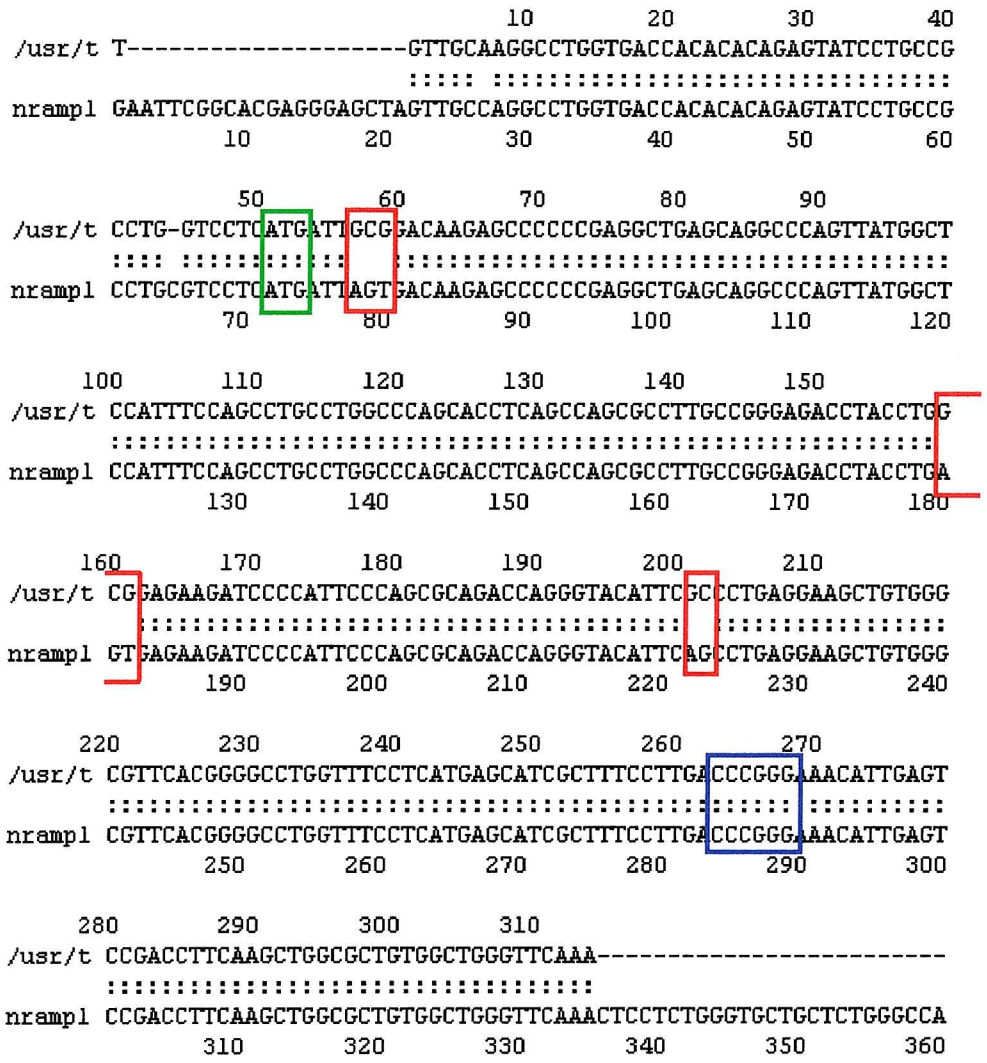

Figure 5.2.17. p-nut sequencing identifies that all modifications are complete. Sequencing of the mutant construct shows that all three serine codons have been modified to alanine codons (red squares) removing the putative PKC sites. Wildtype *Nramp1* sequence corresponds to the bottom sequence and the PKC mutant to the top. The ATG codon is highlighted in green and the blue square indicates the consensus XmaI site.

5.2.2 Expression Of The Mutant Construct In RAW 264.7 Cells

Immune blotting of Nramp1 using extracts from stable clones expressing the mutant construct (referred to as p-nut from here on) show protein mobility discrepancies in comparison to wildtype extracts. The HMW, 90-100 kDa in

wildtype, bands from p-nut extracts progress further into the denaturing gel than that of the wildtype, however the 45-kDa LMW Nramp1 band appears to be affected in this manner only slightly or not at all (fig.**5.2.21**).

Figure 5.2.21

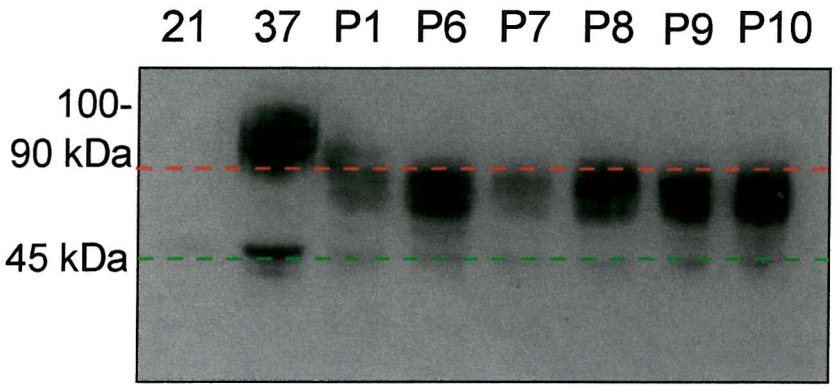

Figure 5.2.21. P-nut protein size shifts. Samples were western blotted using an 8 % denaturing acrylamide gel. P1/P6-P10 are individual p-nut clones. The red line depicts the difference between the upper mature Nramp1 wildtype and lower p-nut bands. The green line shows that the immature band may only shift slightly.

Analysis of RAW p-nut clones. Unlike wildtype Nramp1 expression in RAW cells, levels of p-nut protein were gradually lost over two months limiting experimental analysis of these clones. Inspection of the p-nut DNA sequence showed that the alanine codons replacing those of serine in the wildtype sequence introduced possible methylation sites. Methylation has been implicated in extinction of transfected gene expression over a similar time period in other cell lines(152). No further study of this phenomenon was carried out.

Removal of carbohydrate using PNGaseF treatment of protein extracts from wildtype and p-nut expressing cell lines reconstitutes a protein species that when run on

a SDS gel produces a diffuse band of roughly similar mass between all lines. This migrates a little further through the gel than the 45kDa band and consists of a single sharp intense band that can be followed by 1-3 sharp less intense bands or diffuse protein becoming weaker towards the end of the gel (fig.**5.2.22**). Fig.**5.2.22 (a)** compare two p-nut lines (3/4 and 5/6) with the wildtype line 37 (1/2) before and after treatment with PNGaseF. Before treatment there is a striking difference between the sizes of the HMW bands {1(**a**) compared to 3 and 5 (**a**)}, as seen before. After treatment reconstitution of Nramp1 protein without carbohydrate produces, as described, sharp and diffuse bands with both p-nut and wildtype extracts. The primary band to appear resides slightly lower than that of the LMW polypeptide shown clearly in fig.**5.2.22 (a)** highlighted by the black star. Both the LMW band and reconstituted band are similar between all lines tested.

If the ratio of protein concentration:PNGaseF is varied to favour a greater proportion of protein then it is possible to see a partial removal of carbohydrate from Nramp1 protein. Fig.**5.2.22 (b)** lane 2 shows this occurring in cell extracts from 37s (wildtype) with an intermediately diffuse band (white star) that travels to a similar point as the lower portion of the HMW untreated p-nut Nramp1 polypeptide in lane 3. Unfortunately this partial action could never be reproduced in p-nut cell lines. Although partial digestion of 37 extracts occurs, reconstitution of the lower sharp band is also seen in both lanes 2 and 4 containing wildtype and p-nut extracts respectively.

Figure 5.2.22

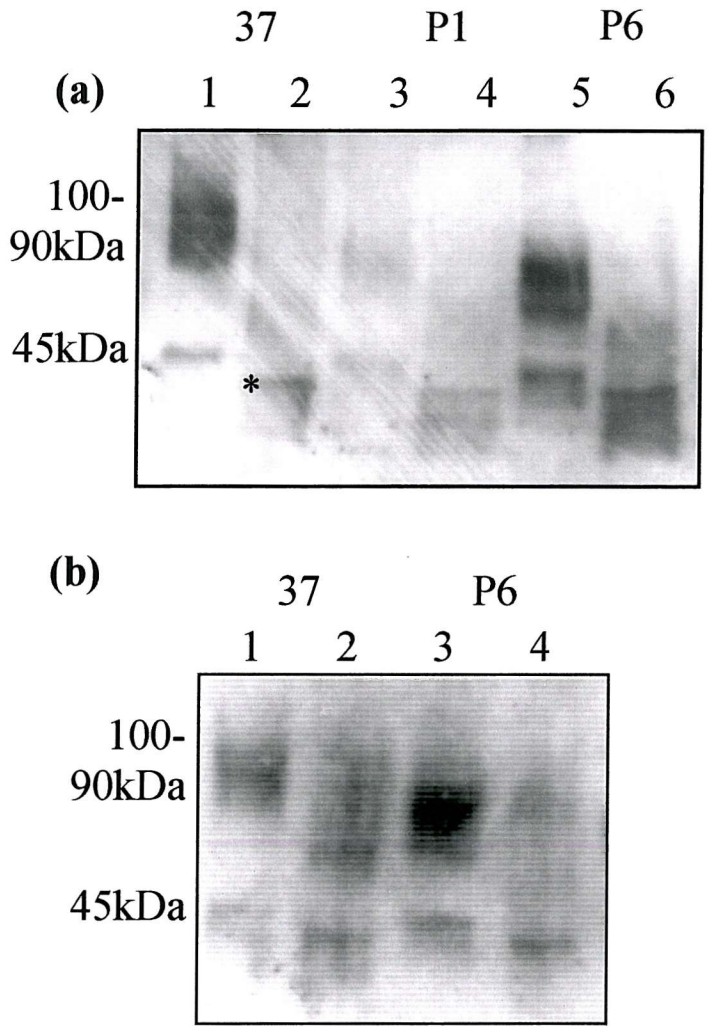

Figure 5.2.22. Removal of p-nut and Nramp1 carbohydrate: 25μg of total protein from each sample was analysed using western blotting and an 8 % denaturing acrylamide gel. All cell extracts were treated in the same way with the exception that cell extracts from (b) contained twice the protein concentration as those from (a) but were digested with the same concentration of PNGaseF (2.2.19). Lanes 2, 4 and 6 in (**a**) have been treated with PNGaseF, and 2 and 4 in (**b**). In (**a**) lanes 1/2 contain extracts from 37s, 2/4 from P1s and 5/6 from P6s. In (**c**) lanes 1/2 contain extracts from 37s and 2/4 from P6s.

Figure 5.2.23

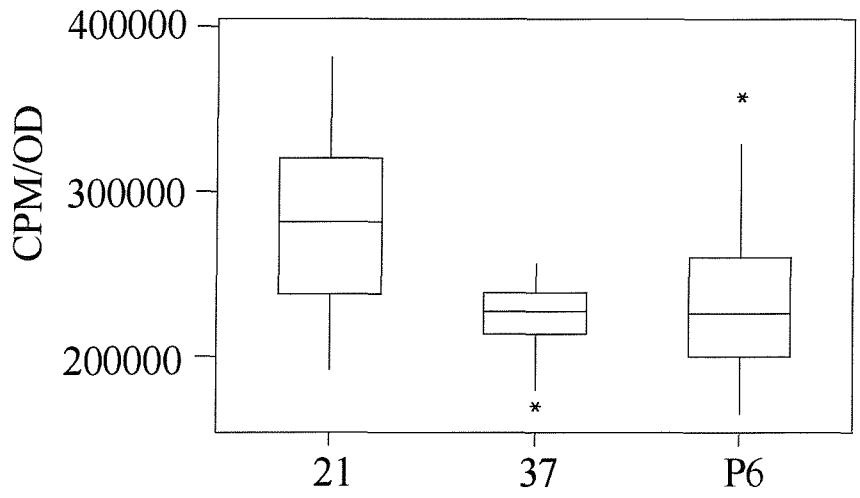

Figure 5.2.23. Box plot showing the distribution of [^{3}H]-thymidine DNA incorporation into 21,37 and P6 RAW cell lines. Counts per minute have been standardised according to the absorbance recorded for crystal violet cell counting (2.2.5). Both 37 and P6 cell lines incorporate significantly less [^{3}H]-thymidine than 21s using the Mann-Whitney Test, $P<0.05$. Lines 37 and P6 are not significantly different. Results show a typical experimental outcome.

RAW cell growth regulation by p-nut was studied to decipher if the substitution of three serine residues for alanine affected the reduced growth induced by wildtype *Nramp1*. Tests of [^{3}H]-thymidine incorporation into the DNA of phenotypically null *Nramp1*^{Asp169} cells (**21**), wildtype *Nramp1*^{Gly169} constitutive expressing cells (**37**) and p-nut constitutive expressing cells (**P6**) show that resting cells producing p-nut protein have the same growth deficit, ~22% less, as those expressing wildtype Nramp1 (fig.**5.2.23**). Unfortunately only limited studies could be conducted due to the loss of p-nut protein expression and no studies on the effect of iron over the growth deficiency caused by P6 could be carried out.

5.2.3 *Ex-vivo* De-phosphorylation Of Wildtype Nramp1

The substitution of three of Nramp1's N-terminal serine residues for alanine produces a mobility shift on an SDS denaturing gel when compared to wildtype Nramp1. The three serine residues substituted are critical for the putative PKC phosphorylation motifs that they are contained within. In order to ascertain if the mobility shift was due to an inability of p-nut to be phosphorylated it was necessary to disrupt the function of cellular PKC in wildtype *Nramp1* cell lines.

Use of bisindolylmaleimide I hydrochloride: This drug is a highly selective cell-permeable PKC inhibitor (K_i = 10 nM) that is structurally similar to staurosporine. It acts as a competitive inhibitor for the ATP-binding site of PKC and shows high selectivity for PKCα, β_I, β_{II}, γ-, δ-, and ε- isozymes. It is known that Nramp1 is phosphorylated but unknown where this occurs in the protein and which kinase(s) are involved (44). Treatment of 32 and 37 cell lines (fig.**4.2.11 (b)**) with bisindolylmaleimide I (BSM) did not cause a mobility shift like that of p-nut protein (fig.**5.2.31**). There is no change in the LMW 45kDa band. Just above the LMW band lays a sharp band, this is inconsistently detected during immune blotting and is believed to be non-specific (43). Removal of the putative phosphorylation sites from Nramp1's N-terminal domain was hypothesised to alter the proteins translocation around the cell. If indeed this does occur then it is expected that co-localisation of Nramp1 with pathogen containing vesicles may lead to such a change in phosphorylation.

It is not known if phosphorylation is important in Nramp1 translocation or if indeed de-phosphorylation is an essential part of this if it were to occur. However, based on three facts: the first that Nramp1 is phosphorylated in resting cells, the second; data showing that the N-terminal domain can bind α and β tubulin (40), and

Figure 5.2.31

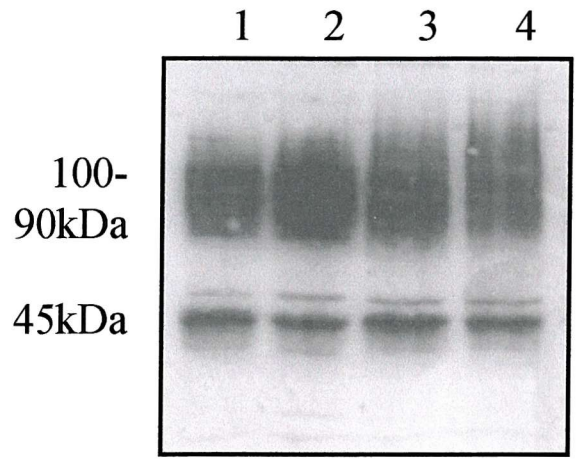

Figure 5.2.31. Treatment of wildtype *Nramp1* Expressing RAW cells with a specific PKC inhibitor. Cells were treated overnight with 20μM BSM then harvested and western blotted using an 8% denaturing gel. Lanes 1and 2 are untreated 32 and 37 cells respectively. Lanes 3 and 4 are treated 32 and 37s respectively.

the third demonstrating the replacement of serine residues (above) causes a change in protein gel mobility, it could be that the three are inter-linked. To this end gel mobility of wildtype Nramp1 was studied after cellular uptake of pathogens.

Overnight IFN-γ activation of RAW cells, constitutively expressing Nramp1, followed by uptake of salmonella for two hours had no effect on the protein's gel mobility (not shown). Overnight uptake of zymosan (yeast cell wall) had the remarkable effect of increasing the expression of Nramp1 protein but had no effect on its mobility. Further study of the augmented expression identified enhanced β-actin promoter activity, recognised as an increase in constitutive expression of *Nramp1* upon uptake of zymosan (not shown).

5.2.4 Cellular Localisation Of Nramp1 and p-nut Protein

The primary goal after removing the three putative PKC phosphorylation sites from the N-terminal portion of Nramp1 was to analyse the ensuing effect on Nramp1 localisation within the cell. In order to do this it was necessary to have a system that allowed visual examination of Nramp1's location. This involved staining of Nramp1 with specific antibodies and synthesis of fluorescent-tagged Nramp1 and p-nut fusion proteins. Ultimately, however, the fusion protein was more appropriate for a majority of experiments.

Construction Of GFP-tagged p-nut Construct

The p-nut vector sequence was amplified using PCR primers (2.2.22) to the start and stop codons with the addition of 5' SalI and 3' BamHI restriction sites (fig.**5.2.40 (a)**). The PCR product was subsequently TA subcloned using the pGEM-T vector system (fig.**5.2.40 (b)**). From here the sequence was cloned via its SalI and BamHI restriction sites into pEGFP-N3 (Clontech) using XhoI and BamHI polylinker restriction sites (fig.**5.2.40 (c)**). The second from top band in clone 2 is likely to be the result of partial digestion.

Figure 5.2.40

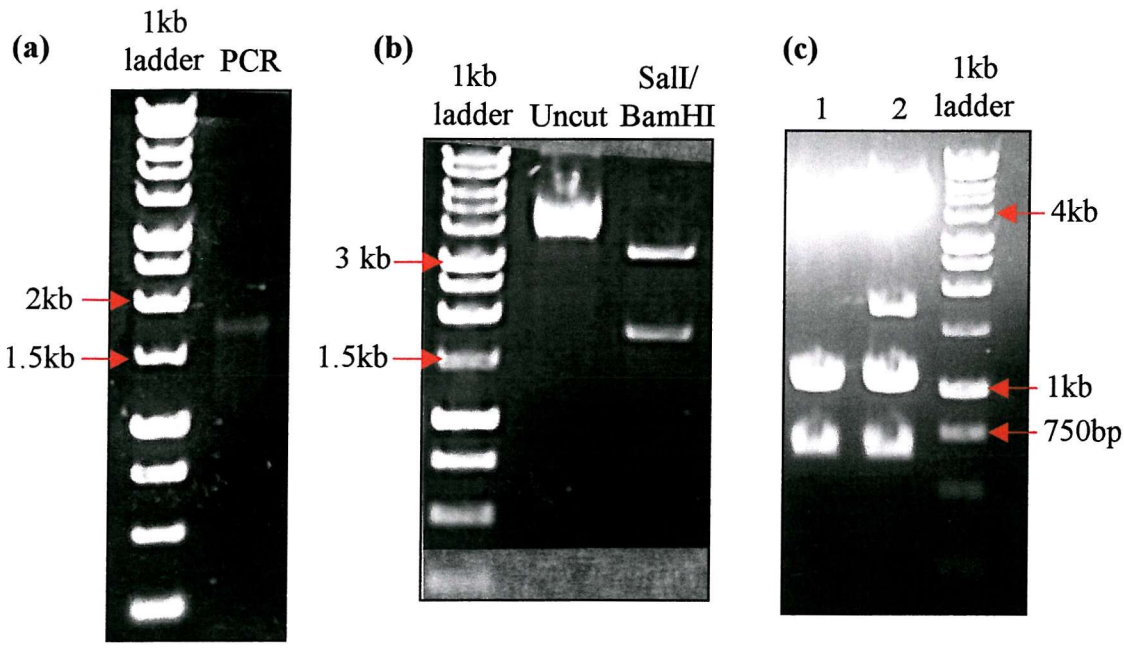

Figure 4.2.40. Restriction digests of p-nut pEGFP-N3 cloning steps. (**a**) PCR using primers to the p-nut vector to amplify the sequence from the start codon to the stop codon with the addition of 5' SalI and 3' BamHI restriction sites (total length 1662bp). (**b**) PCR TA cloned into pGEM-T vector, showing uncut plasmid and the subsequent drop out upon SalI and BamHI digestion also 1662bp. (**c**) Cloning of SalI/BamHI drop out into pEGFP-N3 vector via XhoI and BamHI polylinker restriction sites. Shows 2 clones, 1 and 2, that have been digested with BglII and BamHI with the correct drop outs of ~1kb and 700bp demonstrating the correct cloning of the p-nut sequence into pEGFP-N3. (pEGFP-N3 ~ 4.5kb).

Testing correct cellular expression of fluorescent labelled Nramp1 and p-nut. In addition to the EGFP-p-nut construct described above three other fluorescent-tagged fusion proteins were made. These are described in 2.1.18 and were produced by other members of the group. They specifically included: EGFP labelled wildtype *Nramp1*, DsRed labelled wildtype *Nramp1*, and EGFP labelled *Nramp2*. Nramp2 does not co-localise with Nramp1 (86), primarily a lysosomal protein, but instead to early endosomes. For this reason co-expression of tagged Nramp1 and Nramp2 should produce cell staining that is discrete.

These constructs were first tested in COS-1 cells as they have a greater transfection efficiency than RAW264.7 cells making detection of co-transfections a simpler task. Fig.**5.2.41 (a)** and **(b)** are two such co-transfections. All transient transfections took place over 48 hours unless otherwise stated. In fig.**5.2.41 (a)** COS-1 cells have been transfected with both EGFP-*Nramp1* and DsRed-*Nramp1* expression vectors. The settings used to capture these images enabled optimal lateral resolution, indicating that EGFP-Nramp1 and DsRed-Nramp1 were no more than ~0.2 μm away from each other in the cell where co-localisation produces yellow staining. The close proximity of the two proteins is also exhibited by the large amount of orange staining seen on the image. Knowing that DsRed and EGFP did not differentially effect Nramp1 localisation within the cell it was possible to test DsRed-Nramp1 and EGFP-Nramp2 co-localisation fig.**5.2.41 (b)**. These two fusion proteins are targeted differently and do not co-localize; green Nramp2 staining and red Nramp1 staining are clearly distinct.

Figure 5.2.41

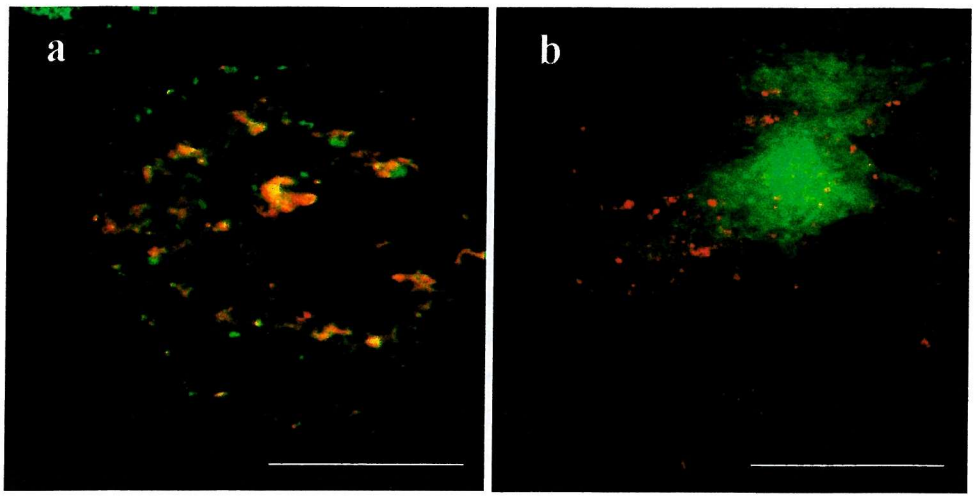

Figure 5.2.41. Nramp1 and Nramp2 do not co-localise in COS-1 cells. All transfections were transient and pictures were taken at 48hrs. (**a**) Confocal microscope image of a single COS-1 cell expressing EGFP-Nramp1 (green) and DsRed Nramp1 (red). Orange/yellow staining shows co-localisation of both tagged proteins. (**b**) Confocal microscope image of a single COS-1 cell expressing EGFP-Nramp2 (green) and DS red Nramp1 (red). Above is a representation of a typical image. Bars, 25μm.

It was not possible to co-transfect RAW264.7 cells due to their very low transfection efficiency. Expression of EGFP (fig.**5.2.42** (**a**)) alone or EGFP-fusion proteins (fig.**5.2.42** (**b**) and (**c**)) in RAW264.7 cells, produces markedly different staining patterns. Transfection of EGFP alone leads to its manifestation in the cytoplasm but also within the nucleus, or though it is excluded from an unidentified vesicle system (arrows in (a)) and the plasma membrane. Fusion of EGFP to Nramp1 or p-nut leads to the absence of staining within the cytoplasm and nucleus; there is ribbon-like partially punctate peri-nuclear staining, but again none at the plasma membrane. This staining is subtly different from that observed with transfected

RAW264.7 cell lines using polyclonal antibody against the C-terminal end of Nramp1 and a fluorescent secondary (fig.**5.2.43**). This antibody has previously been shown to

Figure 5.2.42

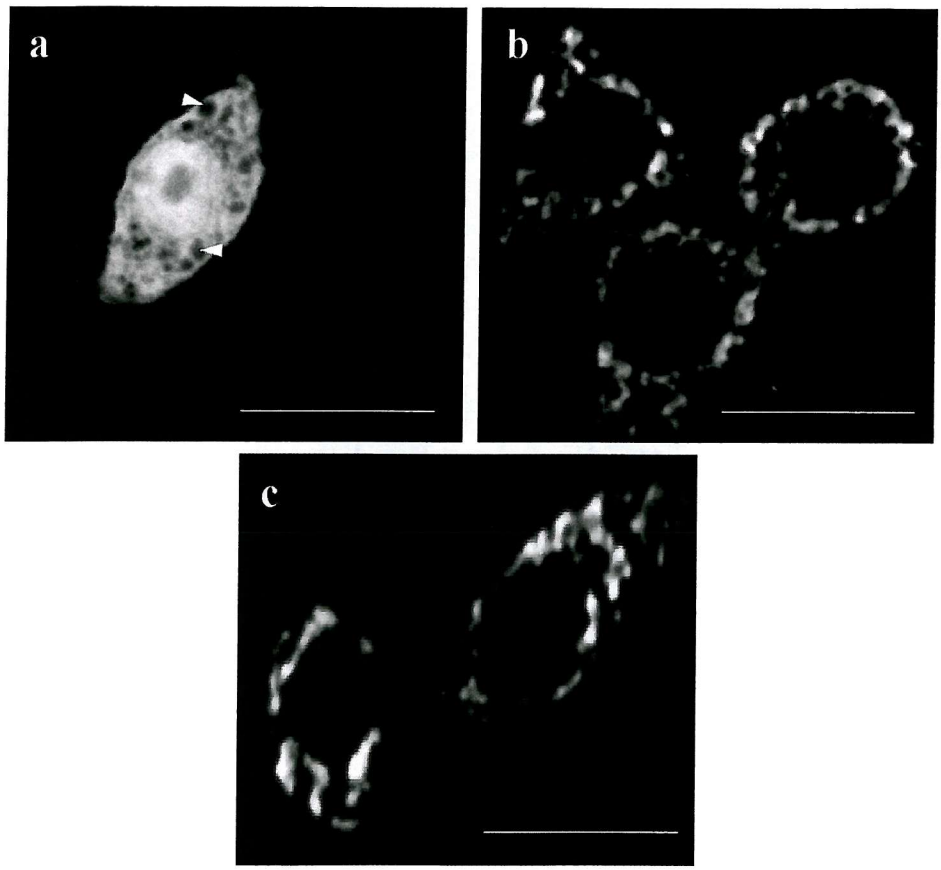

Figure 5.2.42. EGFP, EGFP-Nramp1 and EGFP-p-nut expression in RAW264.7 cells. (**a**) Confocal microscope image illustrating expression of EGFP alone, arrows indicating vesicle system not containing EGFP. (**b**) Confocal image of EGFP-Nramp1 transfected RAW cells. (**c**) Confocal microscope image showing EGFP-p-nut expression in RAW cells. Bars, 25μm.

recognise Nramp1(45;47) and was used here to ensure similar staining patterns between *Nramp1* expressing cell lines and *Nramp1* that have been transfected and visualised using EGFP tagging. Antibody staining of both Nramp1 and p-nut RAW lines (fig.**5.2.43** (**b**) and (**c**) respectively) shows, consistently; largely peri-nuclear staining that does not

intrude into the nucleus or enter the plasma membrane. This staining, however, is more punctate than seen in EGFP-fusion protein transfectants and generally displays less abundant ribbon-like structures. Very little expression is seen in 21 cells that do not express functional *Nramp1* (fig.**5.2.43 (a)**), although this does vary moderately. Oddly the same antibody used by Searle and colleagues (47) produced Nramp1 signal, in other S lines, similar to that of wildtype.

Figure 5.2.43

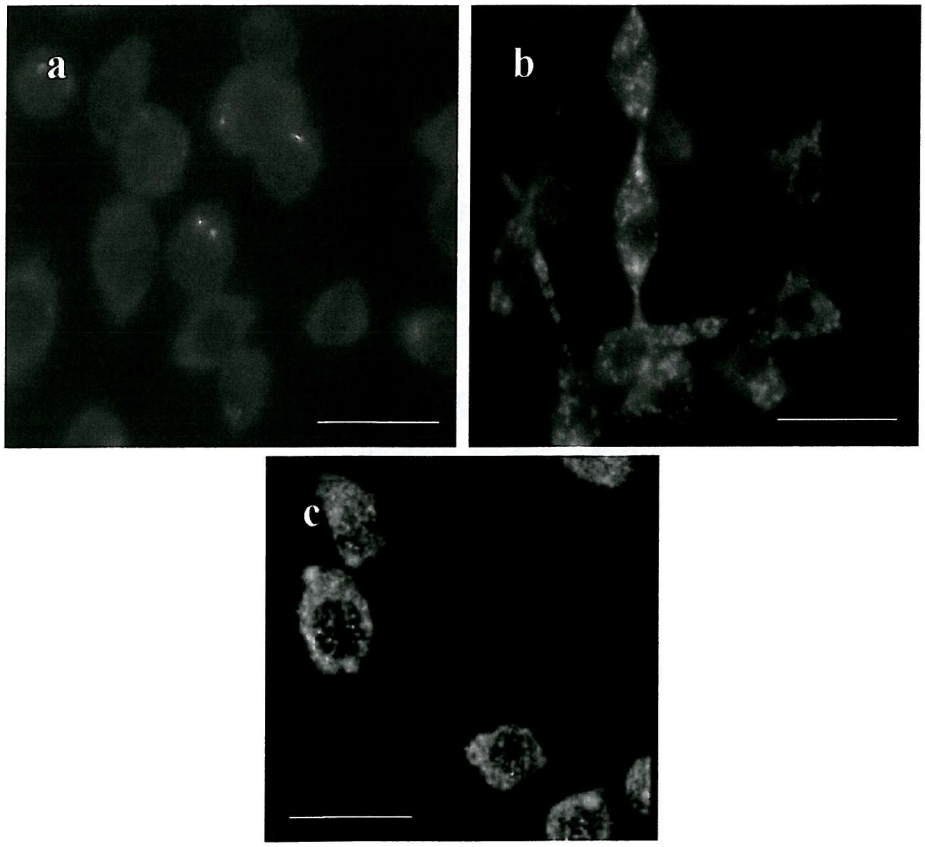

Figure 5.2.43. RAW cell lines constitutively expressing Nramp1 and p-nut proteins stained with anti-Nramp1 antibodies. Digital microscope images of cells stained and prepared as in 2.2.20. (**a**) 21 cells not expressing functional *Nramp1*. (**b**) 37 cells constitutively expressing *Nramp1*. (**c**) P6 cells constitutively expressing p-nut. Bars, 25μm.

Figure 5.2.44

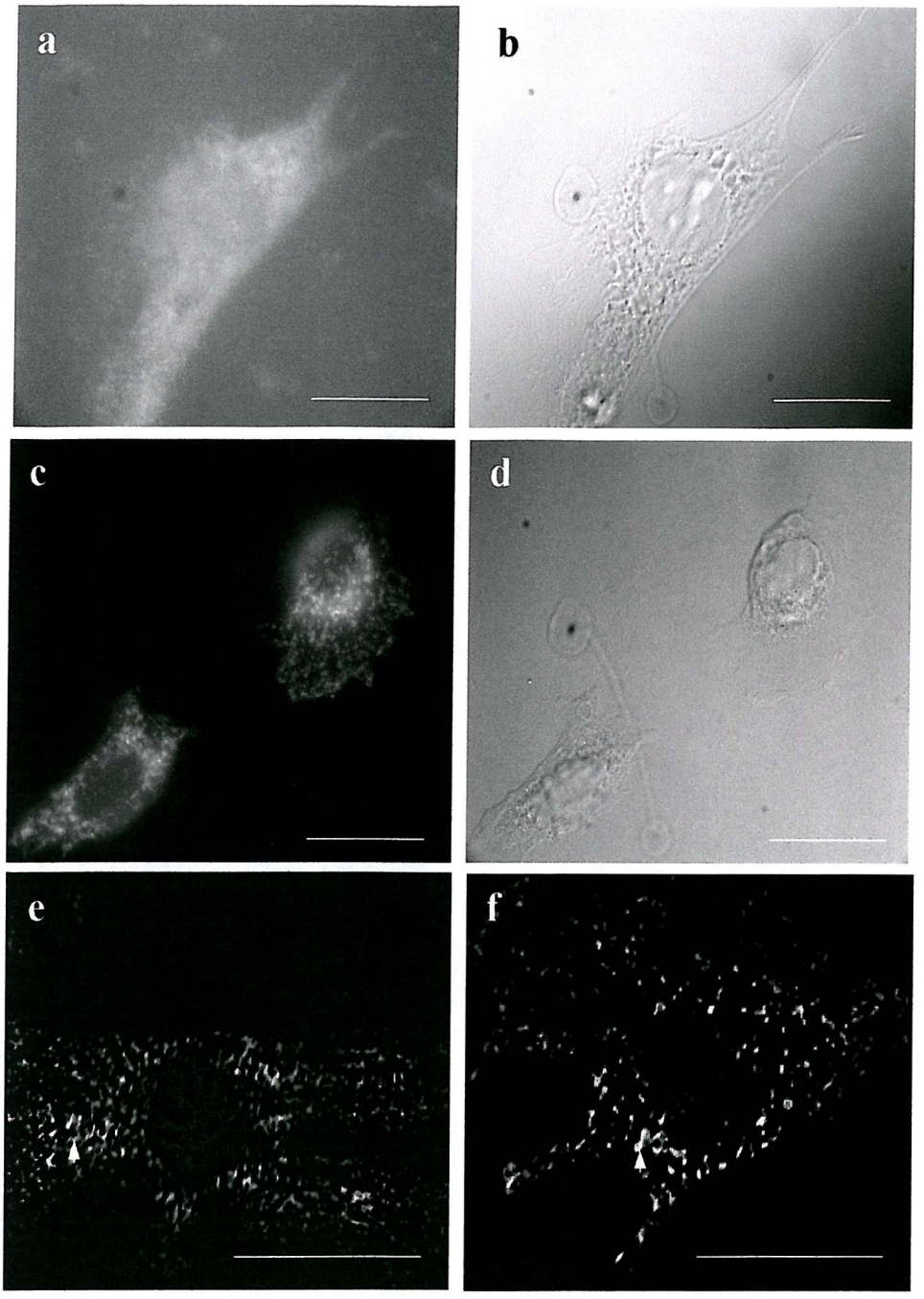

Figure 5.2.44. Fluorescently labelled p-nut and Nramp1 expression in L1 3T3 fibroblast cells. Cells (a) and (c) were stained and prepared as in 2.2.20, and (a)-(d) are images captured by a digital microscope using x40 magnification. (**a**) Shows a wildtype fibroblast with faint background staining. (**b**) Shows the brightfield image of this fibroblast. (**c**) Shows two stained fibroblasts that are stably transfected with p-nut. (**d**) Brightfield image of (c). (**e**) Confocal image of a fibroblast expressing EGFP-Nramp1. (**f**) Confocal image of a fibroblast expressing EGFP-p-nut. Bars, 25μm.

The dissimilarity between RAW cell lines stained with antibody and cells transfected with EGFP Nramp1 or p-nut constructs does not occur in fibroblasts. Immune stained fibroblasts stably expressing p-nut display comparable patterns of expression to fibroblasts transfected with EGFP-p-nut (fig.**5.2.44** compare (**c**) with (**f**)). The staining is again more intense closer to the nucleus but is punctate not only here but also throughout the cytoplasm. The greater magnification of the confocal images (~2 fold), fig.**5.2.44** (**e**) and (**f**), does reveal some ribbon-like structures (arrows) but these are not as *en masse* as those seen in RAW cells. Consistent among all staining is the absence of nuclear and plasma membrane staining and by eye there is little, if any difference in the pattern of staining seen in Nramp1 and p-nut cell lines; fig.**5.2.43** (**b**) compared to (**c**). In addition to this, comparison of EGFP-Nramp1 and EGFP-p-nut expression within cell types is also very similar; fig. **5.2.42** (**b**) compared to (**c**) and fig.**5.2.44** (**e**) compared to (**f**). This would suggest that the substitution of the serine residues in p-nut has no effect on the gross anatomy of its targeting.

Due to the relatively easy handling of the EGFP constructs the work from here focuses on their use. Antibody staining was in comparison a far longer protocol and in addition to this the use of EGFP allows dynamic measurement of protein movement, as cell fixing is not required in the protocol.

In order to test the EGFP constructs further it was necessary to check that they were targeted to acidic, lysosome like, vesicles. To complement these studies, and also as experiments with co-localisation of Nramp2 could not be done in RAW cells, co-localisation with transferrin was studied. Transferrin has itself been shown to co-localise with Nramp2 (86).

Co-localisation of lysoTracker: lysoTracker red, molecular probes, is an acidotropic probe that accumulates in vesicles of low pH. In this way it has been used to stain lysosomes in RAW cells and fibroblasts to study co-localisation of EGFP-tagged Nramp1 and p-nut. Uptake was achieved over 10 minutes using 50nM lysoTracker.

Figure 5.2.45

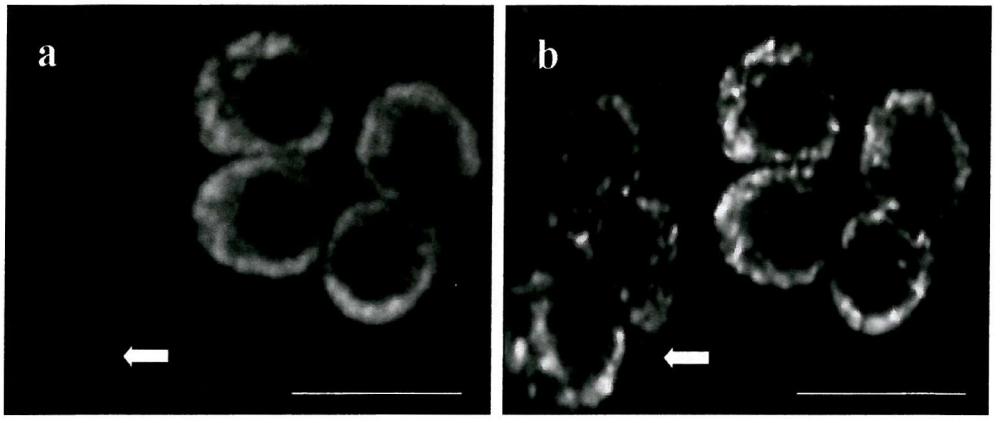

Figure 5.2.45. LysoTracker red emission does not crossover to the green channel. Confocal captured images from RAW cells expressing EGFP-Nramp1 that have taken up lysoTracker. (**a**) Green channel showing EGFP-Nramp1. Arrow indicates lack of crossover from red channel (b). (**b**) Red channel showing uptake of lysoTracker. Arrow indicates presence of red emission that is not contained in (a). Bars, 25μm.

Fig.**5.2.45** shows that there is no crossover from the red channel to the green (comparison of arrows in (**a**) and (**b**)). There is also very little crossover of green into red with the level of laser power used throughout this study (not shown).

Uptake of lysoTracker into RAW cells produces staining that is similar but distinct to that of Nramp1 and p-nut EGFP. Accumulation seems to be at its greatest within more spherical vesicles that often look as though they are attached to the

Figure 5.2.46

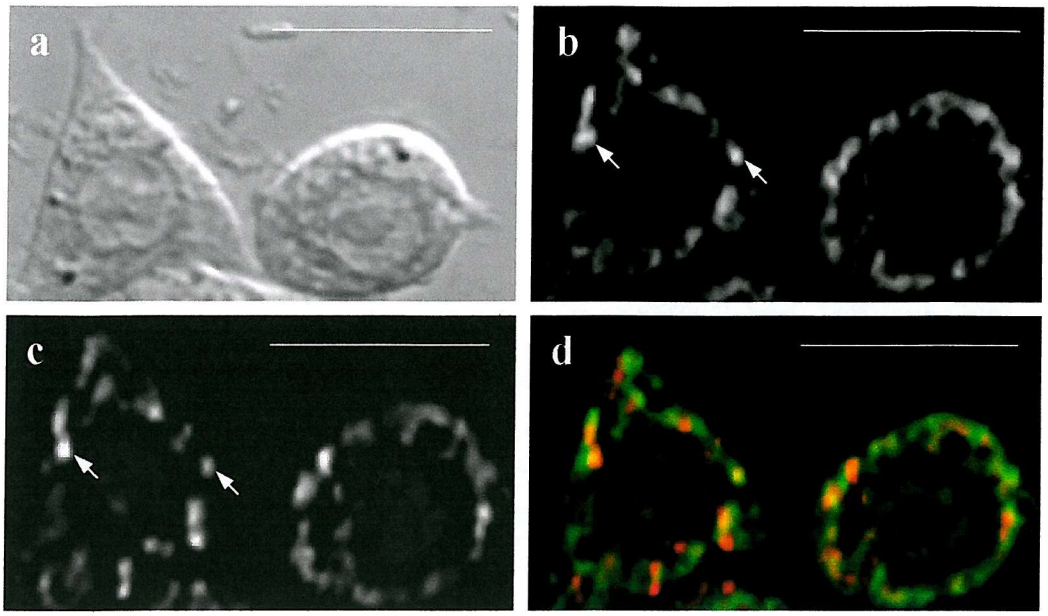

Figure 5.2.46. Co-localisation of lysoTracker with EGFP-Nramp1: Confocal captured images. (**a**) Transmission image of RAW cells. (**b**) EGFP-Nramp1 expression. (**c**) LysoTracker uptake. (**d**) Merged green EGFP-Nramp1 and red lysoTracker channels. Yellow/orange shows co-localisation. Confocal: Power-30%, Red and green iris-3.5, Red gain-1269, green gain-1307. Bars, 25μm.

ribbon-like structures that are less heavily stained. Frequently the more spherical staining coincides with areas of Nramp1 or p-nut EGFP staining that is more punctate/intense; this can be distinguished by comparing the white arrows in (**b**) and (**c**) in fig.**5.2.46**. Like Nramp1 and p-nut, lysoTracker staining is peri-nuclear and dispersed throughout the cytoplasm with no nuclear of membrane staining. LysoTracker does co-localise with both EGFP-Nramp1 and EGFP-p-nut (yellow/orange staining in (**d**), figures **5.2.46** and **5.2.47** respectively), but this is not absolute and may reflect lysoTracker that has only just been absorbed.

Fig.**5.2.48** shows the uptake of lysoTracker into fibroblasts and the expression of EGFP-Nramp1 in one of these fibroblasts. The appearance of lysoTracker in

Figure 5.2.47

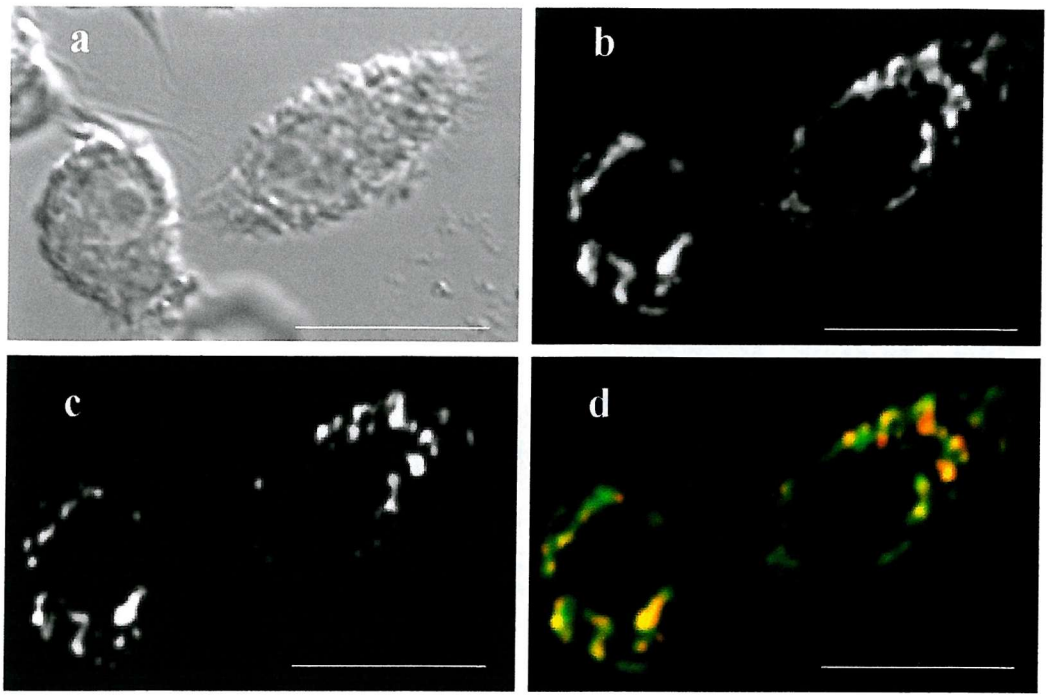

Figure 5.2.47. Co-localisation of EGFP-p-nut and lysoTracker in RAW264.7 cells: Confocal captured images. (**a**) Transmission picture of transfected RAW cells. (**b**) EGFP-p-nut green channel. (**c**) LysoTracker uptake, red channel. (**d**) Merged images, yellow shows co-localisation. Confocal: Power-30%, red and green iris-2.9, red gain-826, green gain-1500. Bars, 25μm.

fibroblasts is again, like RAW cells, similar but distinct from that of the EGFP fusion proteins. They have the same overall organisation, peri-nuclear and throughout the cytoplasm, but the vesicles are like RAW cells, more spherical or punctate. Co-localisation of EGFP-p-nut and lysoTracker in fibroblasts is akin to that of EGFP-Nramp1 in fibroblasts. There is good co-localisation between the two but once again this is not complete (fig.**5.2.49 (d)**). There are often parts were the two remain exclusive of one another. This is especially true of EGFP tagged Nramp1 and p-nut, as a large amount of green staining can still be seen where lysoTracker does not accumulate.

Figure 5.2.48

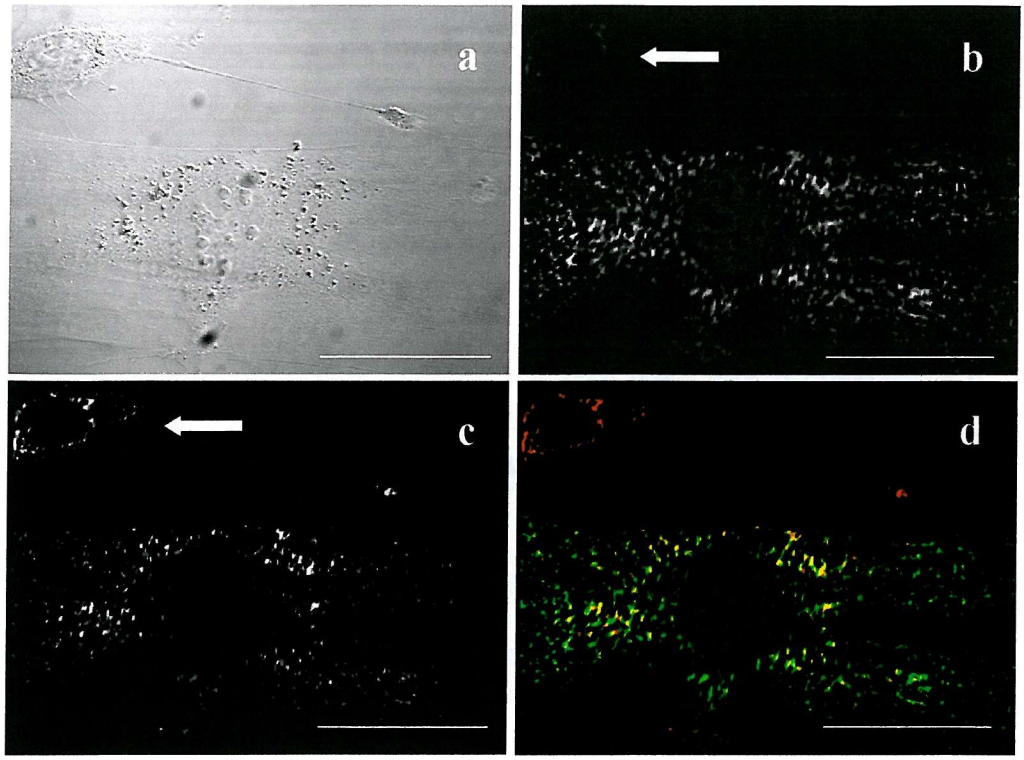

Figure 5.2.48. Co-localisation of lysoTracker with EGFP-Nramp1 in 3T3 L1 fibroblasts: Images were captured using a confocal microscope. (**a**) Transmission image of two fibroblasts. (**b**) EGFP-Nramp1 expression. (**c**) LysoTracker uptake. (**d**) Co-localisation of green EGFP-Nramp1 and red lysoTracker. Yellow/orange shows co-localisation. White arrows in (b) and (c) show no red auto-fluorescence from fibroblasts in (b). Confocal: power-30%, red and green iris-5, red gain-961, green gain-1500. Bars, 25μm.

The lack of exclusive expression of EGFP constructs within acidic, likely lysosomal, vesicles suggests that these fusion proteins are either being retained in the ER/Golgi and perhaps targeted to late endosomes, or incorrectly to less acidic vesicles such as early and recycling endosomes. Another possibility is that lysoTracker has not had a chance to accumulate in all areas of the cell.

Figure 5.2.49

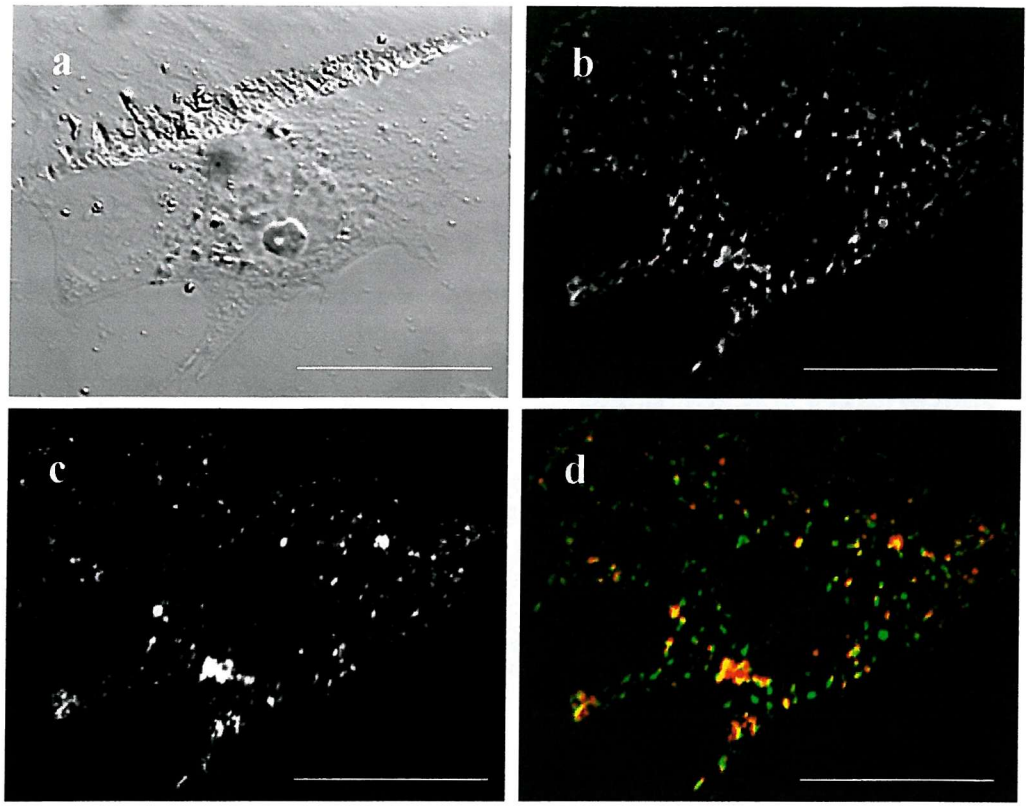

Figure 5.2.49. Co-localisation of EGFP-p-nut with lysoTracker in 3T3 L1 fibroblasts: Images were captured using a confocal microscope. (**a**) Transmission image of a single fibroblast. (**b**) EGFP-p-nut expression. (**c**) Red lysoTracker uptake. (**d**) Co-localisation of EGFP-p-nut and red lysoTracker. Yellow/orange shows co-localisation. Confocal: power-30%, red and green iris-2.7, red gain-1000, green gain-1500. Bar, 25μm.

Uptake of transferrin: This was carried out to determine if Nramp1 and p-nut EGFP proteins were being targeted to Nramp2 like previously characterised vesicles [86]. If this were the case then it would mean that incorrect targeting was taking place.

Figure 5.2.410

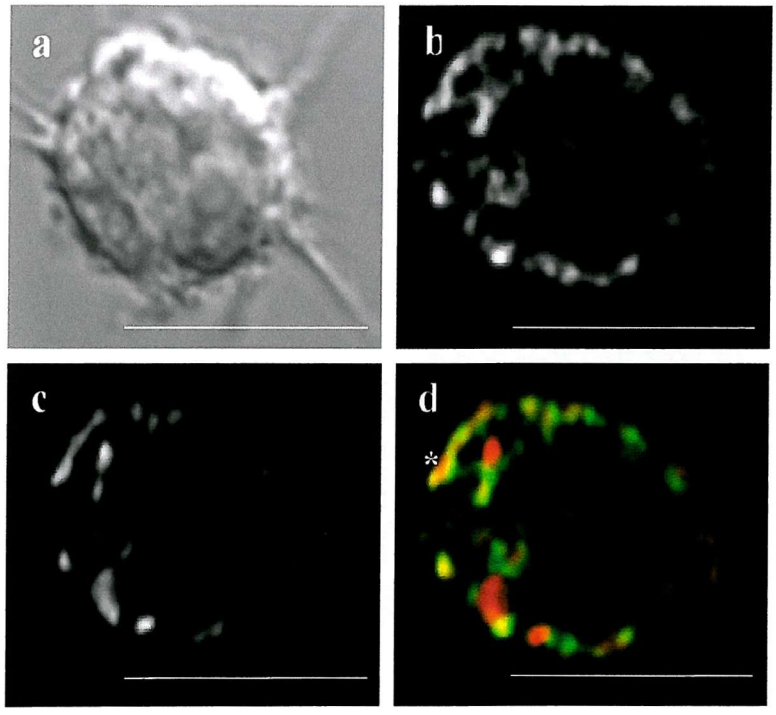

Figure 5.2.410. Transferrin does not co-localise with EGFP-Nramp1. Images were captured using a confocal microscope. (**a**) Transmission image of a single RAW cell. (**b**) EGFP-Nramp1 expression. (**c**) Transferrin localisation after uptake. (**d**) Transferrin (red) and EGFP-Nramp1 (green) and largely exclusive of one another. Confocal: power-30%, red and green iris-2.6, red gain-1200, green gain-1500. Bars, 25μm.

Raw cells were incubated in the presence of TRITC-transferrin (molecular probes) that emits red light upon excitation allowing it to be distinguished from EGFP. This was done for 3 hours using 3μl/ml of media. Unfortunately fibroblasts

did not take up sufficient quantities of transferrin to make analysis possible. Both EGFP-fusion proteins remained largely exclusive of transferrin in RAW cells (figs.**5.2.410 (d)** and **5.2.411 (d)**) with the residual overlap perhaps due to partial degradation of transferrin and targeting to lysosomes (white star, fig.**5.2.10 (d)**).

Figure 5.2.411

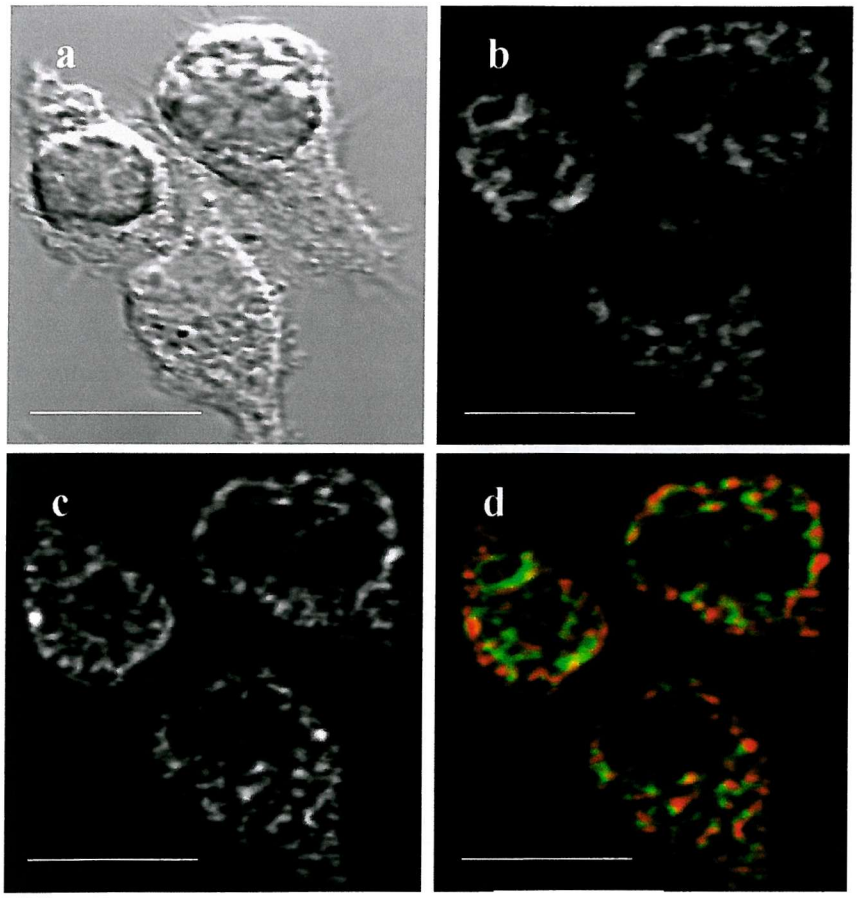

Figure 5.2.411. Transferrin remains exclusive of EGFP-p-nut expression in RAW cells. Images were captured using a confocal microscope. (**a**) Transmission image of three RAW cells. (**b**) EGFP-p-nut expression. (**c**) Localisation of transferrin after uptake. (**d**) Merged (b) and (c) show that EGFP-p-nut (green) does not co-localise with transferrin (red). Confocal: power-30%, red and green iris-3.8, red gain-1096, green gain-1500. Bar, 25μm

Transferrin, like the chimeras, is contained within a tubular network with some punctate markings.

5.2.5 Targeting of Nramp1 and p-nut

Tests of Nramp1 and p-nut expression suggested that both proteins were being targeted to acidic vesicles that do not contain transferrin: the pattern of expression was largely peri-nuclear with less staining throughout the cytoplasm that could be described as ribbon-like and punctate. There was no staining in the nucleus or at the plasma membrane. This pattern of expression is consistent with the available data for Nramp1 targeting and does not show any prominent diversity when using p-nut, suggesting that the phosphorylation mutant does not interfere with normal targeting in resting cells. The next step was to test Nramp1 targeting under an appropriate stimulus. It was of interest to study Nramp1 movement to the membrane under stimuli that are known to cause fusion of secretory lysosomes with the plasma membrane. To this end zymosan (in RAW264.7 cells) and the calcium ionophore A23187 (both RAW264.7 and 3T3 L1 fibroblasts) were used in static and time-lapse experiments, respectively.

Zymosan uptake into RAW264.7 cells was initially found to cause auto-fluorescence during early incubation (up to 5 hours); this consisted of fluorescence in the green channel that could not be distinguished from that produced by EGFP. The consequence of this was an inability to test early movement of Nramp1 and p-nut to the plasma membrane or to phagosomes containing zymosan. This fluorescence was only acute and had disappeared completely by 24 hours after washing (not shown). Figure **5.2.51 (a)** shows the presence of two zymosan particles (arrow heads) next to a RAW cell and gives an indication of their size and shape.

Figure 5.2.51

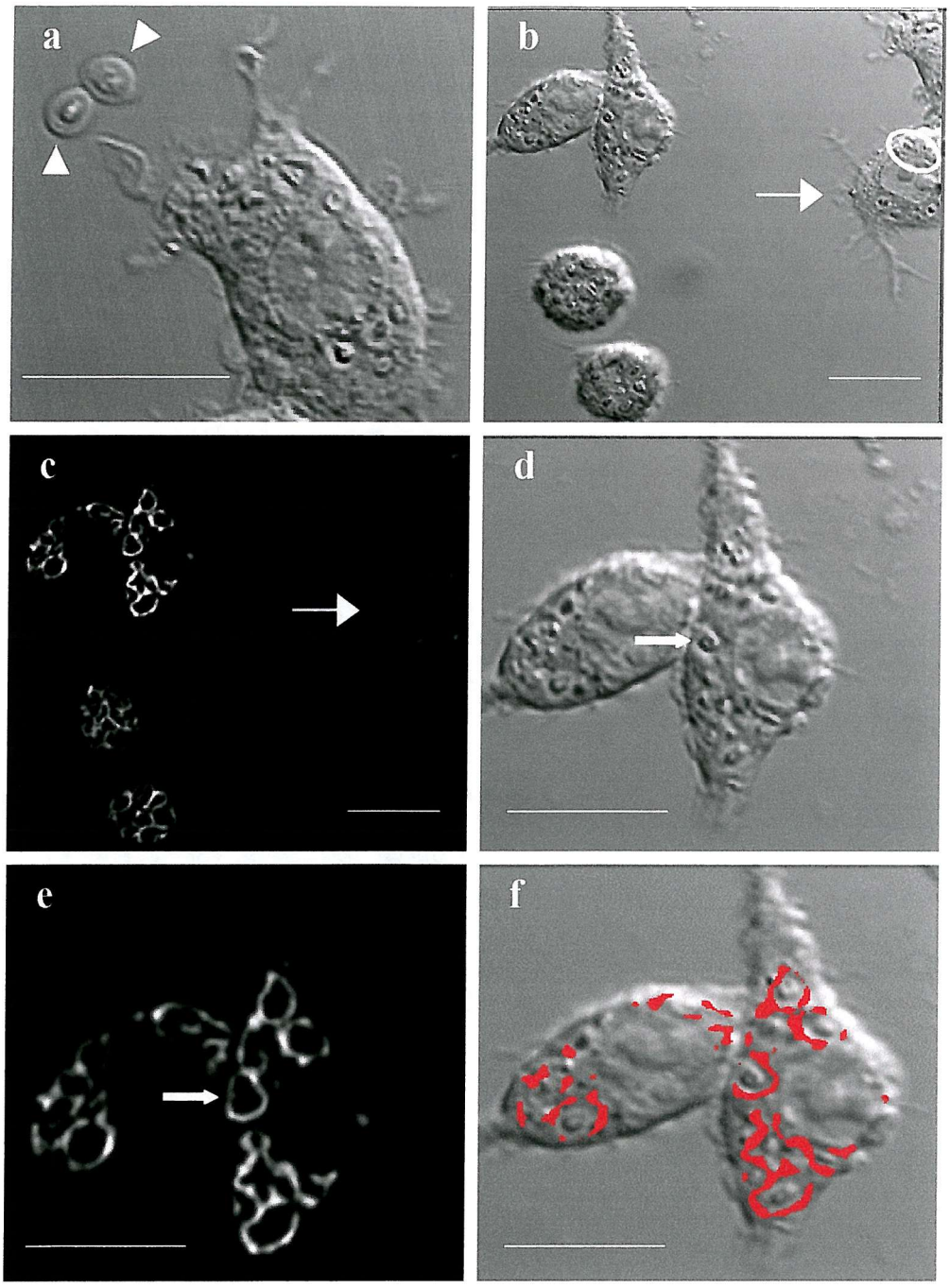

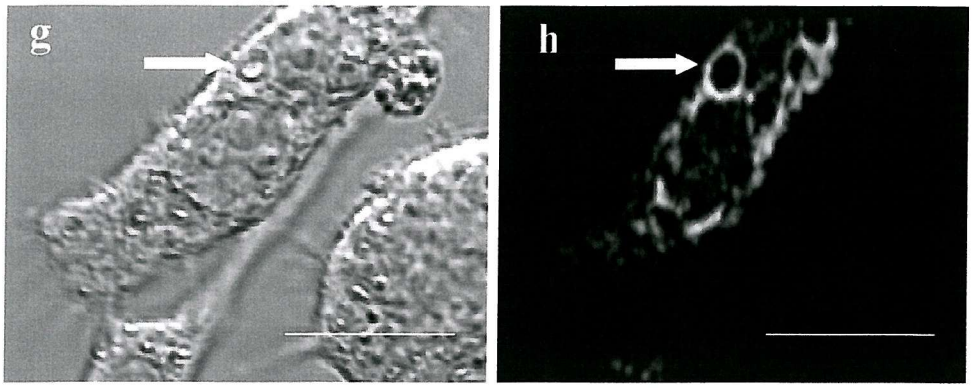

Figure 5.2.51. Targeting of Nramp1 and p-nut to zymosan containing phagosomes: Images were captured using a confocal microscope. Cells were transfected for 24 hours before being incubated in zymosan for 5 hours at which point they were washed and left for a further 24 hours before use. (**a**) Transmission image showing two zymosan particles (arrowheads) next to a RAW cell. (**b**) Transmission image of RAW cells that have been transfected with EGFP-Nramp1. Arrow indicates a cell that does not contain EGFP-Nramp1 but is not fluorescing (compare to (c)). White circle shows the presence of two zymosan particles within the cell. (**c**) As in (b) but showing green channel fluorescence. (**d**) Transmission image of two RAW cells that have been transfected with EGFP-Nramp1, the arrow highlights a zymosan particle contained within the RAW cell. (**e**) EGFP-Nramp1 expression in RAW cells, arrow indicates the localisation of Nramp1 with a zymosan particle as seen in (d). (**f**) Merged image of (d) and (e) showing extent of co-localisation of EGFP-Nramp1 with the many zymosan particles phagocytosed by these RAW cells. (**g**) Transmission image of a RAW cell that is expressing EGFP-p-nut. The arrow indicates a phagocytosed zymosan particle. (**h**) EGFP-p-nut expression showing co-localisation with a zymosan particle, arrow. Confocal: power-30%, iris-2.3, gain-1500. Bars, 25μm.

At ~30 hours cells no longer auto-fluoresce, which consists of cytoplasmic and nuclei (both RAW and zymosan) fluorescence; figure **5.2.5** (**b**) and (**c**), the white arrow indicating the lack of fluorescence in this cell which contains zymosan (white circle). Although it was not possible to determine if Nramp1 or p-nut move to the plasma membrane during uptake of zymosan, phagocytosis of zymosan did lead to targeting

of Nramp1 and p-nut to zymosan phagosomes. Fig.**5.2.51** (**d**)-(**f**) illustrates this clearly for EGFP-Nramp1, the arrow in (**d**) highlighting the presence of a zymosan particle that is surrounded by EGFP-Nramp1 as a ring structure in (**e**) also highlighted by an arrow. These particular RAW cells have engulfed multiple zymosan particles that are surrounded by EGFP-Nramp1 (**f**). This pattern of expression is very different from resting cells with near total loss of ribbon-like and punctate markings. It is not always the case however, and is liable to be a reflection of the large number of zymosan particles contained within these macrophages. Figure **5.2.51** (**g**) and (**h**) demonstrate a RAW cell expressing EGFP-p-nut containing far fewer zymosan particles, one of these zymosan particles is highlighted by an arrow and demonstrates clear, ring-like, EGFP-p-nut localisation. In addition to this the normal ribbon-like expression is also present surrounding the nucleus. Therefore both EGFP-Nramp1 and EGFP-p-nut are targeted to phagosomes containing zymosan by 30 hours.

A23187 treatment of RAW cells has no effect on Nramp1 and p-nut movement (not shown). In addition to this uptake of lysoTracker into RAW cells followed by treatment with A23187 has no effect on the vesicles containing it over 20 minutes (not shown). This would suggest that A23187 does not give an appropriate stimulus in RAW cells for lysosomal secretion, an observation already described (153;154).

A23187 treatment of fibroblasts leads to movement of EGFP-tagged Nramp1 and p-nut to the cell membrane over a time period of ~10 minutes. This can clearly be seen in figure **5.2.52** (**a**) where a single vesicle is shown moving to the membrane (arrow head), and after multiple fusion events there is clearly plasmalemma EGFP-p-nut expression (201s).

Figure 5.2.52

(a)

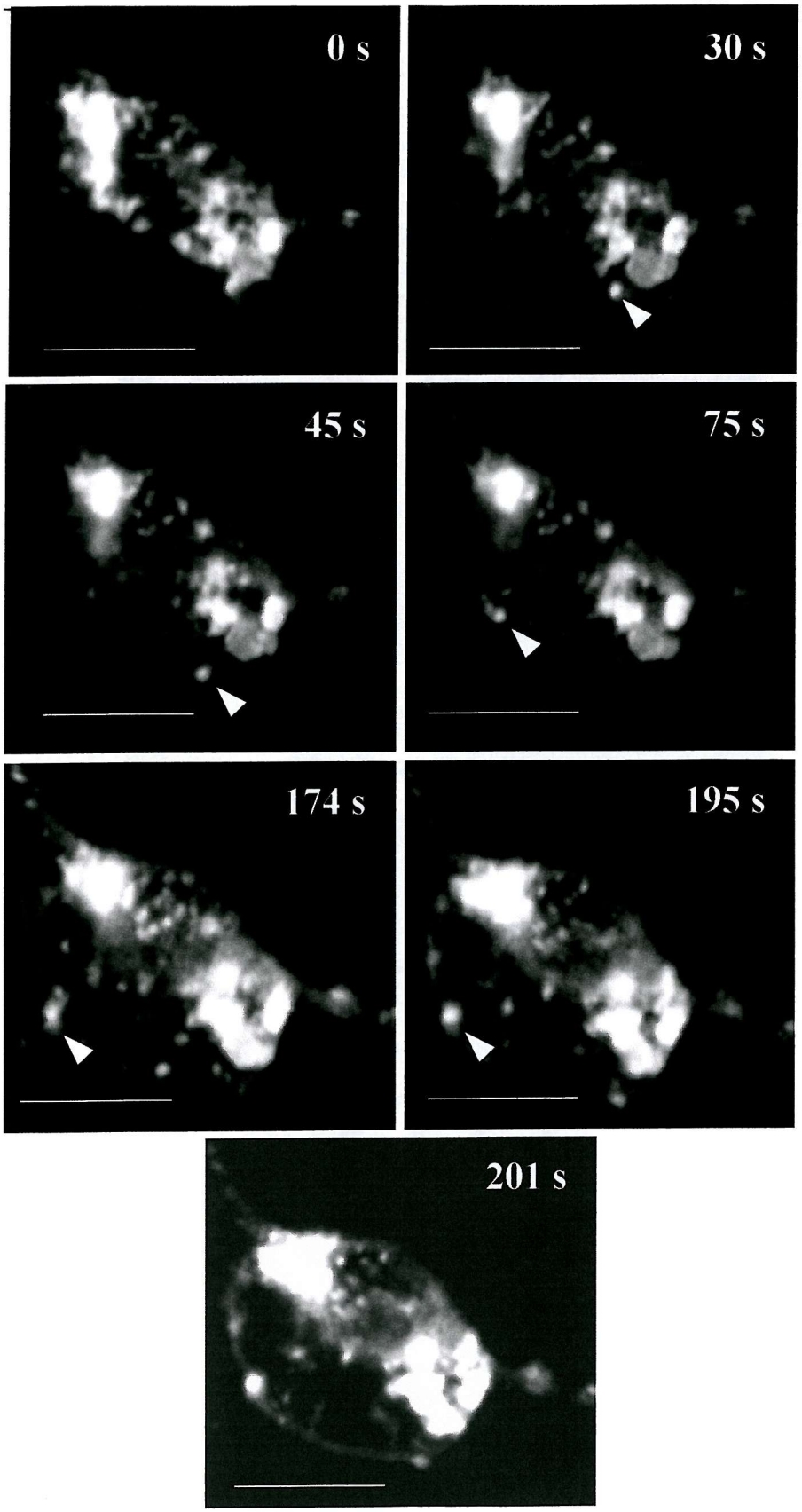

(b)

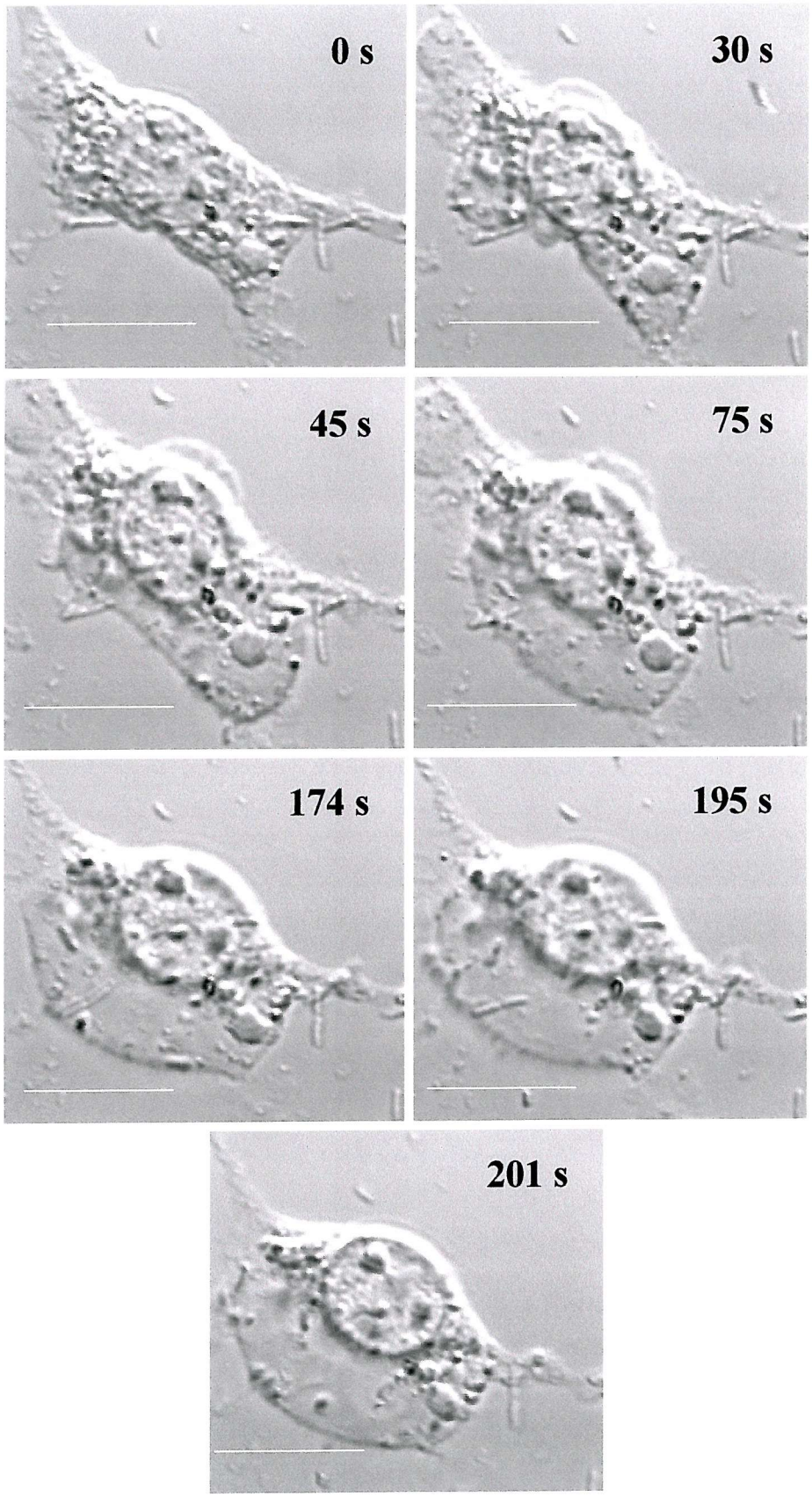

Figure 5.2.52. A23187 treatment of fibroblasts expressing EGFP-p-nut leads to plasma membrane targeting. Images are from confocal microscopy time-lapse experiments. . Cells were treated as in methods (2.2.21). (**a**) The seven images are of a single fibroblast cell expressing EGFP-p-nut. A23187 (25μM) and $CaCl_2$ (1μM) were added to the system 4 minutes and 45 seconds before the first picture (0 s) that is shown here. The following pictures are actual time points from then on coming to a total of 3 minutes and 21 seconds. The arrows indicate the movement of a single vesicle to the membrane. The last image shows the ensuing plasma membrane staining. (**b**) Transmission images of the same fibroblast cell at identical time points. Bars, 25μm.

Interestingly ionophore treatment is accompanied by a dramatic change in fibroblast cell morphology indicated by a large increase in the width of the cell and an expansion in the size of the cytosol that appears smooth (fig.**5.2.52 (b)**). This also occurs in EGFP-Nramp1 transfected fibroblasts (fig.**5.2.53 (d)**). In addition EGFP-Nramp1 plasma membrane staining can clearly be seen by 8-10 minutes of treatment (fig.**5.2.53 (c)**), suggesting that both wildtype and mutant proteins have an equal ability to translocate under an appropriate stimulus.

Figure 5.2.53

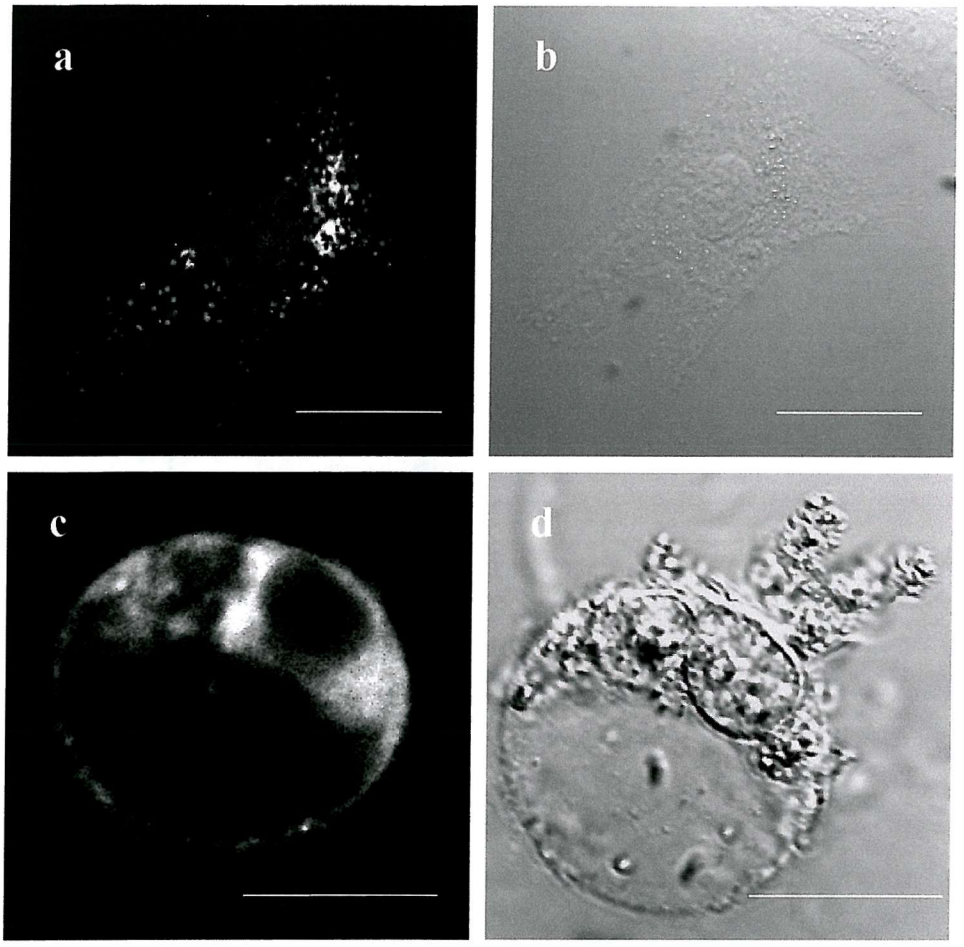

Figure 5.2.53. A23187 treatment of fibroblasts expressing EGFP-Nramp1 causes plasma membrane targeting. Images were captured using a confocal microscope. (**a**) Shows the expression of EGFP-Nramp1 before the addition of A23187, confocal: power-30%, iris-5, gain-1200, temp- 35 ^{0}C. (**b**) Transmission image of (a) showing the cell itself. (**c**) After 9 minutes of A23187 (25μM) and $CaCl_2$ (1μM) treatment EGFP-Nramp1 has translocated to the plasma membrane, confocal: power-30%, iris-5, gain-1500, temp- 35 ^{0}C. (**d**) Transmission image of (c) showing the cell morphology. Bars, 25μm.

5.3 Discussion

Three of *Nramp1*'s N-terminal serine residues were mutated to alanine in an effort to understand their relevance to the protein's cellular localisation. This mutant 'p-nut' protein was stably expressed in the macrophage like cell line RAW264.7 in the hope that antibody staining would reveal disparity to Nramp1. The loss of p-nut protein in stable lines and the unreliability of parental RAW264.7 antibody staining as a control meant that another technique was needed. The technique chosen was to create fluorescent-tagged Nramp1 and p-nut chimeras that would also allow the study of real time protein movement. No gross differences in Nramp1 and p-nut localisation were detected in resting or stimulated RAW264.7 and 3T3 L1 fibroblasts. It was shown however that Nramp1 containing vesicles fuse with the plasma membrane during increases in cytosolic calcium concentration in 3T3 L1 fibroblasts and also that Nramp1 co-localises with phagocytosed zymosan particles in RAW264.7 cells, information previously unknown. Although removal of the N-terminal serine residues had no evident affect on localisation, the size of p-nut after western blotting is markedly different from Nramp1. The reason for this discrepancy is still an enigma but glycosylation is a part of the puzzle.

Constitutive p-nut expression in RAW cells produces comparable growth defects to those caused by wildtype Nramp1 expression (fig.**5.2.23**). As this is the case it is reasonable to assume that the mutant p-nut protein has retained gross *Nramp1* function; allowing greater confidence in results attained from p-nut analysis.

P-nut mobility shifts. Western blotting Nramp1 and p-nut containing cell extracts exposed a dramatic difference in appearance (figs.**5.2.21** & **5.2.22**). The major form of Nramp1 found on a denaturing gel migrated substantially further into the gel when missing its three N-terminal serines, substituted for alanine. Mobility

shifts on SDS denaturing gels can occur with proteins that become phosphorylated, such as ERK1/2(155). This type of mobility shift is often subtle and unlike that seen for p-nut upper bands. The treatment of p-nut and Nramp1 extracts with PNGaseF reconstitutes a primary band that is lower than the 45kDa band in untreated extracts. This band migrates to a similar distance in p-nut and Nramp1 extracts, contrasting to the mobility shift seen when carbohydrate is attached. The formation of a smear or set of bands below this primary band is probably a result of protease digestion: glycosylation often acting as a barrier against protease attack (156-159). Such a problem is more likely to occur in *Nramp1* extracts as they cannot be boiled before SDS-PAGE, but also because treatment with PNGaseF requires incubation at room temperature or 37°C. These conditions could allow residual active proteases, especially concentrated in macrophages, to attack. Interestingly later examination using a PNGaseF protocol containing protease inhibitors (2.2.19) and using membrane isolation to increase the ratio of Nramp1: cellular protein showed this to be the case (fig.**5.3.1**, lane 2), also leading to improvement in quality of untreated extracts (fig.**5.3.1**, lane 1). Unfortunately p-nut lines had already been lost.

Figure 5.3.1

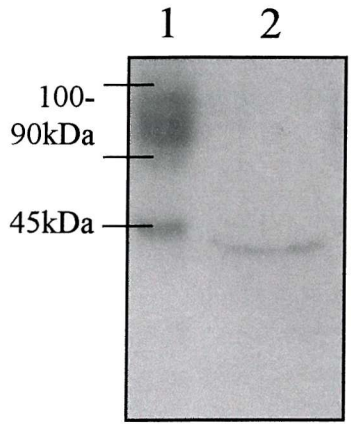

Figure 5.3.1. Treatment of 37 cells with PNGaseF: Western blot of Nramp1 from 37 cells without treatment, lane **1** and with treatment, lane **2** using the modified method (2.2.19).

The similarity between Nramp1 and p-nut reconstituted and 45kDa bands would suggest that the difference seen between HMW bands would have to be a consequence of alternative glycosylation in p-nut lines. The fact that the 45kDa band

resides slightly higher above the reconstituted band would advocate that this band is itself glycosylated; perhaps a precursor as has been mentioned: this is supported by the HMW bands absence in *Nramp1* G169A mutant macrophages. The data therefore insinuate that p-nut can either form a normal precursor Nramp1 glycoprotein with highly modified end glycosylated products, or that only one of the N-linked glycosylation sites is active during protein maturation. The later theory is to some extent supported by the observation that partial digestion of Nramp1 with PNGaseF, an enzyme that hydrolyses the bond between asparagine and proximal N-acetyl-glucosamine, 'all or nothing' loss, leads to formation of an intermediate band with similar size to the lower portion of p-nut untreated protein (fig.**5.2.22**). These experiments, however, were hard to produce due to the action of proteases and likely variable because of this, consequently they were difficult to assess reliably.

The altered mobility of p-nut could not be reproduced artificially in Nramp1 expressing cell lines. This was attempted through the use of a broad-spectrum PKC inhibitor, BSM, but also through uptake of pathogens that lead to recruitment of Nramp1 to phagosomes. The inability of BSM to produce the desired response (fig.**5.2.31**) could be interpreted in at least two ways. (**1**) BSM is unable to inhibit Ca^{2+}-independent and DAG insensitive atypical PKCs ζ/λ, of which both are present in RAW264.7 cells (160). Nramp1 may be a substrate for these PKCs. (**2**) Putative PKC sites are not phosphorylated but instead the removal of three hydroxyl groups in p-nut may cause modifications in protein folding leading to alternative glycosylation.

In both cases the enigma lies in how either phosphorylation of N-terminal serine residues or removal of hydroxyl groups could affect glycosylation as both modifications are putatively contained in the cytoplasm and separated from the glycosylation machinery by a lipid bilayer. There is no direct evidence but

complementary information does support theory (2). Alternative glyco-forms occur in a hormone known as hCG where removal of a C-terminal portion of its β-subunit, not present in other family members, causes alteration but not removal of N-terminal glycosylation (161). It is difficult to conceive how three cytoplasmic contained N-terminal amino acids could affect glycosylation in this way except that the process may be exquisitely sensitive, demonstrated by Nramp1 G169D mutants; a single amino acid change. This mutant is able to fold soundly as it is targeted correctly (47) (all be it less efficiently) but is not glycosylated appropriately forming LMW but not HMW products, perhaps reflecting a paradigm for p-nut as it too is targeted correctly but differentially glycosylated.

Labeling of Nramp1 proteins with EGFP and DsRed has not been reported before. For this reason EGFP-Nramp1 was tested for correct targeting in cell lines. EGFP-Nramp1 was found to be expressed in a different cellular compartment to DsRed-Nramp2 but also to be targeted to vesicles largely exclusive of transferrin in RAW cells. In addition to this it was found in vesicles that accumulate lysoTracker, an acidotropic probe, in both fibroblast and RAW cells. EGFP-p-nut co-localised with lysoTracker but remained exclusive of transferrin during transferrin uptake experiments, comparable to EGFP-Nramp1. Both Nramp1 and p-nut EGFP-tagged proteins produce staining patterns that are consistent with the literature (47); largely contained within the peri-nuclear region of the cell with some staining throughout the cytoplasm but not in the nucleus or at the plasma membrane. As described they localise to acidic vesicles, likely lysosomes, but remain detached from transferrin containing vesicles which have been shown to co-localise with Nramp2, which itself does not co-localise with Nramp1 (86).

Comparison of antibody stained RAW cell lines stably expressing Nramp1 or p-nut highlighted one major difference to the EGFP-tagged proteins. Antibody staining produced punctate expression whereas tagged protein expression produced ribbon-like staining. The ribbons are most likely tubular lysosomes, which have been reported before in macrophages and tend to cluster toward the cell center (162-164). In addition to this tubular lysosomes are very sensitive to chemical fixation a procedure that is used during antibody staining and is likely to be the cause of the differences seen. In fact studies show that ≥3% paraformaldehyde fixation heavily disrupts tubular lysosomes in macrophages (162), 4% being used in our studies. Interestingly tubular lysosomes are thought to wrap around newly formed phagosomes to form phagolysosomes and it has been established that: the disappearance of tubules is proportional to the total surface area of the particle ingested (163). This was observed for EGFP-Nramp1 and EGFP-p-nut where substantial uptake of zymosan leads to complete removal of any ribbon-like structures (fig.**5.2.51** (**e**)-(**h**)); further support that both fusion proteins are indeed targeted correctly. The extensive tubular lysosomal networks found in macrophages are not as abundant in fibroblasts, which instead have more vesicular lysosomes that spread from the cell center to the periphery frequently in linear arrays (165). This is akin to EGFP tagged Nramp1 and p-nut expression in L1 3T3 fibroblasts.

No difference between EGFP tagged Nramp1 and p-nut staining was observed in resting cells, but it was necessary to analyse behavior during cell activation. Unfortunately macrophages become autofluorescent during 5 hours of zymosan uptake making study of early lysosome/EGFP-protein movement to the plasma membrane very difficult. Inflammatory macrophages are known to intensely fluoresce but the cause is unidentified (166;167) and autofluorescence in RAW cells

due to zymosan was not found in the literature. However it would seem that autofluorescence could go hand in hand with inflammatory activation.

Interestingly both EGFP-Nramp1/EGFP-p-nut are recruited to phagolysosomes containing zymosan, an effect suggesting that phagocytosis leads to a general recruitment of Nramp1 that is not specific to intracellular parasites and opsonised beads. P-nut movement to phagolysosomes strengthens the notion that the putative PKC phosphorylation sites are not involved in Nramp1 translocation.

Fibroblasts also have the ability to secrete lysosomal contents but through a mechanism that involves increases in cytosolic calcium concentration (153;168). In the literature calcium has only a minor role in macrophage lysosomal secretion (149;154), comparable to observations in this report; no fusion of lysoTracker containing vesicles occurred in RAW264.7 cells during calcium ionophore treatment. In addition there was no movement of Nramp1 to the plasma membrane. The opposite occurs during calcium ionophore treatment of fibroblasts transiently expressing Nramp1 and p-nut EGFP fusion proteins. Movement of both Nramp1 and p-nut EGFP proteins to the plasma membrane occurred over ~10 minutes of A23187 treatment known to cause secretion of lysosomal contents (153;169). Of interest during this process was the dramatic change in cell morphology with the appearance of a extended cytoplasm; lysosome fusion in fibroblasts has been studied as a mechanism for membrane healing (169) and aberrant induction of such a mechanism is known to cause massive increases in membrane surface area (170), perhaps the cause of the extended cytoplasm.

Although not the natural cell type, movement of Nramp1 to the fibroblast plasma membrane rules 'in' rather than out a hypothesis involving Nramp1 targeting to the macrophage plasma membrane during lysosome exocytosis. Tests of iron

release from fibroblast lines stably expressing Nramp1 could not be carried out, as these lines were lost. Nevertheless, increased iron release from lysosomes of RAW cells expressing *Nramp1* (5.1 introduction), during zymosan uptake but not when resting, and membrane binding of Nramp1 during lysosome exocytosis in fibroblasts is very suggestive.

The putative presence of an Nramp1 positive vesicle system accumulating and storing iron that can be released under conditions promoting lysosomal exocytosis begs the question why? *In vivo* analysis of iron overloaded mice expressing phenotypically null (mutant) or wildtype *Nramp1* shows that the processing of iron in the spleen of mutant mice is compromised (121). Further un-published results in our group demonstrate that the spleens of several strains of mutant mice are larger than those of wildtype counterparts. The functional significance of these observations is not known, but the possible presence of a subset of iron laden lysosomes in cultured macrophages and impaired iron processing in mutant mice in addition to their enlarged spleens indicates that Nramp1 is involved in an aspect of iron recycling. This role is subtle however and except for the enlarged spleens is only observed during iron stress (121). Interestingly, analogous to fibroblast membrane healing, exocytosis of intracellular vesicles occurs during uptake of erythrocytes and involves the cells' need to replenish membrane surface area during phagocytosis (171). This mechanism entails the action of a family of SNARE and SNAP proteins that specifically interact and orchestrate fusion events through location of different family members on different membranes. Specifically it has been found that plasma and endomembrane fusion requires VAMP-2 or a related SNARE and that this process is essential for optimal phagocytosis of opsonised red blood cells and zymosan particles in J774 cells (171); a murine macrophage cell line. Although the location of

Figure 5.3.2

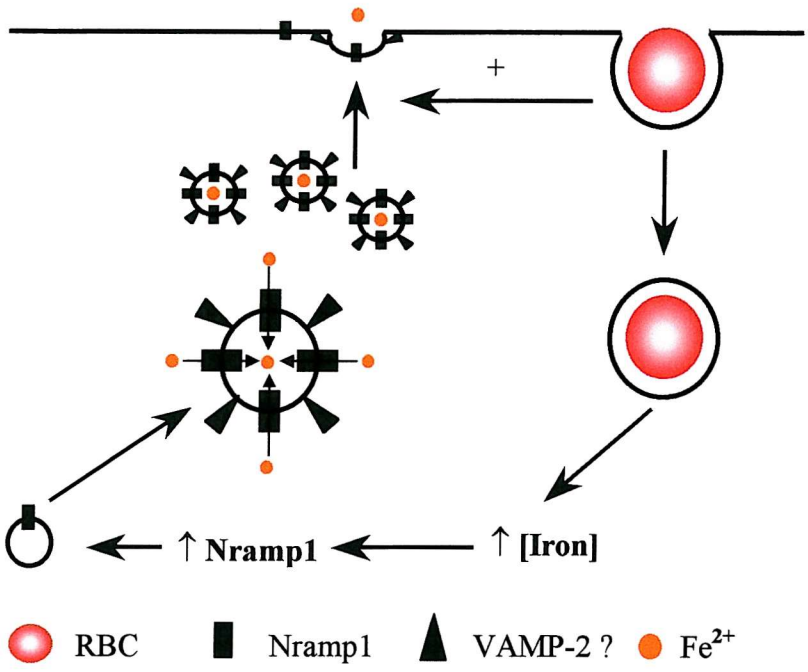

Figure 5.3.2. Diagram depicts possible events occurring during macrophage erythrophagocytosis.

VAMP-2 in macrophages is unknown VAMP-2 in neutrophils localises to secretory vesicles and tertiary granules both of which are secreted during phagocytosis (171;172) suggesting it has a general role in this pathway. This system may link Nramp1, iron-laden lysosomes, and the differential iron release absent in resting cells (5.3.2).

In summary it was found that three putative PKC phosphorylation sites in Nramp1's N-terminal domain are not involved in protein targeting. It is not known if these residues are phosphorylated *in vivo* but alternative glycosylation of the mutant protein would suggest that one or a combination of these sites is important in this process. Nramp1 is targeted to fibroblast plasmalemma under conditions that are known to cause lysosome exocytosis. Physiologically it is suggested that *Nramp1*, aside from innate immunity, may aid in a pathway culminating in release of iron from

oxidized and ageing red blood cells. How this occurs is not known but phagocytosis of immune complexed iron leads to release of similar levels of iron in resting RAW cells that express or do not express wildtype *Nramp1*. As this is the case Nramp1 mediated increases in lysosomal iron do not affect this cations eventual release, explaining the absence of an iron disorder with a strong phenotype in mutant mice. Instead Nramp1 may increase the efficiency of iron recycling, through exocytosis of iron-laden lysosomes, an outcome that evolution has exploited in pathogen resistance.

Chapter 6

General Discussion And Future Work

This thesis has provided evidence that *Nramp1* expression leads to lower levels of cytoplasmic iron but also that *Nramp1* expression is regulated by this cation. The ability of iron to augment *Nramp1* mRNA and protein expression but also that Nramp1 can in turn deplete levels of cytoplasmic iron suggests that this protein may be able to autoregulate its own expression through a negative feedback loop. *In vivo* support for iron regulation of Nramp1 expression manifests as this protein's tissue specific expression within the liver and spleen, areas of senescent erythrocyte iron recycling (121). In addition *Nramp1* mRNA is regulated by the synthetic analogue of haem, hemin. It was originally remarked by Flemming *et al.* that *Nramp1* might be involved in RBC iron recycling (79). The general recruitment of this protein to newly formed phagosomes may also allow its movement to phagosomes containing RBC, although this has never been shown. Still it remains that if *Nramp1* can be regulated by RBCs but also by catabolites of their breakdown then perhaps it is also involved in the recycling of RBC derived iron to the plasma. Interestingly this study has observed the first induced movement of Nramp1 to a membrane other than that of newly formed phagosomes. Indeed this year Mulero and colleagues have shown that uptake of transferrin-anti-transferrin immune complexes by resistant and susceptible macrophages leads, later, to differential NO induced iron release; resistant macrophages showing a 2.4 fold better release (173). It was remarked that this could be due to the NO induced exocytosis of lysosomes that occurs in other cell types.

Interestingly this group also recognized decreased ferritin levels in resistant macrophages consistent with lower cytoplasmic iron and the results within this report.

In summary Nramp1 is known to localise to late endosomes and lysosomes but also to phagolysosomes (87). Its expression increases the iron levels within isolated phagosomes and it has been shown to act as an anti-port transporter for hydrogen ions and divalent cations (94). Its close orthologue *Nramp2* has been conclusively shown to not only transport iron but to have a major regulatory role in mammalian homeostatic control of this cation (79;86;90;174-176). The work in this report shows that *Nramp1* is regulated positively by iron but also that it reduces the levels of cytoplasmic iron. In addition it is able to translocate to the plasma membrane under an appropriate stimulus suggesting it is expressed upon lysosomes with the necessary machinery for this to occur. In light of this evidence it is proposed that Nramp1 acts as an anti-port transporter transporting ferrous iron from the cytoplasm to the lumen of late endosomes, lysosomes and phagolysosomes using the hydrogen iron gradient created by v-ATPase on these vesicles. During phagocytosis and degradation of RBCs *Nramp1* expression is increased, an action that in turn causes greater levels of iron to be withheld within the cells vesicular system. Under an appropriate stimulus, which may involve general phagocytosis (chapter 5, fig.5.3.2) or NO induced reduction in lysosomal acidity (173), a known mechanism for lysosomal secretion (149;177;178), Nramp1 translocates to the plasma membrane with subsequent release of iron from the secretory vesicles it is expressed upon. Functionally this may act to create an inducible pathway for the release of iron from iron-laden vesicles brought about by the expression of Nramp1. Finally, NO induced secretion of iron from macrophages may act to reduce cellular iron levels during attack of bacteria favoring

the intracellular environment of this cell, an ability enhanced by *Nramp1* and explaining abrogation of resistance during iron overload.

The study of this mechanism requires further analysis of Nramp1 movement during phagocytosis of senescent RBCs and also during NO treatment in macrophages, two assays that could use EGFP tagged *Nramp1* and time lapse confocal microscopy. Interestingly a study by Gruenheid *et al.* looking at the rate of Nramp1 recruitment to latex bead containing phagosomes did not comment on movement of Nramp1 to the cell membrane(24); an observation also not recorded by others using bacteria (47). The reason for this is not known but may have been a result of the static nature of these experiments using antibodies and therefore cell fixing. EGFP-tagged Nramp1 analysis would allow real time study of Nramp1 movement and would prove useful in determining any plasma membrane targeting over an extended time period, an event that is likely to be transient.

Examination of the three putative PKC phosphorylation sites within the N-terminal domain of Nramp1 has revealed, that together, they have no role in the gross anatomy of its localisation or targeting. In addition this mutant protein could also attenuate DNA synthesis within RAW264.7 cells to a level seen using wildtype *Nramp1* expressing cells; implying that they have little role in its function and that the protein is folding correctly. It was not determined in this investigation if removal of the three PKC sites reduced Nramp1 phosphorylation, it is therefore not possible to say if glycosylation is affected by their removal or by the absence of three hydroxyl groups. It was shown that a broad spectrum PKC inhibitor could not affect Nramp1 glycosylation but this compound is unable to inhibit the atypical PKCs ζ/λ. Due to the lack of a highly specific inhibitory compound for these proteins studies have used anti-sense (99), transfection of kinase inactive isoforms (179) and production of cell

permeable peptides containing the pseudosubstrate for these PKCs (180) to inhibit their activity. Transfection of macrophages is very difficult and produces very low transfection rates making use of promoter driven anti-sense and kinase inactive isoform constructs difficult. Pseudosubstrates have been successfully used by Bhattacharyya *et al.* in macrophages (181), however, and may provide the best opportunity for analysis of the role of atypical PKC isoforms in the glycosylation of Nramp1. The activity of these putative PKC sites should first be examined though, requiring the immunoprecipitation of Nramp1/p-nut and analysis of phosphorylation using mass spectrometry. This should reveal whether the N-terminal domain of Nramp1 is phosphorylated and in turn, together with PKC inhibition studies, answer whether the hydroxyl groups are of importance to glycosylation of this protein.

The identification of two putative antioxidant response elements in an unpublished (our group) extended part of the promoter has provided a possible pathway for induction of *Nramp1* transcription by radicals/hemin. Chapter 3 demonstrated that Nramp1 protein expression was enhanced by superoxide but attenuated by superoxide dismutase. In addition SNP was also able to induce protein and mRNA expression. This compound however produces both nitrosonium ions and superoxide in addition to containing iron. In the absence of tests using a specific compound producing nitric oxide it was not possible to demonstrate a role for this molecule in induction studies. Studies with SNP did reproducibly produce observed better induction than iron or paraquat alone though, and may reflect synergy between molecules and ions produced by this compound. Further study should clarify the role of nitric oxide by using compounds such as SIN-1 (a compund specifically releasing NO into the cell) and perhaps identify whether it is important in IFN-γ/LPS signaling, molecules that potently stimulate NO production by iNOS, using aminoguanidine – an

inhibitor of iNOS activity. The involvement of the ARE elements in these pathways could be studied through the use of luciferase *Nramp1* promoter constructs carrying these elements or mutated variations. The participation of Nrf2 could be grossly examined through the use of stable macrophage lines expressing the Nrf2 transcription factor or dominant negative isoforms (182). In addition band shifts/supershifts could be used to analyse the transcription factors that bind to the ARE during oxidative stress/iron conditions. These, as described in 3.3, may involve small Maf proteins or Jun/Fos interactions with Nrf2. The limitation of these experiments may involve the inappropriate use of dividing cell lines. As mentioned in 3.3 there are 6 non-canonical c-myc sites within the extended *Nramp1* promoter and its insensitivity in RAW264.7 cells may be reflected through the interference of abnormally expressed transcription factors. If this is the case stable cell lines expressing Nrf2 will be of no use and analysis of this transcription factor and its dominant negative isoforms would require the dual transfection of murine tissue macrophages. This is an extremely difficult task that would also require an assay to test dual expression of both the promoter construct and of Nrf2 expression within the same cell. This could perhaps be done through dual fluorescence analysis tagging the promoter construct with EGFP and the Nrf2 constructs with a ribosomal re-entry site for DsRed. Cells expressing both constructs could be sorted using fax analysis and the effect of Nrf2 on the promoter construct later measured as a positive or negative effect upon the EGFP fluorescence compared to a set of controls.

The classic method of DNA foot printing could also be used to study transcription factor binding to the ARE.

In conclusion it is interesting to speculate on the diverse roles of *Nramp1*, a protein originally identified as being able to increase resistance to intracellular

parasites in mice. Although studies are still conflicting it would appear that *Nramp1* codes for an anti-port transporter able to transport iron across vesicle membranes of acidic organelles to which it is targeted. The way in which this attenuates the growth of bacteria has been postulated to involve the production of radicals, although it may now seem that Nramp1 is involved in increased iron release through exocytosis of lysosomes under an appropriate stimulus, such as NO. This molecule is itself produced during the attack of bacteria upon macrophages and the expression of iNOS is enhanced in resistant macrophages. Together this may act to reduce the iron content of resistant macrophages starving the bacteria of this essential nutrient.

The exocytosis of iron-laden lysosomes may have a role in the recycling of iron from senescent erythrocytes but evidence is required to show that there are greater levels of iron release from resistant macrophages during erythrophagocytosis. Still it remains that this does not have a major effect on mammalian iron homeostasis, as susceptible animals do not show iron-associated disease phenotypes, although a brain-lesion model and iron overload studies do demonstrate that *Nramp1* has an iron modulatory effect in stress-associated circumstances (121).

Lastly a novel aspect of Nramp1 function may involve its use as a putative antioxidant protein. Indeed this study demonstrated enhanced resistance to paraquat induced stress by resistant macrophages and also the putative presence of an ARE element within the *Nramp1* promoter, additionally Nramp1 expression is regulated by oxidative radicals.

References

1. **Molbak,K., Baggesen,D.L., Aarestrup,F.M., Ebbesen,J.M., Engberg,J., Frydendahl,K., Gerner-Smidt,P., Petersen,A.M., and Wegener,H.C.,** An outbreak of multidrug-resistant, quinolone-resistant *Salmonella* enterica serotype *typhimurium* DT104. *N.Engl.J.Med.* 1999. **341**: 1420-1425.
2. **Sreevatsan,S., Pan,X., Zhang,Y., Kreiswirth,B.N., and Musser,J.M.,** Mutations associated with pyrazinamide resistance in pncA of *Mycobacterium tuberculosis* complex organisms. *Antimicrob.Agents Chemother.* 1997. **41**: 636-640.
3. **Sun,Z., Scorpio,A., and Zhang,Y.,** The pncA gene from naturally pyrazinamide-resistant *Mycobacterium avium* encodes pyrazinamidase and confers pyrazinamide susceptibility to resistant M. tuberculosis complex organisms. *Microbiology* 1997. **143 (Pt 10)**: 3367-3373.
4. **Zhang,Y., Scorpio,A., Nikaido,H., and Sun,Z.,** Role of acid pH and deficient efflux of pyrazinoic acid in unique susceptibility of *Mycobacterium tuberculosis* to pyrazinamide. *J.Bacteriol.* 1999. **181**: 2044-2049.
5. **Orme,I.M.,** Beyond BCG: the potential for a more effective TB vaccine. *Mol.Med.Today* 1999. **5**: 487-492.
6. **Skamene,E., Schurr,E., and Gros,P.,** Infection genomics: Nramp1 as a major determinant of natural resistance to intracellular infections. *Annual Review of Medicine* 1998. **49**: 275-287.
7. **Hill,A.V.,** Genetics of infectious disease resistance. *Curr.Opin.Genet.Dev.* 1996. **6**: 348-353.
8. **McLeod,R., Buschman,E., Arbuckle,L.D., and Skamene,E.,** Immunogenetics in the analysis of resistance to intracellular pathogens. *Curr.Opin.Immunol.* 1995. **7**: 539-552.
9. **Jouanguy,E., Altare,F., Lamhamedi,S., Revy,P., Emile,J.F., Newport,M., Levin,M., Blanche,S., Seboun,E., Fischer,A., and Casanova,J.L.,** Interferon-gamma-receptor deficiency in an infant with fatal bacille Calmette-Guerin infection. *N.Engl.J.Med.* 1996. **335**: 1956-1961.
10. **Bellamy,R. and Hill,A.V.,** Genetic susceptibility to mycobacteria and other infectious pathogens in humans. *Curr.Opin.Immunol.* 1998. **10**: 483-487.
11. **Bellamy,R. and Hill,A.V.,** Genetic susceptibility to mycobacteria and other infectious pathogens in humans. *Curr.Opin.Immunol.* 1998. **10**: 483-487.
12. **Roy,S., Frodsham,A., Saha,B., Hazra,S.K., Mascie-Taylor,C.G., and Hill,A.V.,** Association of vitamin D receptor genotype with leprosy type. *J.Infect.Dis.* 1999. **179**: 187-191.
13. **Hill,A.V.,** Genetic susceptibility to malaria and other infectious diseases: from the MHC to the whole genome. *Parasitology* 1996. **112 Suppl** : S75-S84.
14. **Sauer,B.,** Inducible gene targeting in mice using the Cre/lox system. *Methods* 1998. **14**: 381-392.
15. **Plant,J. and Glynn,A.A.,** Genetics of resistance to infection with Salmonella typhimurium in mice. *J.Infect.Dis.* 1976. **133**: 72-78.
16. **Gros,P., Skamene,E., and Forget,A.,** Genetic control of natural resistance to Mycobacterium bovis (BCG) in mice. *J.Immunol.* 1981. **127**: 2417-2421.
17. **Bradley,D.J. and Kirkley,J.,** Variation in susceptibility of mouse strains to Leishmania donovani infection. *Trans.R.Soc.Trop.Med.Hyg.* 1972. **66**: 527-528.

18. **Glynn,A.A.,** Resistance to infection: looking for new genes. *Bull.Eur.Physiopathol.Respir.* 1983. **19**: 143-145.

19. **Pelletier,M., Forget,A., Bourassa,D., Gros,P., and Skamene,E.,** Immunopathology of BCG infection in genetically resistant and susceptible mouse strains. *J.Immunol.* 1982. **129**: 2179-2185.

20. **Buschman,E. and Skamene,E.,** From bcg/lsh/ity to nramp1: three decades of search and research. *Drug Metab Dispos.* 2001. **29**: 471-473.

21. **Morrison,D.C., Duncan,R.L., Jr., and Goodman,S.A.,** In vivo biological activities of endotoxin. *Prog.Clin.Biol.Res.* 1985. **189**: 81-99.

22. **Nishimoto,T.,** Upstream and downstream of ran GTPase. *Biol.Chem.* 2000. **381**: 397-405.

23. **Yuan,Q., Zhao,F., Chung,S.W., Fan,P., Sultzer,B.M., Kan,Y.W., and Wong,P.M.,** Dominant negative down-regulation of endotoxin-induced tumor necrosis factor alpha production by Lps(d)/Ran. *Proc.Natl.Acad.Sci.U.S.A* 2000. **97**: 2852-2857.

24. **Gruenheid,S., Pinner,E., Desjardins,M., and Gros,P.,** Natural resistance to infection with intracellular pathogens: the Nramp1 protein is recruited to the membrane of the phagosome. *J.Exp.Med.* 1997. **185**: 717-730.

25. **Gros,P., Skamene,E., and Forget,A.,** Cellular mechanisms of genetically controlled host resistance to Mycobacterium bovis (BCG). *J.Immunol.* 1983. **131**: 1966-1972.

26. **Skamene,E., Gros,P., Forget,A., Kongshavn,P.A., St Charles,C., and Taylor,B.A.,** Genetic regulation of resistance to intracellular pathogens. *Nature* 1982. **297**: 506-509.

27. **Denis,M., Forget,A., Pelletier,M., Gervais,F., and Skamene,E.,** Killing of Mycobacterium smegmatis by macrophages from genetically susceptible and resistant mice. *J.Leukoc.Biol.* 1990. **47**: 25-30.

28. **Lissner,C.R., Swanson,R.N., and O'Brien,A.D.,** Genetic control of the innate resistance of mice to Salmonella typhimurium: expression of the Ity gene in peritoneal and splenic macrophages isolated in vitro. *J.Immunol.* 1983. **131**: 3006-3013.

29. **Crocker,P.R., Blackwell,J.M., and Bradley,D.J.,** Expression of the natural resistance gene Lsh in resident liver macrophages. *Infect.Immun.* 1984. **43**: 1033-1040.

30. **Goto,Y., Buschman,E., and Skamene,E.,** Regulation of host resistance to Mycobacterium intracellulare in vivo and in vitro by the Bcg gene. *Immunogenetics* 1989. **30**: 218-221.

31. **Vidal,S.M., Malo,D., Vogan,K., Skamene,E., and Gros,P.,** Natural resistance to infection with intracellular parasites: isolation of a candidate for Bcg. *Cell* 1993. **73**: 469-485.

32. **Buckler,A.J., Chang,D.D., Graw,S.L., Brook,J.D., Haber,D.A., Sharp,P.A., and Housman,D.E.,** Exon amplification: a strategy to isolate mammalian genes based on RNA splicing. *Proc.Natl.Acad.Sci.U.S.A* 1991. **88**: 4005-4009.

33. **Barton,C.H., White,J.K., Roach,T.I., and Blackwell,J.M.,** NH2-terminal sequence of macrophage-expressed natural resistance- associated macrophage protein (Nramp) encodes a proline/serine-rich putative Src homology 3-binding domain. *J.Exp.Med.* 1994. **179**: 1683-1687.

34. **Malo,D., Vogan,K., Vidal,S., Hu,J., Cellier,M., Schurr,E., Fuks,A., Bumstead,N., Morgan,K., and Gros,P.,** Haplotype mapping and sequence analysis of the mouse Nramp gene predict susceptibility to infection with intracellular parasites. *Genomics* 1994. **23**: 51-61.

35. **Vidal,S., Tremblay,M.L., Govoni,G., Gauthier,S., Sebastiani,G., Malo,D., Skamene,E., Olivier,M., Jothy,S., and Gros,P.,** The Ity/Lsh/Bcg locus: natural resistance to infection with intracellular parasites is abrogated by disruption of the Nramp1 gene. *J.Exp.Med.* 1995. **182**: 655-666.

36. **Govoni,G., Vidal,S., Gauthier,S., Skamene,E., Malo,D., and Gros,P.,** The Bcg/Ity/Lsh locus: genetic transfer of resistance to infections in C57BL/6J mice transgenic for the Nramp1 Gly169 allele. *Infect.Immun.* 1996. **64**: 2923-2929.

37. **Gruenheid,S., Cellier,M., Vidal,S., and Gros,P.,** Identification and characterization of a second mouse Nramp gene. *Genomics* 1995. **25**: 514-525.

38. **Cellier,M., Prive,G., Belouchi,A., Kwan,T., Rodrigues,V., Chia,W., and Gros,P.,** Nramp defines a family of membrane proteins. *Proc.Natl.Acad.Sci.U.S.A* 1995. **92**: 10089-10093.

39. **Makui,H., Roig,E., Cole,S.T., Helmann,J.D., Gros,P., and Cellier,M.F.,** Identification of the Escherichia coli K-12 Nramp orthologue (MntH) as a selective divalent metal ion transporter. *Mol.Microbiol.* 2000. **35**: 1065-1078.

40. **Kishi,F., Yoshida,T., and Aiso,S.,** Location of NRAMP1 molecule on the plasma membrane and its association with microtubules. *Mol.Immunol.* 1996. **33**: 1241-1246.

41. **Tokuraku,K., Nakagawa,H., Kishi,F., and Kotani,S.,** Human natural resistance-associated macrophage protein is a new type of microtubule-associated protein. *FEBS Lett.* 1998. **428**: 63-67.

42. **Gruenheid,S. and Gros,P.,** Genetic susceptibility to intracellular infections: Nramp1, macrophage function and divalent cations transport. *Current Opinion in Microbiology* 2000. **3**: 43-48.

43. **Atkinson,P.G.P. and Barton,C.H.,** Ectopic expression of Nramp1 in COS-1 cells modulates iron accumulation. *Febs Letters* 1998. **425**: 239-242.

44. **Vidal,S.M., Pinner,E., Lepage,P., Gauthier,S., and Gros,P.,** Natural resistance to intracellular infections: Nramp1 encodes a membrane phosphoglycoprotein absent in macrophages from susceptible (Nramp1 D169) mouse strains. *J.Immunol.* 1996. **157**: 3559-3568.

45. **Atkinson,P.G., Blackwell,J.M., and Barton,C.H.,** Nramp1 locus encodes a 65 kDa interferon-gamma-inducible protein in murine macrophages. *Biochem.J.* 1997. **325 (Pt 3)**: 779-786.

46. **Niu,L., Heaney,M.L., Vera,J.C., and Golde,D.W.,** High-affinity binding to the GM-CSF receptor requires intact N- glycosylation sites in the extracellular domain of the beta subunit. *Blood* 2000. **95**: 3357-3362.

47. **Searle,S., Bright,N.A., Roach,T.I., Atkinson,P.G., Barton,C.H., Meloen,R.H., and Blackwell,J.M.,** Localisation of Nramp1 in macrophages: modulation with activation and infection. *J.Cell Sci.* 1998. **111 (Pt 19)**: 2855-2866.

48. **Govoni,G., Vidal,S., Cellier,M., Lepage,P., Malo,D., and Gros,P.,** Genomic structure, promoter sequence, and induction of expression of the mouse Nramp1 gene in macrophages. *Genomics* 1995. **27**: 9-19.

49. **Govoni,G., Vidal,S., Cellier,M., Lepage,P., Malo,D., and Gros,P.,** Genomic structure, promoter sequence, and induction of expression of the mouse Nramp1 gene in macrophages. *Genomics* 1995. **27**: 9-19.

50. **Kaufmann,J., Verrijzer,C.P., Shao,J., and Smale,S.T.,** CIF, an essential cofactor for TFIID-dependent initiator function. *Genes Dev.* 1996. **10**: 873-886.

51. **Sprenger,H., Lloyd,A.R., Lautens,L.L., Bonner,T.I., and Kelvin,D.J.,** Structure, genomic organization, and expression of the human interleukin-8 receptor B gene. *J.Biol.Chem.* 1994. **269**: 11065-11072.

52. **Wyllie,S., Seu,P., and Goss,J.A.,** The natural resistance-associated macrophage protein 1 Slc11a1 (formerly Nramp1) and iron metabolism in macrophages. *Microbes.Infect.* 2002. **4**: 351-359.

53. **Klemsz,M.J., McKercher,S.R., Celada,A., Van Beveren,C., and Maki,R.A.,** The macrophage and B cell-specific transcription factor PU.1 is related to the ets oncogene. *Cell* 1990. **61**: 113-124.

54. **Zhang,D.E., Hetherington,C.J., Chen,H.M., and Tenen,D.G.,** The macrophage transcription factor PU.1 directs tissue-specific expression of the macrophage colony-stimulating factor receptor. *Mol.Cell Biol.* 1994. **14**: 373-381.

55. **Brown,D.H., Lafuse,W., and Zwilling,B.S.,** Cytokine-mediated activation of macrophages from Mycobacterium bovis BCG-resistant and -susceptible mice: differential effects of corticosterone on antimycobacterial activity and expression of the Bcg gene (Candidate Nramp). *Infect.Immun.* 1995. **63**: 2983-2988.

56. **Liu,J., Fujiwara,T.M., Buu,N.T., Sanchez,F.O., Cellier,M., Paradis,A.J., Frappier,D., Skamene,E., Gros,P., and Morgan,K.,** Identification of polymorphisms and sequence variants in the human homologue of the mouse natural resistance-associated macrophage protein gene. *Am.J.Hum.Genet.* 1995. **56**: 845-853.

57. **Singal,D.P., Li,J., Zhu,Y., and Zhang,G.,** NRAMP1 gene polymorphisms in patients with rheumatoid arthritis. *Tissue Antigens* 2000. **55**: 44-47.

58. **Bellamy,R.,** Identifying genetic susceptibility factors for tuberculosis in Africans: a combined approach using a candidate gene study and a genome-wide screen. *Clinical Science* 2000. **98**: 245-250.

59. **Bellamy,R., Ruwende,C., Corrah,T., McAdam,K.P.W.J., Whittle,H.C., and Hill,A.V.S.,** Variations in the Nrampi gene and susceptibility to tuberculosis in West Africans. *New England Journal of Medicine* 1998. **338**: 640-644.

60. **North,R.J. and Medina,E.,** How important is Nramp1 in tuberculosis? *Trends Microbiol.* 1998. **6**: 441-443.

61. **Searle,S. and Blackwell,J.M.,** Evidence for a functional repeat polymorphism in the promoter of the human NRAMP1 gene that correlates with autoimmune versus infectious disease susceptibility. *Journal of Medical Genetics* 1999. **36**: 295-299.

62. **Gao,P.S., Fujishima,S., Mao,X.Q., Remus,N., Kanda,M., Enomoto,T., Dake,Y., Bottini,N., Tabuchi,M., Hasegawa,N., Yamaguchi,K., Tiemessen,C., Hopkin,J.M., Shirakawa,T., and Kishi,F.,** Genetic variants of NRAMP1 and active tuberculosis in Japanese populations. International Tuberculosis Genetics Team [letter] [In Process Citation]. *Clin.Genet.* 2000. **58**: 74-76.

63. **Sanjeevi,C.B., Miller,E.N., Dabadghao,P., Rumba,I., Shtauvere,A., Denisova,A., Clayton,D., and Blackwell,J.M.,** Polymorphism at NRAMP1 and D2S1471 loci associated with juvenile rheumatoid arthritis. *Arthritis Rheum.* 2000. **43**: 1397-1404.

64. **Yang,Y.S., Kim,S.J., Kim,J.W., and Koh,E.M.,** NRAMP1 gene polymorphisms in patients with rheumatoid arthritis in Koreans. *J.Korean Med.Sci.* 2000. **15**: 83-87.

65. **Shaw,M.A., Clayton,D., and Blackwell,J.M.,** Analysis of the candidate gene NRAMP1 in the first 61 ARC National Repository families for rheumatoid arthritis. *J.Rheumatol.* 1997. **24**: 212-214.

66. **Shaw,M.A., Clayton,D., Atkinson,S.E., Williams,H., Miller,N., Sibthorpe,D., and Blackwell,J.M.,** Linkage of rheumatoid arthritis to the candidate gene NRAMP1 on 2q35. *J.Med.Genet.* 1996. **33**: 672-677.

67. **Brown,D.H., Lafuse,W.P., and Zwilling,B.S.,** Stabilized expression of mRNA is associated with mycobacterial resistance controlled by Nramp1. *Infect.Immun.* 1997. **65**: 597-603.

68. **Brown,D.H., Miles,B.A., and Zwilling,B.S.,** Growth of Mycobacterium tuberculosis in BCG-resistant and -susceptible mice: establishment of latency and reactivation. *Infect.Immun.* 1995. **63**: 2243-2247.

69. **Arias,M., Rojas,M., Zabaleta,J., Rodriguez,J.I., Paris,S.C., Barrera,L.F., and Garcia,L.F.,** Inhibition of virulent Mycobacterium tuberculosis by Bcg(r) and Bcg(s) macrophages correlates with nitric oxide production. *J.Infect.Dis.* 1997. **176**: 1552-1558.

70. **North,R.J., LaCourse,R., Ryan,L., and Gros,P.,** Consequence of Nramp1 deletion to Mycobacterium tuberculosis infection in mice. *Infect.Immun.* 1999. **67**: 5811-5814.

71. **Medina,E. and North,R.J.,** Evidence inconsistent with a role for the Bcg gene (Nramp1) in resistance of mice to infection with virulent Mycobacterium tuberculosis. *J.Exp.Med.* 1996. **183**: 1045-1051.

72. **Medina,E., Rogerson,B.J., and North,R.J.,** The Nramp1 antimicrobial resistance gene segregates independently of resistance to virulent Mycobacterium tuberculosis. *Immunology* 1996. **88**: 479-481.

73. **Cellier,M., Govoni,G., Vidal,S., Kwan,T., Groulx,N., Liu,J., Sanchez,F., Skamene,E., Schurr,E., and Gros,P.,** Human natural resistance-associated macrophage protein: cDNA cloning, chromosomal mapping, genomic organization, and tissue-specific expression. *J.Exp.Med.* 1994. **180**: 1741-1752.

74. **Marks,M.S., Woodruff,L., Ohno,H., and Bonifacino,J.S.,** Protein targeting by tyrosine- and di-leucine-based signals: evidence for distinct saturable components. *J.Cell Biol.* 1996. **135**: 341-354.

75. **Sturgill-Koszycki,S., Schaible,U.E., and Russell,D.G.,** Mycobacterium-containing phagosomes are accessible to early endosomes and reflect a transitional state in normal phagosome biogenesis. *EMBO J.* 1996. **15**: 6960-6968.

76. **Hackam,D.J., Rotstein,O.D., Zhang,W., Gruenheid,S., Gros,P., and Grinstein,S.,** Host resistance to intracellular infection: mutation of natural resistance-associated macrophage protein 1 (Nramp1) impairs phagosomal acidification. *J.Exp.Med.* 1998. **188**: 351-364.

77. **Pinner,E., Gruenheid,S., Raymond,M., and Gros,P.,** Functional complementation of the yeast divalent cation transporter family SMF by NRAMP2, a member of the mammalian natural resistance- associated macrophage protein family. *J.Biol.Chem.* 1997. **272**: 28933-28938.

78. **Gunshin,H., Mackenzie,B., Berger,U.V., Gunshin,Y., Romero,M.F., Boron,W.F., Nussberger,S., Gollan,J.L., and Hediger,M.A.,** Cloning and characterization of a mammalian proton-coupled metal-ion transporter. *Nature* 1997. **388**: 482-488.

79. **Fleming,M.D., Trenor,C.C., III, Su,M.A., Foernzler,D., Beier,D.R., Dietrich,W.F., and Andrews,N.C.,** Microcytic anaemia mice have a mutation in Nramp2, a candidate iron transporter gene. *Nat.Genet.* 1997. **16**: 383-386.

80. **Su,M.A., Trenor,C.C., Fleming,J.C., Fleming,M.D., and Andrews,N.C.,** The G185R mutation disrupts function of the iron transporter Nramp2. *Blood* 1998. **92**: 2157-2163.

81. **Canonne-Hergaux,F., Gruenheid,S., Ponka,P., and Gros,P.,** Cellular and subcellular localization of the Nramp2 iron transporter in the intestinal brush border and regulation by dietary iron. *Blood* 1999. **93**: 4406-4417.

82. **Le,N.T. and Richardson,D.R.,** Ferroportin1: a new iron export molecule? *Int.J.Biochem.Cell Biol.* 2002. **34**: 103-108.

83. **Roy,C.N. and Enns,C.A.,** Iron homeostasis: new tales from the crypt. *Blood* 2000. **96**: 4020-4027.

84. **Garrick,L.M., Dolan,K.G., Romano,M.A., and Garrick,M.D.,** Non-transferrin-bound iron uptake in Belgrade and normal rat erythroid cells. *J.Cell Physiol* 1999. **178**: 349-358.

85. **Tabuchi,M., Yoshimori,T., Yamaguchi,K., Yoshida,T., and Kishi,F.,** Human NRAMP2/DMT1, which mediates iron transport across endosomal membranes, is localized to late endosomes and lysosomes in HEp-2 cells. *J.Biol.Chem.* 2000. **275**: 22220-22228.

86. **Gruenheid,S., Canonne-Hergaux,F., Gauthier,S., Hackam,D.J., Grinstein,S., and Gros,P.,** The iron transport protein NRAMP2 is an integral membrane glycoprotein that colocalizes with transferrin in recycling endosomes. *J.Exp.Med.* 1999. **189**: 831-841.

87. **Kuhn,D.E., Lafuse,W.P., and Zwilling,B.S.,** Iron transport by isolated phagolysosomes (PL) obtained from the RAW264.7 macrophage (M phi) cell line transfected with resistant or susceptible Nramp1. *Faseb Journal* 1998. **12** : 1611.

88. **Kuhn,D.E., Lafuse,W.P., and Zwilling,B.S.,** Iron transport into mycobacterium avium-containing phagosomes from an Nramp1(Gly169)-transfected RAW264.7 macrophage cell line. *J.Leukoc.Biol.* 2001. **69**: 43-49.

89. **Zwilling,B.S., Kuhn,D.E., Wikoff,L., Brown,D., and Lafuse,W.,** Role of iron in Nramp1-mediated inhibition of mycobacterial growth. *Infect.Immun.* 1999. **67**: 1386-1392.

90. **Fleming,M.D., Romano,M.A., Su,M.A., Garrick,L.M., Garrick,M.D., and Andrews,N.C.,** Nramp2 is mutated in the anemic Belgrade (b) rat: evidence of a role for Nramp2 in endosomal iron transport. *Proc.Natl.Acad.Sci.U.S.A* 1998. **95**: 1148-1153.

91. **Gomes,M.S. and Appelberg,R.,** Evidence for a link between iron metabolism and Nramp1 gene function in innate resistance against Mycobacterium avium. *Immunology* 1998. **95**: 165-168.

92. **Baker,S.T., Barton,C.H., and Biggs,T.E.,** A negative autoregulatory link between Nramp1 function and expression. *J.Leukoc.Biol.* 2000. **67**: 501-507.

93. **Jabado,N., Jankowski,A., Dougaparsad,S., Picard,V., Grinstein,S., and Gros,P.,** Natural resistance to intracellular infections: natural resistance- associated macrophage protein 1 (Nramp1) functions as a pH-dependent manganese transporter at the phagosomal membrane. *J.Exp.Med.* 2000. **192**: 1237-1248.

94. **Goswami,T., Bhattacharjee,A., Babal,P., Searle,S., Moore,E., Li,M., and Blackwell,J.M.,** Natural-resistance-associated macrophage protein 1 is an H+/bivalent cation antiporter. *Biochem.J.* 2001. **354**: 511-519.

95. **Olivier,M., Cook,P., DeSanctis,J., Hel,Z., Wojciechowski,W., Reiner,N.E., Skamene,E., and Radzioch,D.,** Phenotypic difference between Bcg(r) and Bcg(s) macrophages is related to differences in protein-kinase-C-dependent signalling. *Eur.J.Biochem.* 1998. **251**: 734-743.

96. **Dempsey,E.C., Newton,A.C., Mochly-Rosen,D., Fields,A.P., Reyland,M.E., Insel,P.A., and Messing,R.O.,** Protein kinase C isozymes and the regulation of diverse cell responses. *Am.J.Physiol Lung Cell Mol.Physiol* 2000. **279**: L429-L438.

97. **Dutil,E.M., Toker,A., and Newton,A.C.,** Regulation of conventional protein kinase C isozymes by phosphoinositide-dependent kinase 1 (PDK-1). *Curr.Biol.* 1998. **8**: 1366-1375.

98. **Gopalakrishna,R. and Jaken,S.,** Protein kinase C signaling and oxidative stress. *Free Radic.Biol.Med.* 2000. **28**: 1349-1361.

99. **Jaken,S. and Parker,P.J.,** Protein kinase C binding partners. *Bioessays* 2000. **22**: 245-254.

100. **Way,K.J., Chou,E., and King,G.L.,** Identification of PKC-isoform-specific biological actions using pharmacological approaches. *Trends Pharmacol.Sci.* 2000. **21**: 181-187.

101. **Schubert,J. and Wilmer,J.W.,** Does hydrogen peroxide exist "free" in biological systems? *Free Radic.Biol.Med.* 1991. **11**: 545-555.

102. **Kuo,P.C., Abe,K., and Schroeder,R.A.,** Superoxide enhances interleukin 1beta-mediated transcription of the hepatocyte-inducible nitric oxide synthase gene. *Gastroenterology* 2000. **118**: 608-618.

103. **Ogata,N., Yamamoto,H., Kugiyama,K., Yasue,H., and Miyamoto,E.,** Involvement of protein kinase C in superoxide anion-induced activation of nuclear factor-kappa B in human endothelial cells. *Cardiovasc.Res.* 2000. **45**: 513-521.

104. **Pratico,D., Pasin,M., Barry,O.P., Ghiselli,A., Sabatino,G., Iuliano,L., FitzGerald,G.A., and Violi,F.,** Iron-dependent human platelet activation and hydroxyl radical formation: involvement of protein kinase C. *Circulation* 1999. **99**: 3118-3124.

105. **Klann,E., Roberson,E.D., Knapp,L.T., and Sweatt,J.D.,** A role for superoxide in protein kinase C activation and induction of long-term potentiation. *J.Biol.Chem.* 1998. **273**: 4516-4522.

106. **Lafuse,W.P., Alvarez,G.R., and Zwilling,B.S.,** Regulation of Nramp1 mRNA stability by oxidants and protein kinase C in RAW264.7 macrophages expressing Nramp1Gly169. *Biochem.J.* 2000. **351**: 687-696.

107. **Barrera,L.F., Kramnik,I., Skamene,E., and Radzioch,D.,** I-A beta gene expression regulation in macrophages derived from mice susceptible or resistant to infection with M. bovis BCG. *Mol.Immunol.* 1997. **34**: 343-355.

108. **Rojas,M., Olivier,M., Gros,P., Barrera,L.F., and Garcia,L.F.,** TNF-alpha and IL-10 modulate the induction of apoptosis by virulent Mycobacterium tuberculosis in murine macrophages. *J.Immunol.* 1999. **162**: 6122-6131.

109. **Lafuse,W.P., Alvarez,G.R., and Zwilling,B.S.,** Regulation of Nramp1 mRNA stability by oxidants and protein kinase C. *Faseb Journal* 2000. **14**: A1231.

110. **Barton,C.H., Whitehead,S.H., and Blackwell,J.M.,** Nramp transfection transfers Ity/Lsh/Bcg-related pleiotropic effects on macrophage activation: influence on oxidative burst and nitric oxide pathways. *Mol.Med.* 1995. **1**: 267-279.

111. **Liew,F.Y., Li,Y., Moss,D., Parkinson,C., Rogers,M.V., and Moncada,S.,** Resistance to Leishmania major infection correlates with the induction of nitric oxide synthase in murine macrophages. *Eur.J.Immunol.* 1991. **21**: 3009-3014.

112. **Brown,D.H., Sheridan,J., Pearl,D., and Zwilling,B.S.,** Regulation of mycobacterial growth by the hypothalamus-pituitary- adrenal axis: differential responses of Mycobacterium bovis BCG-resistant and -susceptible mice. *Infect.Immun.* 1993. **61**: 4793-4800.

113. **Barrera,L.F., Kramnik,I., Skamene,E., and Radzioch,D.,** Nitrite production by macrophages derived from BCG-resistant and - susceptible congenic mouse strains in response to IFN-gamma and infection with BCG. *Immunology* 1994. **82**: 457-464.

114. **Atkinson,P.G.P. and Barton,C.H.,** High level expression of Nramp1(G169) in RAW264.7 cell transfectants: analysis of intracellular iron transport. *Immunology* 1999. **96**: 656-662.

115. **Sagne,C., Isambert,M.F., Henry,J.P., and Gasnier,B.,** SDS-resistant aggregation of membrane proteins: application to the purification of the vesicular monoamine transporter. *Biochem.J.* 1996. **316 (Pt 3)**: 825-831.

116. **Eisenstein,R.S.,** Iron regulatory proteins and the molecular control of mammalian iron metabolism. *Annu.Rev.Nutr.* 2000. **20**: 627-662.

117. **Iwai,K., Drake,S.K., Wehr,N.B., Weissman,A.M., LaVaute,T., Minato,N., Klausner,R.D., Levine,R.L., and Rouault,T.A.,** Iron-dependent oxidation, ubiquitination, and degradation of

iron regulatory protein 2: implications for degradation of oxidized proteins. *Proc.Natl.Acad.Sci.U.S.A* 1998. **95**: 4924-4928.

118. **Muckenthaler,M., Gray,N.K., and Hentze,M.W.,** IRP-1 binding to ferritin mRNA prevents the recruitment of the small ribosomal subunit by the cap-binding complex eIF4F. *Mol.Cell* 1998. **2**: 383-388.

119. **Fleming,R.E., Migas,M.C., Zhou,X., Jiang,J., Britton,R.S., Brunt,E.M., Tomatsu,S., Waheed,A., Bacon,B.R., and Sly,W.S.,** Mechanism of increased iron absorption in murine model of hereditary hemochromatosis: increased duodenal expression of the iron transporter DMT1. *Proc.Natl.Acad.Sci.U.S.A* 1999. **96**: 3143-3148.

120. **Blackwell,J.M., Roach,T.I., Atkinson,S.E., Ajioka,J.W., Barton,C.H., and Shaw,M.A.,** Genetic regulation of macrophage priming/activation: the Lsh gene story. *Immunol.Lett.* 1991. **30**: 241-248.

121. **Hara,E., Takahashi,K., Takeda,K., Nakayama,M., Yoshizawa,M., Fujita,H., Shirato,K., and Shibahara,S.,** Induction of heme oxygenase-1 as a response in sensing the signals evoked by distinct nitric oxide donors. *Biochem.Pharmacol.* 1999. **58**: 227-236.

122. **Biggs,T.E., Baker,S.T., Botham,M.S., Dhital,A., Barton,C.H., and Perry,V.H.,** Nramp1 modulates iron homoeostasis in vivo and in vitro: evidence for a role in cellular iron release involving de-acidification of intracellular vesicles. *Eur.J.Immunol.* 2001. **31**: 2060-2070.

123. **Saito,K., Nishisato,T., Grasso,J.A., and Aisen,P.,** Interaction of transferrin with iron-loaded rat peritoneal macrophages. *Br.J.Haematol.* 1986. **62**: 275-286.

124. **Crocker,P.R., Davies,E.V., and Blackwell,J.M.,** Variable expression of the murine natural resistance gene Lsh in different macrophage populations infected in vitro with Leishmania donovani. *Parasite Immunol.* 1987. **9**: 705-719.

125. **Ding,S., Yao,D., Deeni,Y.Y., Burchell,B., Wolf,C.R., and Friedberg,T.,** Human NADPH-P450 oxidoreductase modulates the level of cytochrome P450 CYP2D6 holoprotein via haem oxygenase-dependent and -independent pathways. *Biochem.J.* 2001. **356**: 613-619.

126. **Durand,G. and Seta,N.,** Protein glycosylation and diseases: blood and urinary oligosaccharides as markers for diagnosis and therapeutic monitoring. *Clin.Chem.* 2000. **46**: 795-805.

127. **Richardson,D.R.,** Iron and gallium increase iron uptake from transferrin by human melanoma cells: further examination of the ferric ammonium citrate- activated iron uptake process. *Biochim.Biophys.Acta* 2001. **1536**: 43-54.

128. **Wingender,E., Chen,X., Hehl,R., Karas,H., Liebich,I., Matys,V., Meinhardt,T., Pruss,M., Reuter,I., and Schacherer,F.,** TRANSFAC: an integrated system for gene expression regulation. *Nucleic Acids Res.* 2000. **28**: 316-319.

129. **Kehres,D.G., Zaharik,M.L., Finlay,B.B., and Maguire,M.E.,** The NRAMP proteins of Salmonella typhimurium and Escherichia coli are selective manganese transporters involved in the response to reactive oxygen. *Mol.Microbiol.* 2000. **36**: 1085-1100.

130. **Nguyen,T., Huang,H.C., and Pickett,C.B.,** Transcriptional regulation of the antioxidant response element. Activation by Nrf2 and repression by MafK. *J.Biol.Chem.* 2000. **275**: 15466-15473.

131. **Jeyapaul,J. and Jaiswal,A.K.,** Nrf2 and c-Jun regulation of antioxidant response element (ARE)- mediated expression and induction of gamma-glutamylcysteine synthetase heavy subunit gene. *Biochem.Pharmacol.* 2000. **59**: 1433-1439.

132. **Ishii,T., Itoh,K., Takahashi,S., Sato,H., Yanagawa,T., Katoh,Y., Bannai,S., and Yamamoto,M.,** Transcription factor Nrf2 coordinately regulates a group of oxidative stress-inducible genes in macrophages. *J.Biol.Chem.* 2000. **275**: 16023-16029.

133. **Itoh,K., Wakabayashi,N., Katoh,Y., Ishii,T., Igarashi,K., Engel,J.D., and Yamamoto,M.,** Keap1 represses nuclear activation of antioxidant responsive elements by Nrf2 through binding to the amino-terminal Neh2 domain. *Genes Dev.* 1999. **13**: 76-86.

134. **Vaidyanathan,S. and Boroujerdi,M.,** Interaction of dexrazoxane with red blood cells and hemoglobin alters pharmacokinetics of doxorubicin. *Cancer Chemother.Pharmacol.* 2000. **46**: 93-100.

135. **Johnsen,O., Murphy,P., Prydz,H., and Kolsto,A.B.,** Interaction of the CNC-bZIP factor TCF11/LCR-F1/Nrf1 with MafG: binding- site selection and regulation of transcription. *Nucleic Acids Res.* 1998. **26**: 512-520.

136. **Vanin,A.F.,** Dinitrosyl iron complexes and S-nitrosothiols are two possible forms for stabilization and transport of nitric oxide in biological systems. *Biochemistry (Mosc.)* 1998. **63**: 782-793.

137. **Kuhn,D.E., Lafuse,W.P., and Zwilling,B.S.,** Regulation of Nramp1 mediated iron transport. *Faseb Journal* 2000. **14**: A1231.

138. **Baranano,D.E., Wolosker,H., Bae,B.I., Barrow,R.K., Snyder,S.H., and Ferris,C.D.,** A mammalian iron ATPase induced by iron. *J.Biol.Chem.* 2000. **275**: 15166-15173.

139. **Vidal,S., Tremblay,M.L., Govoni,G., Gauthier,S., Sebastiani,G., Malo,D., Skamene,E., Olivier,M., Jothy,S., and Gros,P.,** The Ity/Lsh/Bcg locus: natural resistance to infection with intracellular parasites is abrogated by disruption of the Nramp1 gene. *J.Exp.Med.* 1995. **182**: 655-666.

140. **Kuhn,D.E., Baker,B.D., Lafuse,W.P., and Zwilling,B.S.,** Differential iron transport into phagosomes isolated from the RAW264.7 macrophage cell lines transfected with Nramp1Gly169 or Nramp1Asp169. *J.Leukoc.Biol.* 1999. **66**: 113-119.

141. **Alcantara,O., Obeid,L., Hannun,Y., Ponka,P., and Boldt,D.H.,** Regulation of protein kinase C (PKC) expression by iron: effect of different iron compounds on PKC-beta and PKC-alpha gene expression and role of the 5'-flanking region of the PKC-beta gene in the response to ferric transferrin. *Blood* 1994. **84**: 3510-3517.

142. **Nyholm,S., Mann,G.J., Johansson,A.G., Bergeron,R.J., Graslund,A., and Thelander,L.,** Role of ribonucleotide reductase in inhibition of mammalian cell growth by potent iron chelators. *J.Biol.Chem.* 1993. **268**: 26200-26205.

143. **Furukawa,T., Naitoh,Y., Kohno,H., Tokunaga,R., and Taketani,S.,** Iron deprivation decreases ribonucleotide reductase activity and DNA synthesis. *Life Sci.* 1992. **50**: 2059-2065.

144. **Cellier,M., Shustik,C., Dalton,W., Rich,E., Hu,J., Malo,D., Schurr,E., and Gros,P.,** Expression of the human NRAMP1 gene in professional primary phagocytes: studies in blood cells and in HL-60 promyelocytic leukemia. *J.Leukoc.Biol.* 1997. **61**: 96-105.

145. **Ueda,K., Cardarelli,C., Gottesman,M.M., and Pastan,I.,** Expression of a full-length cDNA for the human "MDR1" gene confers resistance to colchicine, doxorubicin, and vinblastine. *Proc.Natl.Acad.Sci.U.S.A* 1987. **84**: 3004-3008.

146. **Smit,J.J., Schinkel,A.H., Oude Elferink,R.P., Groen,A.K., Wagenaar,E., van Deemter,L., Mol,C.A., Ottenhoff,R., van der Lugt,N.M., van Roon,M.A., and .,** Homozygous disruption of the murine mdr2 P-glycoprotein gene leads to a complete absence of phospholipid from bile and to liver disease. *Cell* 1993. **75**: 451-462.

147. **Kakhlon,O., Gruenbaum,Y., and Cabantchik,Z.I.,** Ferritin expression modulates cell cycle dynamics and cell responsiveness to H-ras-induced growth via expansion of the labile iron pool. *Biochem.J.* 2002. **363**: 431-436.

148. **Epsztejn,S., Kakhlon,O., Glickstein,H., Breuer,W., and Cabantchik,I.,** Fluorescence analysis of the labile iron pool of mammalian cells. *Anal.Biochem.* 1997. **248**: 31-40.

149. **Epsztejn,S., Glickstein,H., Picard,V., Slotki,I.N., Breuer,W., Beaumont,C., and Cabantchik,Z.I.,** H-ferritin subunit overexpression in erythroid cells reduces the oxidative stress response and induces multidrug resistance properties. *Blood* 1999. **94**: 3593-3603.

150. **Tapper,H. and Sundler,R.,** Protein kinase C and intracellular pH regulate zymosan-induced lysosomal enzyme secretion in macrophages. *J.Leukoc.Biol.* 1995. **58**: 485-494.

151. **Yudowski,G.A., Efendiev,R., Pedemonte,C.H., Katz,A.I., Berggren,P.O., and Bertorello,A.M.,** Phosphoinositide-3 kinase binds to a proline-rich motif in the Na+, K+-ATPase alpha subunit and regulates its trafficking. *Proc.Natl.Acad.Sci.U.S.A* 2000. **97**: 6556-6561.

152. **Atkinson,P.G. and Barton,C.H.,** High level expression of Nramp1G169 in RAW264.7 cell transfectants: analysis of intracellular iron transport. *Immunology* 1999. **96**: 656-662.

153. **Pikaart,M.J., Recillas-Targa,F., and Felsenfeld,G.,** Loss of transcriptional activity of a transgene is accompanied by DNA methylation and histone deacetylation and is prevented by insulators. *Genes Dev.* 1998. **12**: 2852-2862.

154. **Rodriguez,A., Webster,P., Ortego,J., and Andrews,N.W.,** Lysosomes behave as Ca2+-regulated exocytic vesicles in fibroblasts and epithelial cells. *J.Cell Biol.* 1997. **137**: 93-104.

155. **Zimmerli,S., Majeed,M., Gustavsson,M., Stendahl,O., Sanan,D.A., and Ernst,J.D.,** Phagosome-lysosome fusion is a calcium-independent event in macrophages. *J.Cell Biol.* 1996. **132**: 49-61.

156. **Kitta,K., Clement,S.A., Remeika,J., Blumberg,J.B., and Suzuki,Y.J.,** Endothelin-1 induces phosphorylation of GATA-4 transcription factor in the HL-1 atrial-muscle cell line. *Biochem.J.* 2001. **359**: 375-380.

157. **Dennis,J.W., Granovsky,M., and Warren,C.E.,** Glycoprotein glycosylation and cancer progression. *Biochim.Biophys.Acta* 1999. **1473**: 21-34.

158. **Dwek,R.A.,** Biological importance of glycosylation. *Dev.Biol.Stand.* 1998. **96**: 43-47.

159. **Hua,X., Sakai,J., Ho,Y.K., Goldstein,J.L., and Brown,M.S.,** Hairpin orientation of sterol regulatory element-binding protein-2 in cell membranes as determined by protease protection. *J.Biol.Chem.* 1995. **270**: 29422-29427.

160. **Rudd,P.M., Joao,H.C., Coghill,E., Fiten,P., Saunders,M.R., Opdenakker,G., and Dwek,R.A.,** Glycoforms modify the dynamic stability and functional activity of an enzyme. *Biochemistry* 1994. **33**: 17-22.

161. **Lin,W.W. and Chen,B.C.,** Distinct PKC isoforms mediate the activation of cPLA2 and adenylyl cyclase by phorbol ester in RAW264.7 macrophages. *Br.J.Pharmacol.* 1998. **125**: 1601-1609.

162. **Muyan,M. and Boime,I.,** The carboxyl-terminal region is a determinant for the intracellular behavior of the chorionic gonadotropin beta subunit: effects on the processing of the Asn-linked oligosaccharides. *Mol.Endocrinol.* 1998. **12**: 766-772.

163. **Robinson,J.M., Chiplonkar,J., and Luo,Z.,** A method for co-localization of tubular lysosomes and microtubules in macrophages: fluorescence microscopy of individual cells. *J.Histochem.Cytochem.* 1996. **44**: 1109-1114.

164. **Knapp,P.E. and Swanson,J.A.,** Plasticity of the tubular lysosomal compartment in macrophages. *J.Cell Sci.* 1990. **95 (Pt 3)**: 433-439.

165. **Hollenbeck,P.J. and Swanson,J.A.,** Radial extension of macrophage tubular lysosomes supported by kinesin. *Nature* 1990. **346**: 864-866.

166. **Heuser,J.,** Changes in lysosome shape and distribution correlated with changes in cytoplasmic pH. *J.Cell Biol.* 1989. **108**: 855-864.

167. **Steinkamp,J.A., Valdez,Y.E., and Lehnert,B.E.,** Flow cytometric, phase-resolved fluorescence measurement of propidium iodide uptake in macrophages containing phagocytized fluorescent microspheres. *Cytometry* 2000. **39**: 45-55.

168. **Njoroge,J.M., Mitchell,L.B., Centola,M., Kastner,D., Raffeld,M., and Miller,J.L.,** Characterization of viable autofluorescent macrophages among cultured peripheral blood mononuclear cells. *Cytometry* 2001. **44**: 38-44.

169. **Martinez,I., Chakrabarti,S., Hellevik,T., Morehead,J., Fowler,K., and Andrews,N.W.,** Synaptotagmin VII regulates Ca(2+)-dependent exocytosis of lysosomes in fibroblasts. *J.Cell Biol.* 2000. **148**: 1141-1149.

170. **Reddy,A., Caler,E.V., and Andrews,N.W.,** Plasma membrane repair is mediated by Ca(2+)-regulated exocytosis of lysosomes. *Cell* 2001. **106**: 157-169.

171. **Coorssen,J.R., Schmitt,H., and Almers,W.,** Ca2+ triggers massive exocytosis in Chinese hamster ovary cells. *EMBO J.* 1996. **15**: 3787-3791.

172. **Hackam,D.J., Rotstein,O.D., Sjolin,C., Schreiber,A.D., Trimble,W.S., and Grinstein,S.,** v-SNARE-dependent secretion is required for phagocytosis. *Proc.Natl.Acad.Sci.U.S.A* 1998. **95**: 11691-11696.

173. **Brumell,J.H., Volchuk,A., Sengelov,H., Borregaard,N., Cieutat,A.M., Bainton,D.F., Grinstein,S., and Klip,A.,** Subcellular distribution of docking/fusion proteins in neutrophils, secretory cells with multiple exocytic compartments. *J.Immunol.* 1995. **155**: 5750-5759.

174. **Mulero,V., Searle,S., Blackwell,J.M., and Brock,J.H.,** Solute carrier 11a1 (Slc11a1; formerly Nramp1) regulates metabolism and release of iron acquired by phagocytic, but not transferrin-receptor- mediated, iron uptake. *Biochem.J.* 2002. **363**: 89-94.

175. **Fleet,J.C.,** Identification of Nramp2 as an iron transport protein: another piece of the intestinal iron absorption puzzle. *Nutr.Rev.* 1998. **56**: 88-89.

176. **Tandy,S., Williams,M., Leggett,A., Lopez-Jimenez,M., Dedes,M., Ramesh,B., Srai,S.K., and Sharp,P.,** Nramp2 expression is associated with pH-dependent iron uptake across the apical membrane of human intestinal Caco-2 cells. *J.Biol.Chem.* 2000. **275**: 1023-1029.

177. **Tandy,S., Williams,M., Leggett,A., Lopez-Jimenez,M., Dedes,M., Ramesh,B., Srai,S.K., and Sharp,P.,** Nramp2 expression is associated with pH-dependent iron uptake across the apical membrane of human intestinal Caco-2 cells. *J.Biol.Chem.* 2000. **275**: 1023-1029.

178. **Tapper,H.,** The secretion of preformed granules by macrophages and neutrophils. *J.Leukoc.Biol.* 1996. **59**: 613-622.

179. **Sundler,R.,** Lysosomal and cytosolic pH as regulators of exocytosis in mouse macrophages. *Acta Physiol Scand.* 1997. **161**: 553-556.

180. **Bandyopadhyay,G., Standaert,M.L., Kikkawa,U., Ono,Y., Moscat,J., and Farese,R.V.,** Effects of transiently expressed atypical (zeta, lambda), conventional (alpha, beta) and novel (delta, epsilon) protein kinase C isoforms on insulin-stimulated translocation of epitope-tagged GLUT4 glucose transporters in rat adipocytes: specific interchangeable effects of protein kinases C-zeta and C-lambda. *Biochem.J.* 1999. **337 (Pt 3)**: 461-470.

181. **Bonnet,D., Thiam,K., Loing,E., Melnyk,O., and Gras-Masse,H.,** Synthesis by chemoselective ligation and biological evaluation of novel cell-permeable PKC-zeta pseudosubstrate lipopeptides. *J.Med.Chem.* 2001. **44**: 468-471.

182. **Bhattacharyya,S., Ghosh,S., Sen,P., Roy,S., and Majumdar,S.,** Selective impairment of protein kinase C isotypes in murine macrophage by Leishmania donovani. *Mol.Cell Biochem.* 2001. **216**: 47-57.

183. **Alam,J., Wicks,C., Stewart,D., Gong,P., Touchard,C., Otterbein,S., Choi,A.M., Burow,M.E., and Tou,J.,** Mechanism of heme oxygenase-1 gene activation by cadmium in MCF-7 mammary epithelial cells. Role of p38 kinase and Nrf2 transcription factor. *J.Biol.Chem.* 2000. **275**: 27694-27702.

183. **Jawetz,** Medical microbiology, nineteenth edition. 1999. Chapters 3, 5 and 9.

184. **Davies.,** Modules in life sciences, infection and immunity. 2001. Chapters 6 and 7.

185. **R.R,Crichton,** Inorganic biochemistry of iron metabolism. 1991. Chapters 10 and 12.